Implementation of Roller Blind, Pleated Drape and Insect Screen Models into the CFC Module of the ESP-r Building Energy Simulation Tool

by

Kenneth Joong

A thesis

presented to the University of Waterloo

in fulfillment of the

thesis requirement for the degree of

Master of Applied Science

in

Mechanical Engineering

Waterloo, Ontario, Canada, 2011

I hereby declare that I am the sole author of this thesis. This is a true copy of the thesis including any required final revisions, as accepted by my examiners.

I understand that my thesis may be made electronically available to the public.

Abstract

The concern of increasing energy consumption with depleting energy resources is ever growing. Though the solution to this problem lies in part in renewable energies, it is becoming increasingly clear that sustainable building design also plays a critical role. Controlling solar gain, for example, can greatly reduce the cooling energy consumption and lowering the peak cooling load. Having the ability to model these effects can have a substantial impact on the sizing of equipment and further reduce operational costs of a building. As a result, renewed interest has been invested by researchers and industry to promote the development and use of building simulation tools to aid in the design process.

Efforts at the University of Waterloo's Advanced Glazing Systems Laboratory have resulted in a set of shading device models, with emphasis on generality and computational efficiency, tailored for use in building simulation. These models have been validated with measurements at the component level and with measurements performed at the National Solar Test Facility (NSTF) on a full scale window system, giving confidence to model validity. Continued research has resulted in the integration of these shading device models into ESP-r via the Complex Fenestration Construction (CFC) module, capable of modelling multi-layer glazing and shading layer systems and greatly improving the value of ESP-r as a design tool.

The objective of the current research was to implement shading device models for roller blinds, pleated drapes and insect screens to the CFC module. These would be in addition to the venetian blind model which had previously been established. A Monte-Carlo ray tracing analysis of pleated drape geometry and incident angle dependent fabric characteristics gave further confidence to the view factor or net reduction method used by the implemented models. On model implementation, a preliminary comparison was performed between a high-slat angle venetian blind, a roller drape and drapery fabric, all given the same material properties, with similar results. Further comparison was then performed using EnergyPlus shading device models to establish further confidence in the functionality of the models. Though there was some discrepancy between the results, primarily due to convective models, good agreement was found, and the effect of the shading device models on building performance was demonstrated.

The successful implementation of roller blind, pleated drape and insect screen shading models to the CFC module in ESP-r has been demonstrated in the current research. It should also be noted that the convective models for indoor shading attachments is a worthwhile topic for further research, at which point it would then be beneficial to conduct further empirical validation on the ESP-r simulation.

Acknowledgements

My first and sincere thanks go to my supervisor, Professor John Wright, for giving me the opportunity to realise this topic of study. I would also like to thank him for the assistance, direction and mentorship throughout the process.

I am forever grateful to Bart Lomanowski for his time and efforts in bringing me up to speed on ESP-r development and providing me with the guidance and confidence required to complete this thesis.

I would also like to give thanks to Professor Mike Collins, Scott Sterling, Andrew Marston, Sebastien Brideau, Will Wager, Carsen Banister and Ned Huang for their continued support and for creating a great, friendly and welcoming, working environment which I looked forward to every day. A special thanks to Christine Rogalsky, with whom I have shared many memorable experiences and interesting discussions as well as for her valuable input throughout my research.

Finally I would like to acknowledge the Solar Buildings Research Network for financial support.

Table of Contents

Appendix C

List of Figures

List of Tables

Nomenclature

Symbols

A	Area	m^2
A_o	Openness Factor	Dimensionless
Fr	Fullness Ratio	Dimensionless
I	Irradiance	W/m^2
N	Inward Flowing Fraction	Dimensionless
n	Number of Bundles	
q	Heat Transfer Rate	W
R	Thermal Resistance	m^2K/W
S	Absorbed Solar Flux	W/m^2
s	Drape Pleat Spacing	m
SD	Standard Deviation	
SHGC	Solar Heat Gain Coefficient	Dimensionless
T	Temperature	K
U	U-Value	W/K
w	Drape Pleat Width	m

Greek Letters

α	Absorptivity	Dimensionless
α_s	Solar Altitude Angle	
γ	Surface Azimuth Angle	
γ_s	Solar Azimuth Angle	
ε	Emissivity	Dimensionless
θ	Solar Incidence Angle	
ρ	Reflectance	Dimensionless
σ	Variance Squared	
τ	Transmittance	Dimensionless
Ω	Profile Angle	

Roman Numerals

I	Open Weave
II	Semi Open Weave
III	Closed Weave

Subscripts

b	Back
bb	Beam-Beam
bd	Beam-Diffuse
bt	Beam-Total
cav	Cavity

cg	Center of Glass
dd	Diffuse-Diffuse
f	Front
gl	Glazing
H	Horizontal
i	Layer i
in	Indoor
j	Layer j
lw	Longwave
net	Net Heat Transfer
out	Outdoor
PARL	Parallel
PERP	Perpendicular
ray	Ray
sol	Incident Solar
surf	Surface
tot	Total
V	Vertical
vis	Visible

Superscripts

f	Fabric
m	Material Property
y	Yarn Property

Chapter 1

Introduction and Background

1.1 Motivation

Today, the world faces the very serious concern of climate change due to a dependence on fossil fuels. As nations expand and increasingly demand more energy, the issue is compounded. Governments are now beginning to take notice of the issue and are increasing funding to renewable energy projects with government subsidies in renewable energy, farming projects, and increased funding into renewable energy research (U.S. Department of Health and Human Services 2011, Government of Canada 2011, Government Grants UK 2011, etc.)

In 2008, the United States Department of Energy (DOE) illustrated that residential and commercial building energy consumption accounted for 39% of total energy use in the US, effectively attributing to 39% of carbon dioxide emissions. In 2010, the U.S. Energy Information Administration (EIA), showed an increase in building energy consumption at 49% of all energy produced in the United States and a subsequent increase in carbon dioxide emissions at 46.9%. The National Renewable Energy Laboratory (NREL) translated this consumption in energy to 71% of the total generated electricity in the United States. It is clear that buildings in the United States account for a significant portion of the energy consumption. Renewable energies can account for some of this consumption; however they require large amounts of resources, capital and space to build and install. Therefore, it is clear that renewable energies alone are not the solution to meet the energy hungry demands of the world. Energy efficiency and energy conservation are critical in the transition from conventional to renewable energies. Better building designs in addition to effective building usage could aide in drastically reducing building loads and as a result, improve the outlook of renewable energies as a real alternative to conventional energy sources.

Though the technology for more efficient building designs exists, the cost of a more efficient office space relative to employee cost is so minimal that there is little incentive for companies to rent this type of space or for building owners to build them. Initiatives such as Leadership in Energy & Environmental Design (LEED) and the American Administration's Better Buildings Initiative (BBI) have been developed to help realise the goal of achieving more sustainable building designs. Although such

development can lead to greater costs during construction, the benefits can outweigh the costs throughout the building's lifetime, critically, without compromising occupant comfort. The net-zero energy building concept has been proven possible (Solar Decathlon Project/Competition, BedZED in London, Riverdale Net Zero Project in Edmonton and many others) by utilizing a more efficient building design and supplementing the energy consumption by means of renewable energy on site. It is often more economical for building owners and operators to design and construct a new building with increased overhead costs than it costs to retrofit a building, which is poorly built, to have the same energy efficiency. However, retrofits have been proven effective, (e.g. The Mission Zero House in Michigan).

A valuable tool aiding in the success of such projects and initiatives is one that predicts the performance of the building design. With increasing efforts being invested in building energy simulation tools; this is becoming more readily available. Simulation tools offer the means of quickly evaluating alternative building designs, where the integration of the multi-disciplinary expertise of engineers, architects and building sciences can occur. Critically, this occurs during the design phase of a project, where changes to the design come at their lowest cost and provide invaluable building performance data aiding in efficient building design.

In spite of the many advantages gained through the application of building simulation software in the design phase of building construction, its adoption has been slow. This is the result of modeling results inaccurately portraying the actual performance of buildings. Although the underlying physics and math behind these programs are often sound, the proper input of material and building characteristics and a good understanding of how the program utilises these inputs is essential. Inexperience of users, compounded with the unintuitive interface many building simulation tools employ can often lead to miscalculations. Therefore it is important to note that although existing simulation tools are capable of closely simulating building performance; this result is heavily dependent on a good understanding of the program being used and the building you wish to simulate.

As programs like LEED and BBI increase in popularity amongst building developers, software companies see the shortcomings of building simulation tools as an opportunity to develop products which reduce their complexity, and increase user-friendliness in order to promote their use. However, this often comes at the cost of performance, the ability to fine-tune properties and hence their ability to accurately represent real-life building performance. Organizations like the International Building Performance Simulation Association (IBPSA) have since been developed to bridge the gap between researchers, developers and designers to help streamline and promote the capabilities of various programs to more accurately predict building performance using building energy simulation software.

1.2 Background

One of the biggest obstacles faced by building designers is the management of solar gain to accommodate for the heating and cooling of a building. Of particular concern in the summer months, is the effort required to remove and/or control solar gain and cool the conditioned space. It was once the case that one would find any means to cope with the heat, by use of awnings, fanning the space and opening the windows. However, the introduction of air-conditioners greatly improved the thermal comfort. Consequently, architects could realise the possibility of designing highly glazed, visually appealing facades, at minimal cost to thermal comfort. In contrast, heating has long since been readily available in the form of wood fires, oil fuelled, natural gas, and more recently electrical heating.

As a result, many buildings today require oversized HVAC systems that would be considered oversized when compared to a well designed building of equivalent floor-space. Therefore, it is not hard to imagine that approximately 25% of a building's energy consumption can be attributed to its windows. This suggests large economic gains for residential and commercial building owners which come as a result of improved window shading systems, increasing building efficiency. Directly correlated to the reduced energy consumption, are reduced greenhouse gas emissions which impact the environment of today and that of future generations. Although renewable energy resources are critical to sustaining the world's increasing energy consumption, even more critical are the means to reduce that demand to a level that can be sustained by renewable energy.

In recent years, increasing interest has been taken in green and net-zero energy building designs. A critical component to these design concepts include heavily insulated envelope, necessary in minimizing heat transfer between the inside space and external surroundings, additionally minimizing solar gains. Inherently obvious in such a building is that any stored heat becomes difficult to remove. This can be seen as a shortcoming or obstacle which must be overcome in order to have a successful design. As such, significant advancements in windows, including the development of low-e coatings, spectrally selective glazing, and the application of fill gases have aided in increasing the thermal resistance (more insulation) and reducing solar gain. However, solar gain is a highly variable source of heat gain for space which must be handled accordingly.

The realisation of comfortable yet efficient building design has brought about a renewed interest in shading devices. The reason for this is the significant role they play in providing the ability to control solar gains through windows as well as the control of occupant comfort. Given the appropriate shading control schemes, the performance of window and shading systems can be drastically improved. Having previously discussed the importance of building energy simulation applied to building design, it should be

noted that until recently, little effort has been invested in the modelling of shading devices. However, it is clear that window shading devices in the form of venetian blinds, roller blinds, pleated drapes and insect screens can be found as a component of almost all window constructions. The need to understand the effects of shading devices on the performance of window systems and consequently building performance is invaluable in terms of building modelling and design. The task of predicting shading device performance has since been undertaken by a number of researchers e.g., (Lomanowski and Wright 2011, Kotey 2009, Yahoda and Wright 2004a, Yahoda and Wright 2004b, Collins and Harrison 2004a, Collins and Harrison 2004b, Breitenbach, et al. 2001 and Rosenfeld, et al. 2000).

1.3 Energy flow through window glazing and shading systems

Considerable research has been invested in the area of window glazing systems over the past half century, establishing a clear understanding of both their solar and thermal characteristics. This process has allowed window glazing manufacturers to develop new glazing and coating technologies (e.g. Hollands, Wright and Granqvist 2001).

In North America, energy distribution through a fenestration system is treated as having three major components; center glass, edge glass and frame, see Figure 1.1. The center glass region can be analysed in one-dimension, while the frame and edge glass require two-dimensional heat transfer analysis. The edge glass on conventional windows accounts for a small amount of the total aperture of the window surface and it is assumed to perform similarly to the center glass. The frame of glass is assumed to have negligible effect on the overall fenestration device performance (Wright et al. 2011). As a result, only the center of glass will be considered in further discussions. It should however be noted that the frame and edge glass have significant influence on condensation.

Before shading layers can be discussed, an understanding of center-of-glass analysis must first be established. The net heat gain in a space, q_{net}, can be viewed as (e.g. Wright and McGowan 1999),

$$q_{net} = U_{cg}(T_{out} - T_{in}) + SHGC_{cg}I_{sol} \tag{1.1}$$

where U_{cg} is the center of glass U-value, T_{out} and T_{in} are the outdoor and indoor temperatures respectively, $SHGC_{cg}$ is the center of glass Solar Heat Gain Coefficient and I_{sol} is the solar irradiance. The U-value is the inverse of the total thermal resistance, R-value, of the glazing system. Thermal resistance can be seen as the resistance resulting from conduction in glass layers, convection between glazing layers and longwave radiation exchange between the glazing layers and indoor and outdoor surfaces.

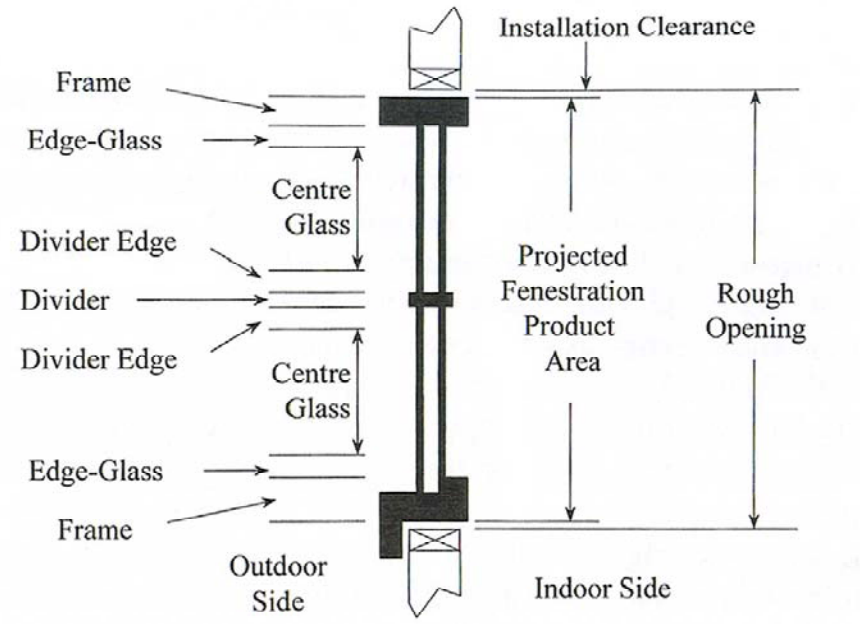

Figure 1.1 - Defining the Center-of-Glass, Edge Glass and Frame - Reproduced from (Hollands, Wright and Granqvist 2001)

The $SHGC_{cg}$ is the fraction of solar incident radiation which is transmitted through the window and absorbed by the room, seen as

$$SHGC_{cg} = \tau_{cg} + \sum_{i=1}^{n} N_i A_i \tag{1.2}$$

Where i denotes the layer, and $i = 1$ refers to the outside layer and n refers to the inside layer, τ_{cg} is the center of glass solar transmittance, N_i is the inward flowing fraction of layer i, A_i is the portion of solar I_{sol} at layer i, and n is the number of layers in the system. The $SHGC_{cg}$ and τ_{cg} apply to the center of glass region of the window.

The inward flowing fraction, N_i, represents the fraction of the total net thermal resistance offered at layer i.

$$N_i = \sum_{j=i}^{n-1} \frac{R_j}{R_{tot}} \tag{1.3}$$

This general equation will apply to any glazing system with any number of glazing layers.

Note: The introduction of shading layers complicates the analysis; a more sophisticated method accommodating for shading layers will be investigated further in subsequent sections.

The $SHGC$ and U-value describe the thermal characteristics of the glazing system. The $SHGC$ is a function of the solar transmittance in addition to the inward flowing fraction of convective and long wave radiant energy from the environment in to the space, see Figure 1.2. The U-value is a function of the temperature difference across each layer and the absorbed flux at each layer due to the various modes of heat transfer. The $SHGC$ and U-value are critically used as window construction performance indices, dependent on the indoor and outdoor temperatures as well as solar irradiance. As such, it is typical for standard environmental conditions to apply in system comparison tests.

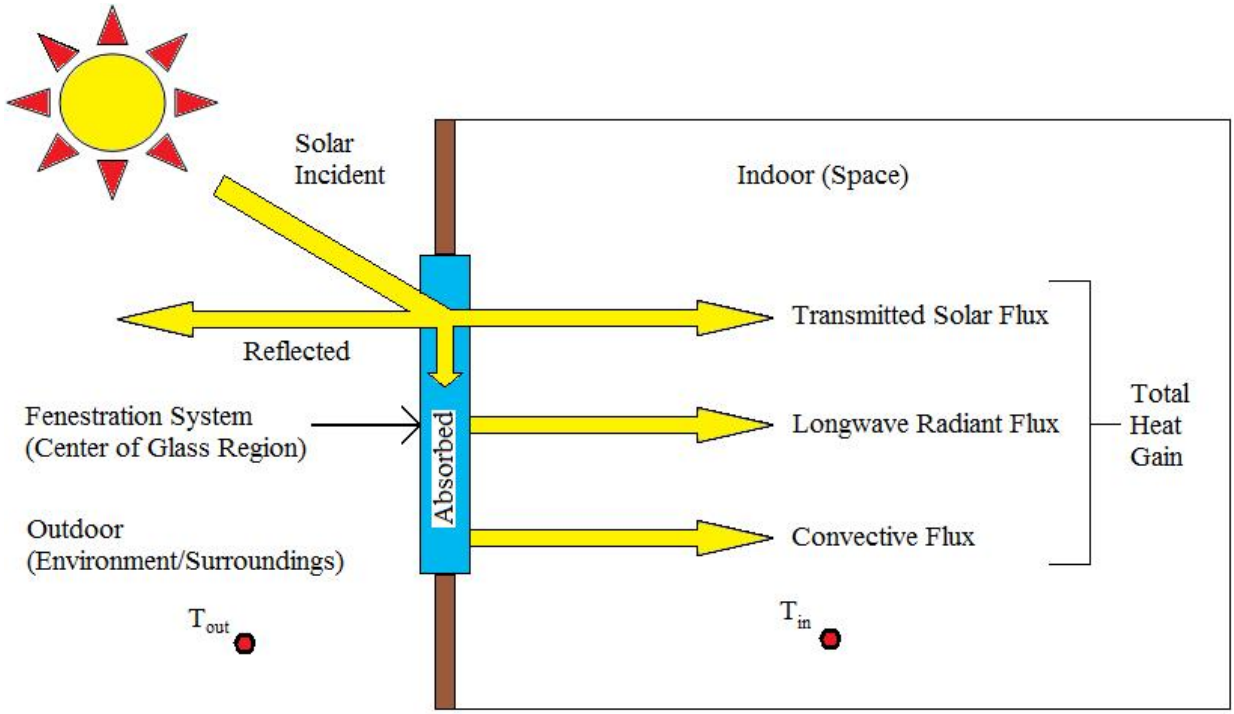

Figure 1.2 - Distribution of Solar Incident Radiation at the Fenestration Construction

1.3.1 Multi-layer analysis

1.3.1.1 Structure

The distribution of solar fluxes can be determined through a multi-layer analysis (Wright et al. 2009, Wright and Kotey 2006, Wright 1998 and Edwards 1977) through a center of glass analysis. This method views the glazing and shading components of a fenestration construction as individual layers separated by gaps. In Figure 1.3, the absorbed solar radiation flux at the i^{th} layer is found to be S_i, a function of the

incident solar flux, I_{sol}. An energy balance is then performed at each layer to account for S_i, thus allowing the corresponding layer temperatures, T_i, to be determined.

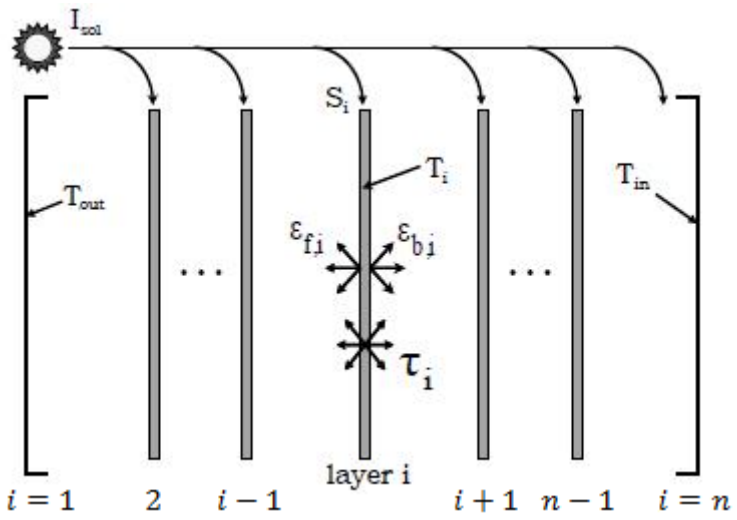

Figure 1.3 - Multi-Layer Analysis Structure - Reproduced from (Wright 2008)

1.3.1.2 Solar Analysis

Models for incident solar radiation interaction with glazing layers have previously been established. The addition of shadings layers has however added to the complexity of this analysis, given that shading layers tend to scatter solar radiation. Therefore the beam and diffuse components of solar radiation are tracked as they interact with the individual components of the multi-layer system. The scheme represented by Figure 1.4, can be used to analyse the beam, diffuse or longwave fluxes incoming and outgoing, I^+ and I^-, at each gap respectively. Although it is not explicitly clear in Figure 1.4, this method also accounts for the beam-diffuse conversion which results from optical layer interactions. Further details describing this method are found in (Wright et al. 2009 and Wright and Kotey 2006).

In order to determine the set of S_i, solar optical properties must be established at each layer. The multi-layer analysis demands an expanded set of 12 solar optical properties for each layer in the multi-layer system. These include; front and back beam-beam transmittances, $\tau_{f,bb}$ and $\tau_{b,bb}$, front and back beam-diffuse transmittances, $\tau_{f,bd}$ and $\tau_{b,bd}$, front and back beam-beam reflectance, $\rho_{f,bb}$ and $\rho_{b,bb}$, front and back beam-diffuse reflectance, $\rho_{f,bd}$ and $\rho_{b,bd}$, in addition to the incident diffuse radiation properties, front and back diffuse-diffuse transmittances, $\tau_{f,dd}$ and $\tau_{b,dd}$, front and back diffuse-diffuse reflectance, $\rho_{f,dd}$ and $\rho_{b,dd}$, and are presented in Figure 1.5.

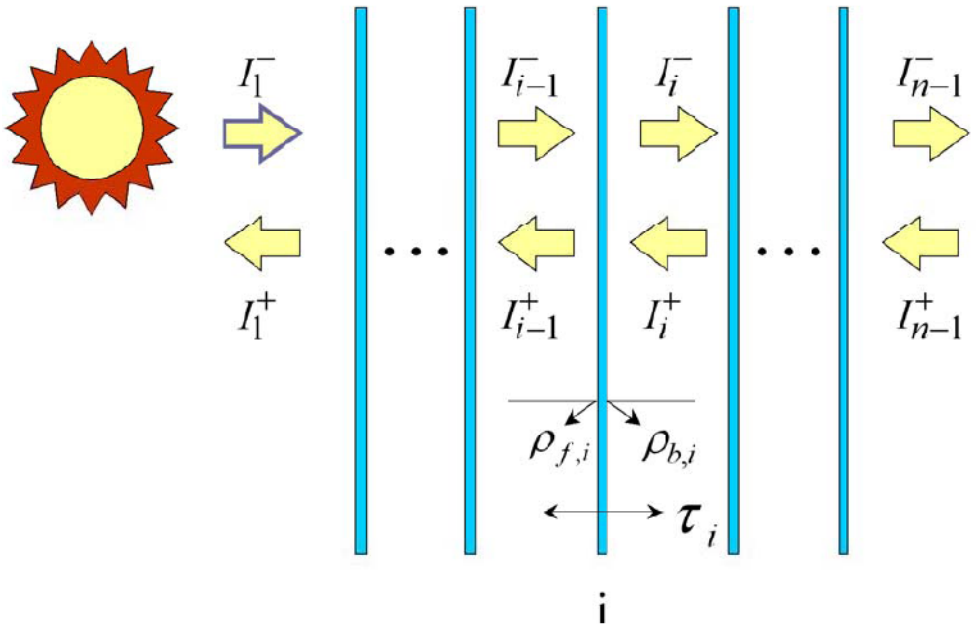

Figure 1.4 - Distribution of Solar Fluxes in an Array of Glazing/Shading Layers - Reproduced from (Lomanowski 2008)

1.3.2 Heat Balance

In the analysis of glazing systems, a one-dimensional heat balance at the center of glass is imposed at each layer of the fenestration construction. Using an equivalent network approach, the equivalent gap resistances are representative of the longwave radiant and convective resistors, as demonstrated in Figure 1.6.

Establishing the absorbed solar flux at each layer as a source term, it is then possible to derive the convective and longwave radiant resistances at each gap and at the indoor and outdoor interfaces. However, the resistances are temperature dependent and thus must resolved iteratively until the fluxes are balanced. Once a solution is reached, the known temperature and heat fluxes can be used to determine the internal gains, gap resistances, total center of glass resistance and thus the $SHGC$ and U-value. This approach is further described in (Lomanowski 2008).

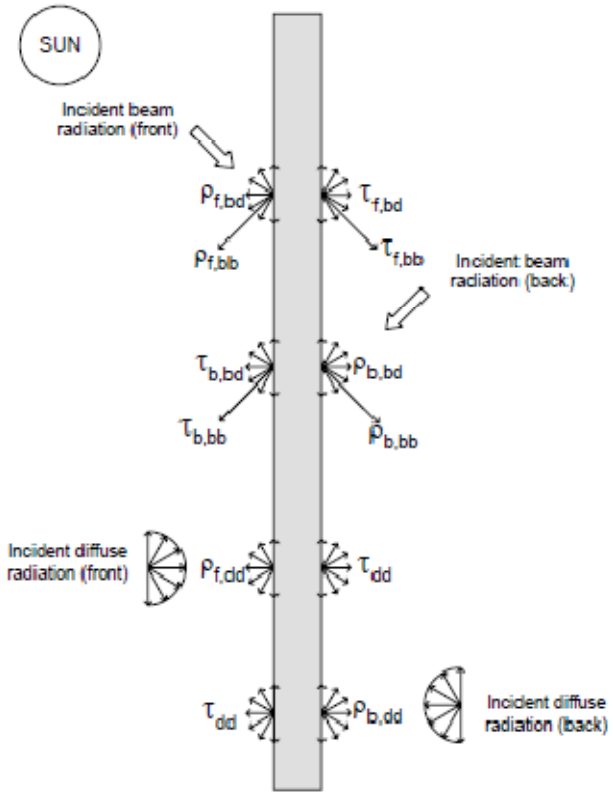

Figure 1.5 Solar Optical Properties Describing a Layer in the Multi-Layer Structure – Reproduced from (Wright et al. 2009)

1.3.3 Shading Layer Analysis

To extend the capability of one-dimensional center of glass glazing analysis to include shading devices, spatially-averaged "effective" solar optical and longwave properties are first established. Methods for determining these properties can be found in (Kotey et al. 2008, Yahoda and Wright 2005, Yahoda and Wright 2004a, Yahoda and Wright 2004b, Rosenfeld, et al. 2000, Pfrommer, Lomas and Kupke 1996, Rheault and Bilgen 1989, Farber, et al. 1963 and Parmelee and Aubele 1952). In doing so, shading layers like slat blinds, roller blinds, drapes and insect screens, shading layers can be treated as planar, homogeneous layers, refer Figure 1.5.

Shading layers in the heat balance analysis creates additional complications since they can be described as diathermanous layers. As a result, longwave "jump resistors" need to be introduced to account for transmission through these layers. Similarly, convective "jump" resistors are introduced to account for the fact that shading devices, unlike glazing layers, do allow air to flow through the layer.

Additionally, the geometry of certain types of shading devices, including slat-type blinds and pleated drapes can further complicate the process of determining the effective solar optical properties of a shading layer. This is a result of inter-reflections which can occur within the shading layer.

However, slat type blinds and pleated drapes further complicate the system analysis as incident beam radiation can be inter-reflected within the shading layer and with adjacent glazing layers. The work described in this document includes a detailed analysis of the pleated drape models demonstrating how the solar optical analysis is handled.

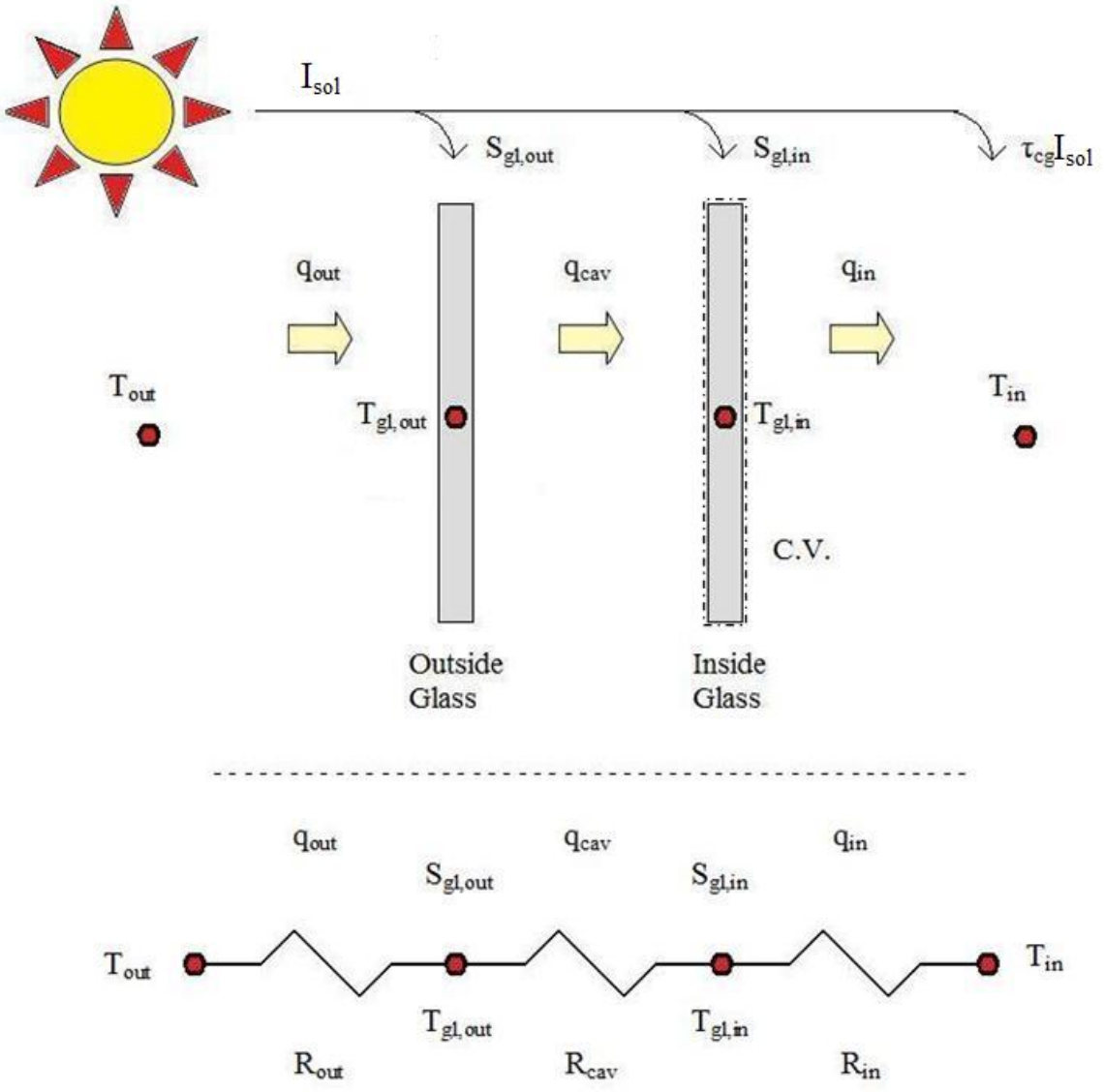

Figure 1.6 - One-Dimensional Heat Transfer Model (Above) and Thermal Equivalent of Electrical Circuit (Below) - Reproduced from (Hollands, Wright and Granqvist 2001)

1.3.4 Longwave Jump Resistors

Shading devices can be described as diathermanous, or layers which can transmit both longwave and shortwave radiation. Therefore the effective radiative properties which describe shading layers must also include longwave transmittance. In terms of the heat transfer analysis, 'jump' resistors must therefore be established in order to accommodate the thermal communication which results between non-adjacent layers. To further complicate matters, when a diathermanous layer is located on the indoor or outdoor face of the glazing and shading system, jump resistors must extend respectively between the external surroundings or internal surfaces, seen in Figure 1.7.

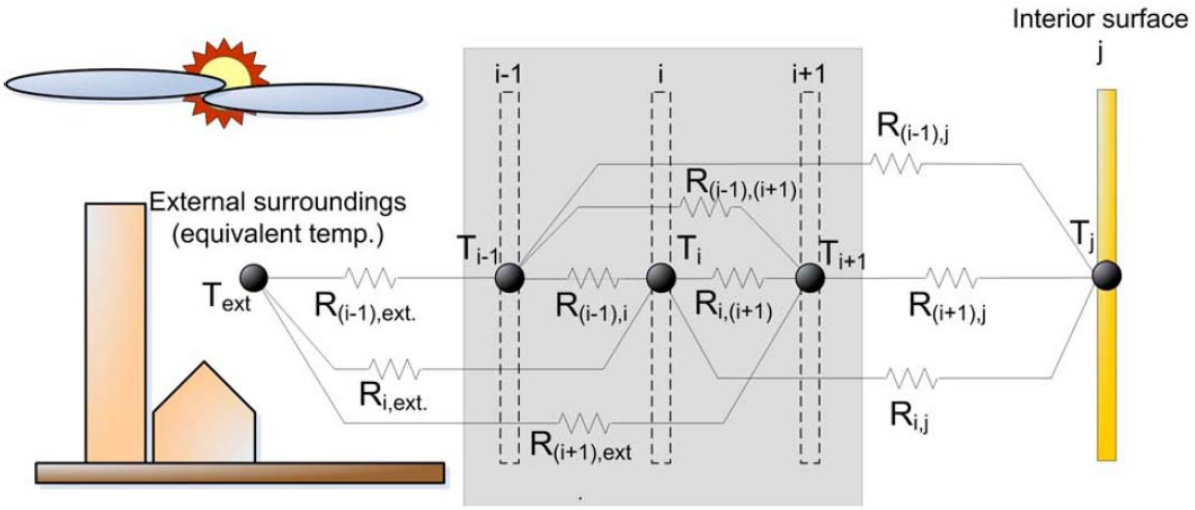

Figure 1.7 - Longwave Heat Transfer Model with "Jump" Resistors to Accommodate for Diathermanous Layer Thermal Communication between Non-Adjacent Layers - Reproduced from (Lomanowski 2008).

The net radiation method of determining radiation exchange is general enough to be able to incorporate jump resistors. However, standard methods of determining a glazing system's U-value and SGHC can produce erroneous results with jump resistors present. Wright (2008) describes a method of integrating diathermanous and opaque layers such as would be found in a glazing and shading system which can calculate the indices of merit correctly. This multi-layer analysis method is based on work previously carried out by Collins and Wright (2006), using Gebhart's analysis of diffuse, grey enclosures (Gebhart 1961, Gebhart 1959 and Gebhart 1957), with an extension to specifically account for diathermanous layers. The method, referred to as the "exchange factor method" (Lomanowski 2008), is similar to the view factor concept. It represents the fraction of radiation leaving surface *i* incident on surface *j*, accounting for direct and inter-reflected radiation in an enclosure. This is achieved by examining the effect of one surface at a time on the surrounding surfaces and determining the irradiation of each interaction by radiosity balance. Further description of this concept is described in (Wright 2008, Hollands 2004, Gebhart 1961, Gebhart 1959 and Gebhart 1957).

1.3.5 Convective Jump Resistors

The presence of shading layers also complicates the convective flows through the glazing and shading systems. Figure 1.8 represents the resistive networks which result with the introduction of external, between-pane and internal shading devices. This analysis relies heavily on empirical information, and has been established for a glazing cavity, (e.g. Shewen, Hollands and Raithby 1996, Wright 1996, ElSherbiny, Raithby and Hollands 1982), and shown to work for a cavity between a window and airtight shading layer. However, airtight shading layers are not common, some information exists on the convective heat transfer of an inter-pane shading layer (Wright et al. 2008, Huang et al. 2006) and even less is known about the convective heat transfer when a shading device is attached outdoors or indoors. The indoor case is particularly critical since shading devices can effectively triple the internal surface area for convective exchange. More evident than in the longwave analysis, convective "jump" resistors are necessary to account for the flow through gaps in slat blinds or fabric gaps in the between-pane case, between the outdoor glass and outdoor surroundings or indoor glass and indoor surfaces, illustrated in Figure 1.8.

Convective flow is well understood for between-pane shading devices and models exist which produce accurate results. However, for indoor and outdoor shading, it is difficult for any one model to account for complex convective flows describing internal free and forced convection, influenced by variable wind, HVAC systems and temperature differences. Still, approximate convection models have been presented to describe the aforementioned cases, see (Wright 2008).

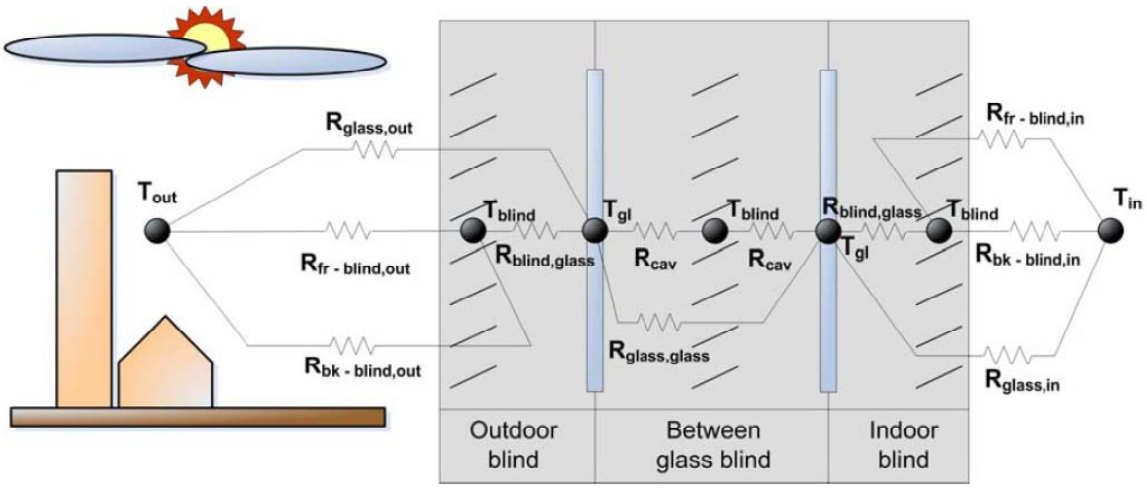

Figure 1.8 - Convective Heat Transfer Model with "Jump" Resistors to Account for Openness in Shading Layers - Reproduced from (Lomanowski 2008).

1.4 Purpose and Objectives

The main purpose of this undertaking is to implement fabric, pleated drape, insect screen and roller blind solar and longwave properties provided largely by (Kotey 2009) in the ESP-r source code distribution package, a project initiated by Lomanowski (2008). As previously discussed, (Kotey 2009) presents a set of simplified, computationally efficient, yet accurate models to estimate the solar gain through window constructions with attached shading devices.

Subroutines added to ESP-r by Lomanowski (2008) have extended the capabilities of the modelling tool to allow for the analysis of shading devices in building energy simulation with the implementation of the Complex Fenestration Construction (CFC) model. This process required a translation of results from the framework analysis presented in (Kotey 2009) to the node system employed by ESP-r. Additionally, the CFC model extended the capability of ESP-r to allow for the flexible definition of shading layers as well as shading layer controls at each time step, such as slat-angle adjustment.

The work of Lomanowski (2008) included the implementation of venetian blind models.

Following, venetian blind shading models were incorporated to demonstrate the CFC models.

The objectives of the current research were:

- To extend the CFC model capabilities to include three additional shading models; roller blinds, insect screens, pleated drapes.
- To develop a better understanding of the pleated drape model, and replicate the results using Monte Carlo Methods, a mathematical approach to model systems based on probabilities to give confidence model validity

The scope of work required to successfully achieve the desired results is as follows:

- Study the underlying theory behind the ESP-r source code, and develop a solid understanding of the shading device models and their subsequent coding.
- Implementation of pleated drape, roller blind and insect screen models to the ESP-r source code, subsequently followed by testing and debugging.
- Utilization of models in a case study to enforce model validity based on a simplified shoebox model used in illustrating predicted shading device effects on building performance.
- Commit the code to the distribution branch of the ESP-r source code, making the models available to all ESP-r users.

Chapter 2

Existing Software for Window Shading Analysis

In the 1970's, during the energy crisis, there was an increased interest in designing more energy efficient buildings. This lead to the development of computer aided tools which could be used in cheaply modeling building performance. However the computational power available at the time required developers to design these programs to be extremely efficient yet capable. As a result tools like ESP-r and DOE-2 were developed. These programs are still used today by government and industry as the engines which drive more user-friendly software. However, the complexity of shading models adding significantly higher computational loads were not considered a priority. With the advancements in technology, more effort is now being put in to developing these models and implementing them in software tools which are able to determine the indices of merit of glazing and shading systems including the U-factor, $SGHC$, G-value and solar transmittance amongst other characterizing properties. A short list of such simulation tools is provided below.

2.1 ASHWAT

ASHWAT is a culmination of FORTRAN subroutines pieced together to model multi-layer complex fenestration systems. An "equivalent layer" framework is implemented generalizing material and solar optical properties of different glazing and shading layers into a uniform set of parameters which describe each layer. Structuring the framework in this manner allows for flexibility and economical use of CPU time as well as the potential for additional shading models. Each layer can be described with a small, basic subset of measurements, and libraries of typical glazing layers, venetian blinds, drapery fabrics, insect screens and roller blinds have been compiled. Models to determine equivalent layer properties of shading devices have been developed by the Advanced Glazing Systems Laboratory (AGSL). A summary of the models and further details are provided in (Kotey 2009).

Each glazing and shading layer in the ASHWAT model is treated as a parallel layer separated by gaps, a proven method of modelling multi-layer systems. Solar-thermal separation is used to determine the flux absorbed at each layer, S_i, from the incident flux, I_{sol} then an energy balance is applied to obtain the set of layer temperatures, T_i, and corresponding heat flux values.

The critical concept behind the ASHWAT model, its simplicity and effectiveness, is spatially-averaged "effective" optical properties. That is, whether a layer is homogeneous or not, it can be represented by a homogeneous layer given equivalent homogeneous layer. (Rheault and Bilgen 1989) This approach has been used and proven in numerous studies (e.g. Yahoda and Wright 2005, Yahoda and Wright 2004a, Yahoda and Wright 2004b, Rosenfeld, et al. 2000, Pfrommer, Lomas and Kupke 1996, Rheault and Bilgen 1989, Farber, et al. 1963 and Parmelee and Aubele 1952). Additionally, it has been shown too accurate characterize venetian blinds (e.g. Huang, Wright and Collins 2006, Wright, Collins, et al. 2009, Kotey, Collins, et al. 2008).

Incident solar radiation which is incident on a structure is then transmitted, reflected or absorbed. The portion unabsorbed by a given layer in the ASHWAT model, which is not transmitted beam radiation, is assumed to be scattered uniformly diffuse. In addition, a shading layer will generally transmit long wave radiation due to its openness, so effective longwave properties are also determined.

ASHWAT is a modelling package capable of determining the indices of merit for a fenestration system comprised of glazing layers and shading devices. Shading device modelling is achieved through the inclusion of diathermanous layer analysis. This multi-layer analysis tool is able to predict the performance of the system based on an expanded set of 12 solar optical properties taken at normal incidence to describe the respective layers in conjunction with approximate convective models described in Appendix C of (Wright et al. 2009).The effective optical properties and beam-diffuse split of solar radiation at each layer used in a multi-layer complex fenestration systems delivers the freedom to describe different shading layers with the computational speed necessary for building simulation.

2.2 ESP-r

ESP-r is an integrated modelling tool designed with the purpose of in-depth analysis of the factors contributing to the performance of buildings. Created at the University of Strathclyde in Scotland during the 1970s, it has since been the subject of sustained development by energy and environmental performance conscious building designers and researchers with the purpose of realistically adhering to physical systems.

The strength of ESP-r is that, while most building analysis tools exclusively simulate thermal processes, ESP-r further strives to integrate all the relevant physical processes as well. (Clarke 1999) The integrated performance of air flow in building zones and plant operations are connected by means of the finite volume, conservation approach, where variable time-steps allow for the user to decide how to balance accuracy of the simulation with computational time required. Levels of system details are also available to

the user to accommodate for knowledge of the modelling tool in addition to depth to which the simulation results must return.

Prior to the work done by the Advanced Glazing Systems Laboratory (AGSL) at the University of Waterloo, the transparent multi-layer construction (TMC) was used for the analysis of fenestration constructions. An extension of the multi-layer nodal scheme used for opaque constructions (MLCs), it is able to determine the fenestration construction's solar and long-wave optical properties, as well as the flow of energy through them as a function of incidence angle. The complex fenestration construction (CFC) as introduced by the AGLS (Lomanowski 2008) further extended the capabilities of the ESP-r framework to incorporate CFCs to the same nodal structure, matrix processing and existing solar gain control methods used by TMCs and MLCs. The result is a functional framework for the analysis of complex fenestration constructions (Lomanowski 2008). Lomanowski (2008) subsequently implemented slat type shading models to the CFC module in ESP-r. Extending the work previously done by the AGSL, the subsequent chapters will explain the development, implementation and results of additional shading devices added to the already comprehensive capabilities of ESP-r.

2.3 Energy Plus 6.0.0

EnergyPlus is a standalone building energy analysis tool developed by the U.S. Department of Energy (DoE). Based on the popular BLAST and DOE-2 energy and load simulation programs of the 1970s and 1980s, EnergyPlus utilizes the characterising attributes of the respective parent programs and improves on their shortcomings. EnergyPlus has been designed for design engineers and architects wishing to optimize building performance in terms of heating loads, cooling loads and energy demands through building simulation models.

EnergyPlus incorporates user based descriptions of building zone constructions, mechanical systems and electrical systems amongst other user specified systems to simulate zone heating and cooling loads as well as system energy consumption. A highly versatile program, buildings can be simplified, or modified to include variable amounts of detail depending on the user's knowledge of the building's future usage and schedules, and as the user gains knowledge of manipulating EnergyPlus's more advanced functions.

Fenestration construction modelling glazing and shading layers is available in EnergyPlus through two different modelling approaches. The first involves a layer-by-layer analysis (Finlayson et al. 1993), integrated into the time-step simulation engine, of the layers which comprise the complex fenestration construction. The second simplifies the calculations by initializing the glazing construction as an equivalent single layer (Arasteh, Kohler and Griffith 2009) by means of the layer-by-layer analysis, or the first approach.

EnergyPlus features the ability to select and modify glazing types, gas layers, frame properties, dividers and critically, shading devices. Shading device capabilities include drapery, roller shades, blinds as well as insect screens. These options are available for more complex analysis of window-shade constructions as per the layer-by-layer analysis.

Note that this method is only applicable to specular glazings. The simplified calculation will accept the effective construction U and SHGC indices to describe the window. This can be a valuable tool, given only the U-value and SHGC of a system at normal incidence as it decreasing calculation times from the multi-construction model. However, the simplified model inherently generates approximate effective system properties as the SHGC will not necessarily reflect angular properties of glazing layers nor accurately reflect the ratio of transmitted to absorbed solar radiation through the system.

2.4 WINDOW 6.3 and THERM 6.3 – Research Version

WINDOW 6.3 and THERM 6.3 are research development computer programs developed by the Lawrence Berkeley National Laboratories (LBNL) used in calculating total, center-of-glass and individual component window indices of merit including; U-value, solar heat gain coefficient ($SGHC$), shading coefficients, visible transmittance and percent relative humidity (R.H.) at which condensation will occur . System off-normal optical properties are determined from normal incidence properties via a 'matrix calculation engine' (Mitchell, et al. 2008). Heat transfer analysis can be performed based on the ISO 15099 standard and aid in the design and development of windows in research and teaching.

The shift from WINDOW 5 and THERM 5 to WINDOW 6 and THERM 6 has further provided the ability to model complex glazing systems or the modeling of shading devices. As with previous versions, WINDOW 6 and THERM 6 is still capable of calculating 2-D frame and edge effects with shading devices and the results can be viewed through a surface temperature map. Radiation is tracked using multi-band spectral analysis with the aid of the extensive Optic 5 glass database. There is also an interface to linking WINDOW and THERM results to DOE-2 and EnergyPlus.

2.5 eQUEST

eQUEST is a whole building performance analysis tool based on the popular DOE-2.2 simulation engine, widely recognized and used in building simulation today. The main feature of the eQUEST package is the wizards included. The eQUEST *Wizards* create a building model based on user defined building attributes, which eQUEST uses to determine building performance. The wizard's allow for users to define simplified models of buildings for quick analysis, or more complex models for more accurate results.

eQUEST is able to accurately predict the effects of fenestration systems including the addition of shading layers. This is achieved by either importing models from LBNL's window software to describe indices of merit and other fenestration system properties or by defining individual layers as per the National Fenestration Research Council (NFRC) or ASHRAE standards, see WINDOW documentation for further details. The result is a functional modelling tool for determining the effects window shading layers on the performance of a building. Further details can be found in the (eQUEST Introductory Tutorial, version 3.64 2010).

2.6 TRNSYS TRNBuild and Type 56

TRNSYS is a commercially available, graphical front-end, simulation software tool capable of modelling multi-zone buildings (TRNBuild and Type 56) with TRNSYS3D and Google SketchUp plug-in capability for creating 3-D models. Rather than having developed custom models for glazing performance, window details can be generated via LBNL's WINDOW 5.x software for use in TRNBuild and Type 56 analysis. Although this capability is designed for glazing systems only, the high dependency on the user to import indices of merit and other glazing system properties including fraction of absorbed radiation, $SGHC$ and U-value allows for the potential capability of modelling glazing and shading systems in TRNBuild and Type 56. See WINDOW documentation for further details.

2.7 WIS version 3.0.1 SP 2

WIS is a multi-purpose European software tool which is a product of the WinDat European thermal Network, and developed closely with the CEN (Comité Européen de Normalisation – European Committee for Standardisation) e.g. (EN 13363-2 E 2004, ISO 15099 2003, EN ISO 10077-1 2000, EN 410 1998 and EN 673 1997). WIS is used in determining thermal and solar characteristics of window systems and window components. This is achieved with the aid of a database of window components and properties as well as routines capable of calculating thermal and optical interactions between them. Based on European standard calculations, window properties can be determined for innovative and customized products. This open and object-oriented, user-friendly tool is available for use by both industry and researchers.

Thermal and solar performance is based on a number of assumptions concerning the layers and surrounding environment as a function of conduction, convection and thermal radiation through glazing layers, fill gas and shading layers. The resulting indices of merit include geometric factors, U-value, solar factor (G-value) and multi-spectrum transmittance for multi-glazing and shading constructions, the frame and edge of glass. Shading effects are determined via ray tracing models for pleated drapes and venetian blinds, roller blinds and screens.

2.8 California Simulation Engine

The California Energy Commission (CEC) maintains and develops a residential standard compliance simulation tool called the California Simulation Engine (CSE) and is supported by the California State-wide Utilities Codes and Standards Program. It is expected to quantify the effects of solar gain, thermal mass and ventilation on building performance. The CSE will achieve this through detailed modelling of opaque surfaces, radiant and convective heat transfer analysis at each surface, infiltration, ventilation and HVAC flows. Additionally, it utilizes ASHWAT fenestration system modelling capabilities for hourly variable analysis through recent work by Wright et al. (2011). The introduction of window modelling constituted a complicated coupled heat balance between the fenestration system and the building presenting computationally intense simulation. However, it was found that indices of merit could be determined at less frequent intervals, pertaining particularly to solar angle and changes in shade geometry, utilizing the thermal network theory (Wright 2008) to calculate the indices of merit for a time interval and to use these indices to replace a complex thermal resistance network with a simple three-node network. This method allows for the generality needed to obtain computational speed while offering the detailed needed to accurately predict the building performance.

Chapter 3

Monte-Carlo Ray Tracing Analysis of a Pleated Drape

Monte Carlo (MC) Methods can be used to solve non-deterministic systems. Utilizing a probability based "hit-and-miss" approach; Monte Carlo simulations are capable of representing a large array of systems, from simple to complex, with foreknowledge of the system boundary conditions. The application of interest to this research is ray tracing, modelling random specular and diffuse interactions at the shading layer. A comparison of methods used in the determination of effective optical properties for shading layers determined by the Kotey view factor models and those determined by ray tracing via Monte Carlo methods is presented and discussed in this chapter.

Kotey et al. (2007) developed simplified models to calculate effective solar optical properties of a drapery for incident beam and diffuse radiation. Modeled as a series of uniform rectangular pleats, the effective optical properties of the drapery layer are functions of the drapery geometry, fabric optical properties and the profile angle of solar radiation. The fabric was assumed to transmit and reflect any incident beam radiation diffusely. Kotey (2009) extended this model to account, in particular, for fabric properties as a function of incidence angle and allow for beam transmission through openings. The effective beam-beam and beam-diffuse properties are determined by tracking both radiation components for a given incidence angle through the various interactions that occur with the fabric pleats. The diffuse-diffuse component is evaluated using a net-radiation analysis with conventional shape factors to track radiant exchange between surfaces. This method of analysis provides the means for determining the effective layer properties of a pleated drape made of practically any fabric as a function of incidence angle.

Little research has since been published in the study of draperies; however the work of Farber et al. (1963) is of particular interest as it includes effective solar optical properties for drapery layers. Using a simple rectangular geometry, Farber et al. assume a fabric to be diffusely reflecting and diffusely transmitting and that reflectance and transmittance were a function of incidence angle. Farber et al. (1963) used the published results of Sparrow and Johnson (1962) to determine effective reflectivity of the cavity portion of the drapery. However, there are limiting assumptions made in the Sparrow and Johnson (1962)

model; without explanation the off-normal transmittance of a pleated drape follows the same pattern as the off-normal reflectance, and the drapery groove is infinitely deep. Pennington et al. (1964) mentioned that as a result, the Farber et al. model was unable to account for the effect of pleating on the effective solar optical properties when solar radiation is at normal or near normal incidence. Still, the front facing and cavity portions of the drapes were treated separately and subsequently averaged to determine effective layer properties.

Pennington et al. (1964) further performed a series of experiments to validate the theoretical analysis of Farber et al. (1963) using an outdoor solar calorimeter. With a pyrheliometer installed in the calorimeter, the solar optical properties of fabrics, draperies and glass-drapery combinations were examined as a function of incidence angle. Particularly, regarding pleated drapes, Pennington et al. found good agreement in the transmittance model, however the reflectance and absorptance did not agree. The discrepancy was likely a result of, amongst other assumptions, the Sparrow and Johnson (1962) model of the groove portion of the drapery. Nonetheless, the results of Kotey (2009) were compared with those of Farber et al. (1963) and can be found in Chapter 8 of (Kotey 2009). In general, given the limitations discussed in the Farber et al. model, agreement was good. Discrepancies in the various comparisons are most likely associated with the inability of the Farber et al. model to account for openness.

Still, little experimental validation of pleated drape models exists; including a solar calorimeter experiment performed at the National Solar Test Facility (NSTF), see Section 5.1.1 for details. The results of this experiment show that a model of the entire fenestration system was able to closely predict the actual performance of the system. However, the shading device layer optical properties were not isolated in this experiment, and as a result, this study is being performed to give further confidence to the view factor approach to modelling pleated drapes.

The material optical properties determined experimentally by Kotey will be used as the bounding conditions in the Monte Carlo analysis. Though Monte-Carlo methods are less computationally efficient than conventional modelling techniques, the results are expected to improve the accuracy of the effective shading layer optical properties determined by Kotey's models by eliminating the assumptions which allow the view factor or net reduction methods to be completed in a practical amount of time. Only the pleated drape model will be studied as it is the most intricate model with geometrical detail in addition to off-normal material properties being considered.

3.1 Fabric Properties - Keyes Universal Chart

The following description is paraphrased from (Kotey 2009).

Fabrics are made up of strands of yarn which are woven or knitted together. Further, the yarn is made of fibres which are twisted or plied together. The yarn can be loosely or tightly woven or knitted which can result in varying amounts of open area for light to be directly transmitted. Keyes (1967) characterised fabrics by yarn colour as Dark (D), Medium (M) and Light (L), and by weave as open (I), semi-open (II) and closed (III), see Figure 3.1. The horizontal axis is the fabric reflectance at normal incidence, $\rho_{bt}^{m}(\theta = 0)$ and the vertical axis represents the fabric beam-total transmittance at normal incidence, $\tau_{bt}^{m}(\theta = 0)$. Both these values are readily available or easy to obtain from manufacturers. The fabric transmittance, τ_{bt}^{m}, is the total amount of incident beam radiation which is transmitted through the drapery fabric. The superscript "m" is a reminder that the topic is the fabric or "material", not the pleated drape. A portion of this radiation encounters the layer structure, and is either absorbed, scattered back, ρ_{bd}^{m}, or scattered in the forward direction, τ_{bd}^{m}. The subscript "d" indicates the subsequent assumption that these scattered components are diffuse. The remaining undisturbed portion is defined as the beam-beam transmittance (or specular transmittance), τ_{bb}^{m}. It was shown experimentally that shading layers exhibit no specular reflection, so $\rho_{bb}^{m} \approx 0$, therefore $\rho_{bd}^{m} = \rho_{bt}^{m}$. Knowing $\tau_{bt}^{m}(\theta = 0)$ and $\rho_{bt}^{m}(\theta = 0)$, it is possible determine the location of the fabric on the chart. However if this information cannot be obtained, it is also possible to less accurately predict the location of the fabric on the chart by approximating the $\tau_{bb}^{m}(\theta = 0)$ = openness, and the $\rho_{bt}^{y}(\theta = 0)$. The "y" denotes yarn optical properties. Keyes chart accounts for all possible fabric materials in the nine possible designations used to describe the various samples, three of which are compared in this study; dark, medium and light draperies.

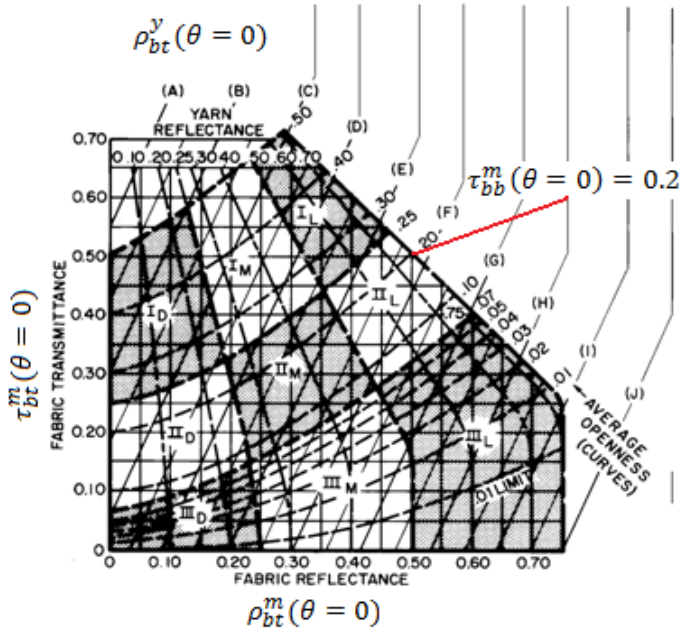

Figure 3.1 - Keyes Universal Chart (ASHRAE 2005)

3.2 Assigning Drape Fabric Off-Normal Properties

The modelling of off-normal solar optical properties of drapery fabrics, with properties denoted by superscript *m*, is critical in the modelling of the effective solar optical properties of the pleated drape layer. Kotey (2009) developed an approach to classify and then determine the off-normal solar optical properties of drapery fabrics, roller blinds and insect screens. The following equations were used to determine the material optical properties of drapery fabrics as a function of incidence angle of oncoming radiation. Refer to Chapter 4 of (Kotey 2009) for further details.

3.2.1 Incidence Angles

The incidence angles as a function of solar profile angle are determined by the following,

$$\cos(\theta_{PARL}) = \cos[\tan^{-1}(\tan\Omega_{\mathrm{V}}\tan\Omega_{\mathrm{H}})] * \cos\Omega_{\mathrm{H}} \tag{3.1}$$

$$\cos(\theta_{PERP}) = \cos[\tan^{-1}(\tan\Omega_{\mathrm{V}}\tan\Omega_{\mathrm{H}})] * \sin\Omega_{\mathrm{H}} \tag{3.2}$$

Where θ_{PARL} refers to the incidence angle on a surface parallel to the face of the drape, and θ_{PERP} is perpendicular to the face of the drape.

3.2.2 Beam-Beam Transmittance

First the yarn reflectance, ρ^{y}, was determined,

$$\rho^{y} = \frac{\rho_{bt}^{m}(\theta = 0)}{1 - A_{o}} \tag{3.3}$$

A normalizing factor for material beam-beam transmittance is used to determine off-normal properties,

$$norm\tau_{bb}^{m} = \frac{\tau_{bb}^{m}(\theta)}{\tau_{bb}^{m}(\theta = 0)} = cos^{b1}(\theta) \tag{3.4}$$

where,

$$b1 = Max\{-\frac{1}{2}\ln\,(Max\{\tau_{bb}(\theta = 0),0.01\},0.35\} \tag{3.5}$$

so,

$$\tau_{bb}^{m}(\theta) = \tau_{bb}^{m}(\theta = 0) * cos^{b1}(\theta) \tag{3.6}$$

3.2.3 Beam-Total Transmittance

Note that,

$$\tau_{bt}^{m}(\theta = 90^{o}) = \tau_{bd}^{m}(\theta = 90^{o}) = 0 \tag{3.7}$$

A normalizing factor for material beam-total transmittance is used to determine off-normal properties,

$$norm\tau_{bt}^{m} = \frac{\tau_{bt}^{m}(\theta)}{\tau_{bt}^{m}(\theta = 0)} = cos^{b2}(\theta) \tag{3.8}$$

where,

$$b2 = Max\{-\frac{1}{2}\ln\ (Max\{\tau_{bt}(\theta = 0),0.01\},0.35\} \tag{3.9}$$

so,

$$\tau_{bt}^{m}(\theta) = \tau_{bt}^{m}(\theta = 0) * cos^{b2}(\theta) \tag{3.10}$$

3.2.4 Beam-Diffuse Transmittance

The fabric has no specular reflection, so,

$$\tau_{bd}^{m}(\theta) = \tau_{bt}^{m}(\theta) - \tau_{bb}^{m}(\theta) \tag{3.11}$$

3.2.5 Beam-Total Reflectance

Recall that,

$$\rho_{bt}^{m} = \rho_{bd}^{m} \tag{3.12}$$

where,

$$\rho_{bt}^{m}(\theta = 90^{o}) = \rho_{bt}^{m}(\theta = 0)(1 - \rho_{bt}^{m}(\theta = 0)) * (0.7(\rho^{y})^{0.7}) \tag{3.13}$$

a normalizing factor for material beam-total reflectance is used to determine off-normal properties,

$$norm\rho_{bt}^{m} = \frac{\rho_{bt}^{m}(\theta) - \rho_{bt}^{m}(\theta = 0)}{\rho_{bt}^{m}(\theta = 90^{o}) - \rho_{bt}^{m}(\theta = 0)} = 1 - cos^{b3}(\theta) \tag{3.14}$$

where,

$$b3 = 0.6$$

or,

$$\rho_{bt}^{m}(\theta) = \rho_{bt}^{m}(\theta = 0) + (\rho_{bt}^{m}(\theta = 90) - \rho_{bt}^{m}(\theta = 0)) * 1 - cos^{b3}(\theta) \tag{3.15}$$

The only input values required for this analysis are $\tau_{bt}^{m}(\theta = 0)$ or $\tau_{bb}^{m}(\theta = 0)$ (or openness) and $\rho_{bt}^{m}(\theta = 0)$, which can easily be determined.

3.2.6 Diffuse-Diffuse Optical Properties

Due to the nature of ray tracing, the diffuse-diffuse models can be neglected as diffuse properties can be determined by beam analysis. Figure 3.2 and Figure 3.3 describe the geometry and terminology used, where the fabric surface properties are a function of drape fabric properties and incidence angle on that surface. The effective drape solar optical properties are a result of the Monte-Carlo analysis.

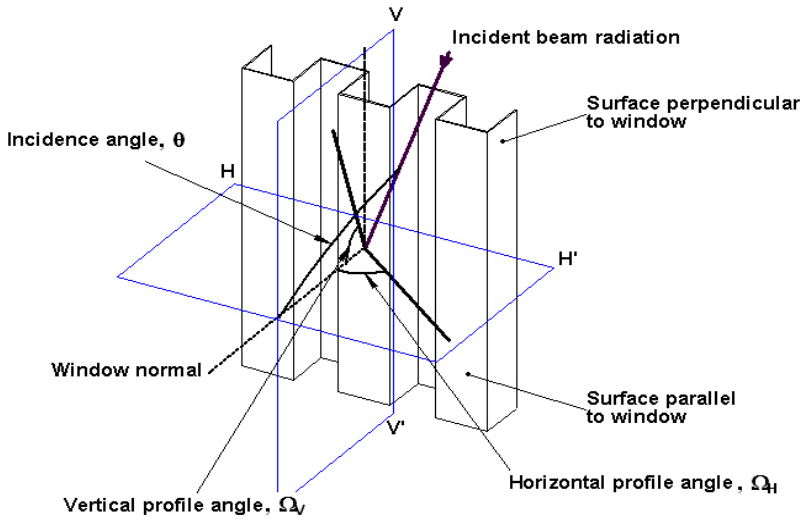

Figure 3.2 - Configuration of Drapery Model with Solar Angles

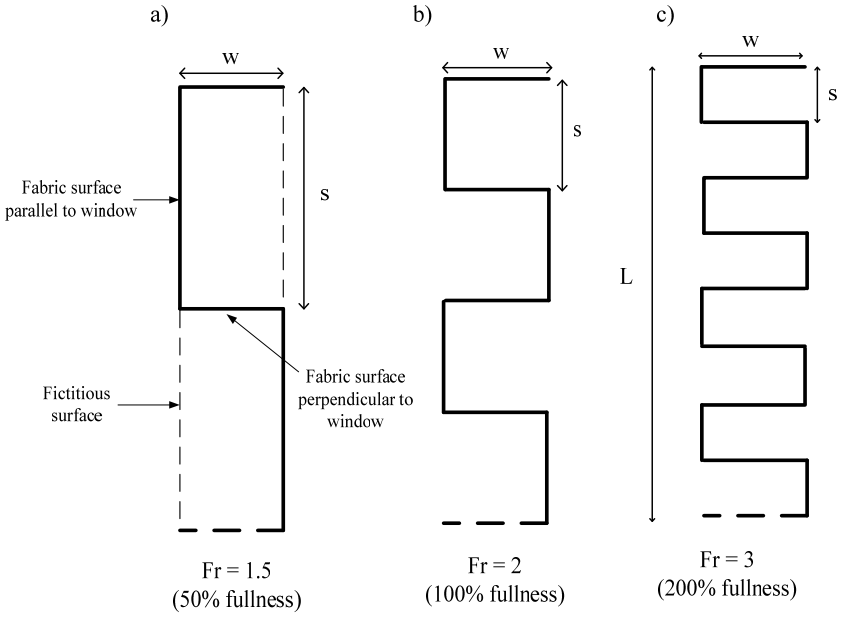

Figure 3.3 - Cross-Section of Drapery Pleats with a Variety of Folding Ratios and Percent Fullness - Reproduced from (Kotey 2009)

By determining the material properties of the drapes, Monte-Carlo simulation can then be implemented to determine the effective properties of the drapery layer as a whole.

3.3 Monte Carlo Framework

The Monte-Carlo simulation was developed by modeling the drape surface as a control volume of infinite length. A seven-surface enclosure was designed to simulate a drape layer of infinite length (see Figure 3.4). The black lines represent the surfaces of the drapery fabric while the dash-dot lines represent imaginary surfaces which are used to complete the enclosure for Monte-Carlo simulation. Note surfaces one and five, for example. Beam transmission through surface one reappears at surface five, thus analogizing a drapery layer of infinite length.

Each surface in the layer is modeled as a parametric vector, and each ray of solar radiation is also modeled with a vector. Through geometric analysis, the intersection of the two lines can be determined giving the resulting vector. To make the system as non-specific as possible, maximizing modularity, a basic formula is used to determine the scalar of the vector component of both the surface and the ray, this means calculating the resulting vectors at all surfaces, then determining which of these results is the one which would actually occur in the given situation.

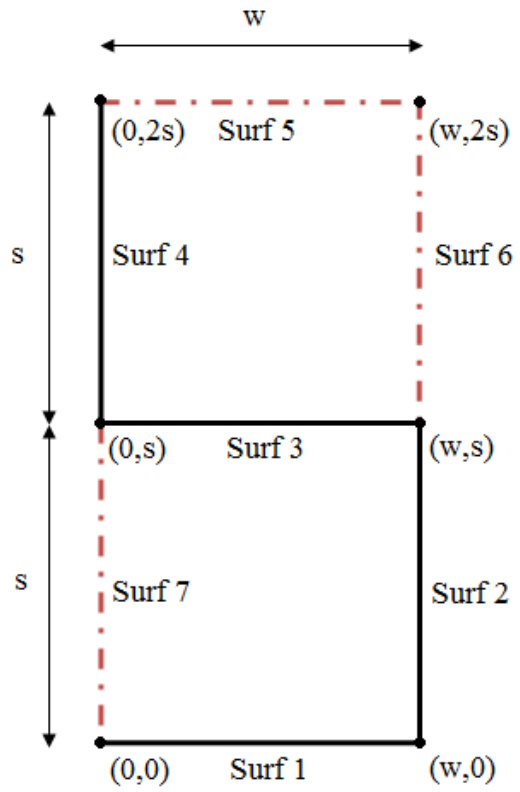

Figure 3.4 - 7-Surface Enclosure Model Describing Pleated Drape Surfaces

3.4 Governing Equation

The following equation is the general expression used for resolving the two vector scalar quantities for the ray and for each surface:

$$\left(x_{0_{surf}}\hat{\imath} + y_{0_{surf}}\hat{\jmath}\right) + s\left(x_{1_{surf}}\hat{\imath} + y_{1_{surf}}\hat{\jmath}\right) = \left(x_{0_{ray}}\hat{\imath} + y_{0_{ray}}\hat{\jmath}\right) + t(x_{1_{ray}}\hat{\imath} + y_{1_{ray}}\hat{\jmath}) \tag{3.16}$$

Where,

$\left(x_{0_{surf}}\hat{\imath} + y_{0_{surf}}\hat{\jmath}\right) = surface\ origin\ position\ vector$

$s = scalar\ product\ of\ surface\ direction\ vector$

$\left(x_{1_{surf}}\hat{\imath} + y_{1_{surf}}\hat{\jmath}\right) = surface\ direction\ vector$

$\left(x_{0_{ray}}\hat{\imath} + y_{0_{ray}}\hat{\jmath}\right) = ray\ origin\ position\ vector$

$t = scalar\ product\ of\ ray\ direction\ vector$

$\left(x_{1_{ray}}\hat{\imath} + y_{1_{ray}}\hat{\jmath}\right) = ray\ direction\ vector$

The *s* and *t,* surface and ray scalar, quantities are found at each surface having two equations and two unknowns. Only the surfaces returning parametric vectors with scalar quantities between 0 and 1 are considered. In the case that two surfaces are hypothetically struck by the ray, the smaller *t*, ray scalar, quantity indicates which surface is struck first. Since In the given seven-surface geometry, a maximum of two results will ever be found per beam emission, making this a relatively quick process. The solar interaction is then determined.

3.5 Determining Surface Interactions

The Monte Carlo method applies when determining the probable surface interaction the ray experience when a surface is struck. The drapery fabric is described to have a certain absorptance, transmittance and reflectance at normal incidence, each a dimensionless quantity, of which the sum for a surface or object is unity.

For each ray that is emitted, the process remains the same on interaction with a surface; the ray is subject to a probable chance of being absorbed, reflected or transmitted, which is a function of a random number between zero and one - generated at the time of contact. To explain when one of the three interactions

occur, an example is described: the dark fabric described in Table 3-1 below would transmit the ray if the random number generated was between 0.00 and 0.14, it would reflect if the number was between 0.14 and 0.49 and it would absorb the ray if the random number generated was between 0.49 and 1.00. A physical representation of this process is presented in Figure 3.5, at point 1, the ray initially intercepts the pleated drape's fabric, it is transmitted through and intercepts the drape again at point 2, where the beam is transmitted again to point 3 where the beam is reflected diffusely out of the system.

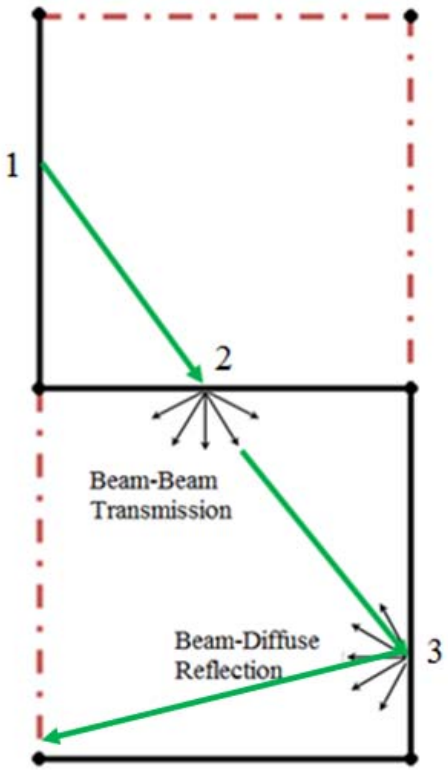

Figure 3.5 - Illustration of Possible Surface Interactions

3.6 Monte-Carlo Algorithm

The following Figure 3.6 outlines the algorithm used in the Monte-Carlo analysis of drapery fabrics. (See Figure 3.6 for further details). Each ray is emitted from a random point outside of the drape enclosure assuming a constant solar incidence angle defined by its vertical component, Ω_V and its horizontal component, Ω_H. When the ray hits a surface, an interaction occurs, where the general expression is used to determine the location of the ray and the surface it struck. Based on the angle of incidence, material off-normal optical properties are used to determine the probability of ray absorptance, transmittance or reflectance (see Section 3.2 and Figure 3.5). If the ray is not; absorbed, transmitted through the drape to the interior of the system, or reflected to the exterior of the system, then the process repeats until one of these things occurs.

3.7 Testing

The baseline for comparison is the system used in Kotey et al. (2009). Kotey previously compared his view factor model results with that of Farber et al. (1963). The comparison included the analysis of a tan, grey and white drape.

The vertical profile angle (Ω_V) was set at zero so the solar optical properties are described only as a function on the incoming horizontal profile angle (Ω_H). The same geometric properties are assumed and the equations for determining off-normal solar optical fabric properties defined by Kotey et al. (described in Section 3.2 above) are used.

3.7.1 Fabric Solar Optical Properties

The fabric solar optical properties at normal incidence used to produce Figure 8.12 in (Kotey 2009) are listed in Table 3-1. These values correspond to the fabrics initially used by Farber et al. (1963) and subsequently in Kotey (2009), the same values were used in this study. Each level of yarn reflectance (light, medium and dark) defined by Keyes was tested at semi-openness.

Table 3-1 - Solar Optical Properties of Fabric at Normal Incidence (Kotey 2009, Table 8.2)

Fabric Description	Transmittance (τ^m_{bt})	Reflectance (ρ^m_{bt})	Absorptance (α^m_{bt})	Openness (τ^m_{bb})
Dark Coloured (IID)	.14	.35	.51	.03
Medium Coloured (IIM)	.23	.30	.47	.12
Light Coloured (IIL)	.35	.39	.26	.16

The effective solar optical properties of a dark, medium and light drapery analyzed in (Kotey 2009) are presented in Figure 3.7, Figure 3.8 and Figure 3.9. The “m” superscript characterizes the material, or fabric, optical properties of the layer. The properties without superscripts represent the effective layer optical properties of the respective coloured drapes. Consequently, the layer effective optical properties are compared in this study.

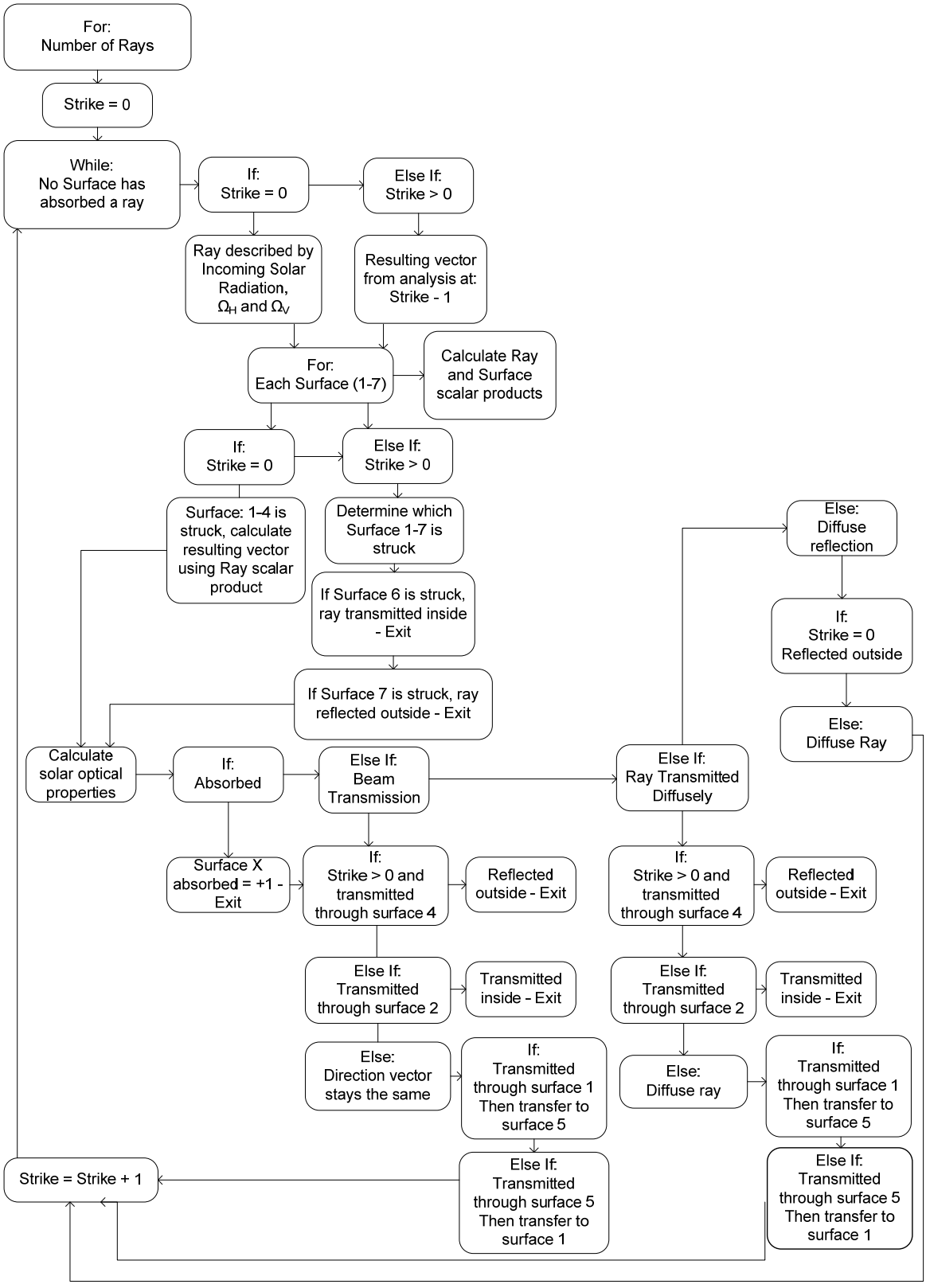

Figure 3.6 - Structure of Program Algorithm for Determining Total Solar Optical Properties

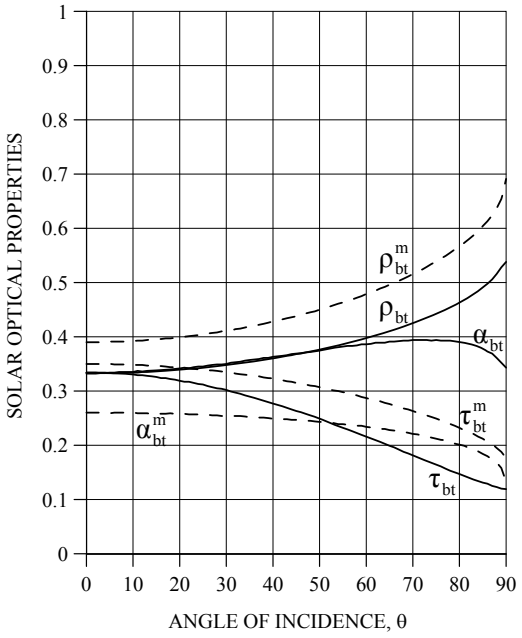

Figure 3.7 - Solar Properties or Pleated Drapes and Fabrics versus Incidence Angle ($\Omega_V = 0$ and $\Omega_H = \theta$) for Dark Coloured Drapes – Reproduced from (Kotey 2009)

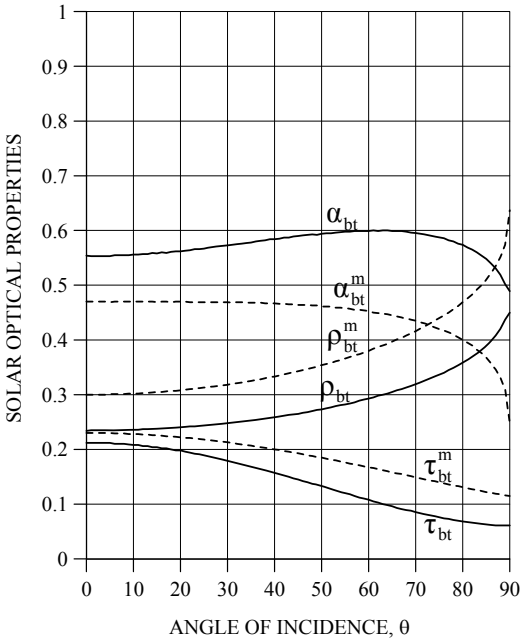

Figure 3.8 - Solar Properties or Pleated Drapes and Fabrics versus Incidence Angle ($\Omega_V = 0$ and $\Omega_H = \theta$) for Medium Coloured Drapes – Reproduced from (Kotey 2009)

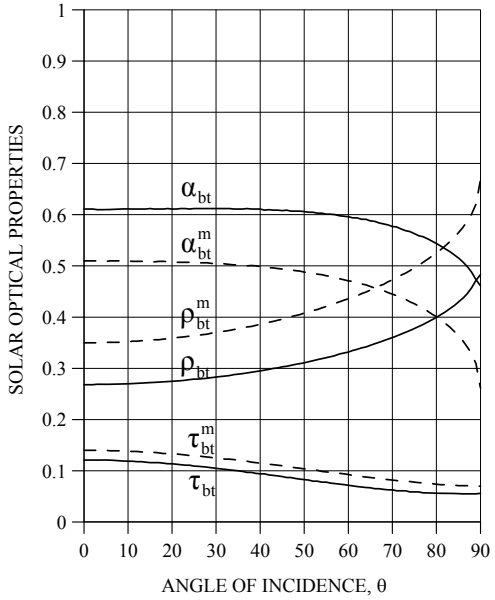

Figure 3.9 - Solar Properties or Pleated Drapes and Fabrics versus Incidence Angle ($\Omega_V = 0$ and $\Omega_H = \theta$) for Light Coloured Drapes - – Reproduced from (Kotey 2009)

3.8 Results

Figure 3.10, Figure 3.11 and Figure 3.12 below illustrate the comparison between the Kotey et al. method of determining effective solar optical properties of drapes using View Factor analysis with those from Monte-Carlo simulation.

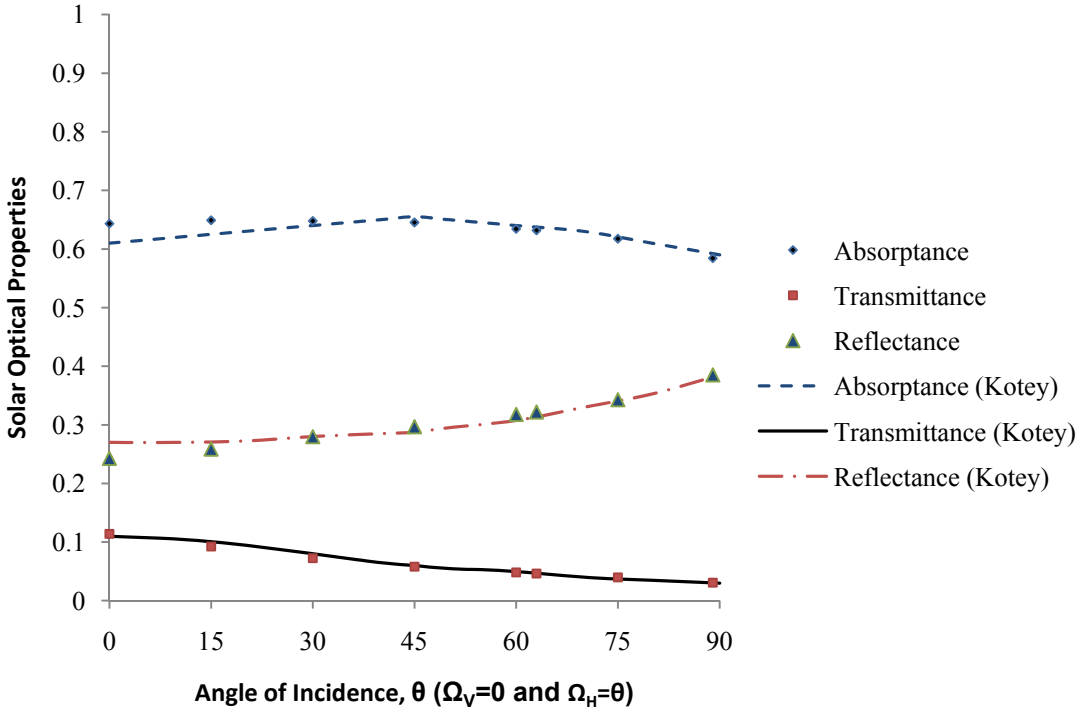

Figure 3.10 - Solar Optical Properties of Dark Coloured Drapes (Kotey taken from (Kotey 2009))

Initially a bundle size of 1000 rays in 30 trials produced a standard deviation greater than that produced with a random number generator. When the bundle size was increased to 5000, the accuracy improved by an average of 0.2 percent, from 0.3 to 0.1 percent variance. When the bundle size was increased to 10000, there was a negligible difference.

The standard deviation of the mean was calculated by, $SD_{\overline{x}} = \frac{\sigma}{\sqrt{n}}$, further details found in Appendix B.

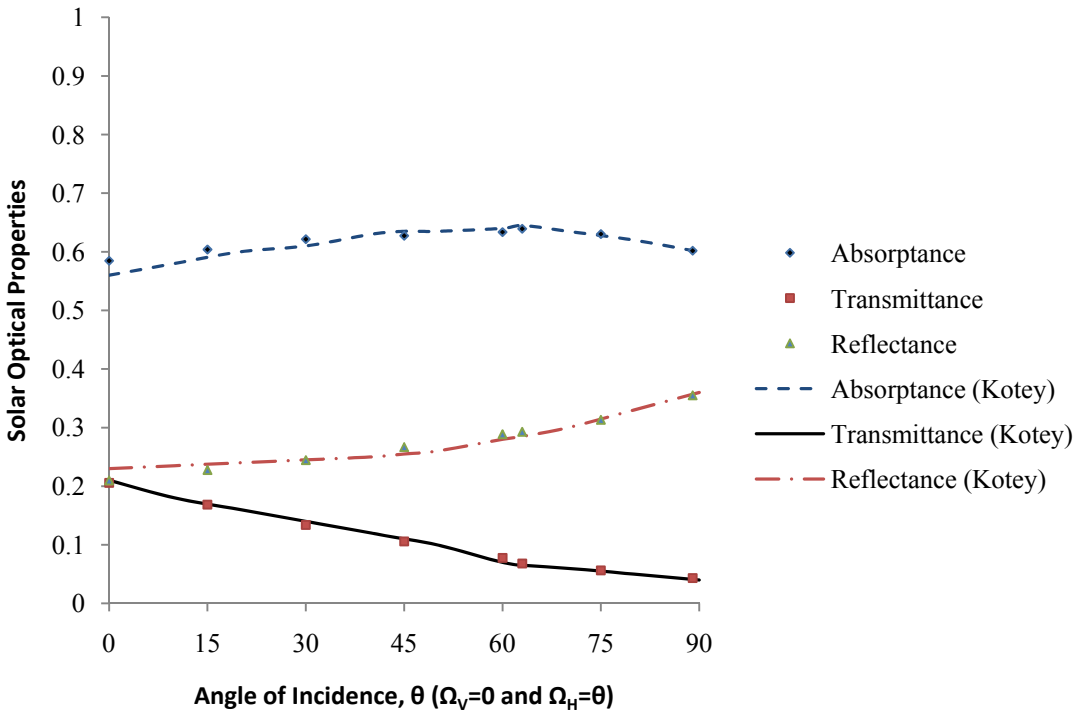

Figure 3.11 - Solar Optical Properties of Medium Coloured Drapes (Kotey data taken from (Kotey 2009))

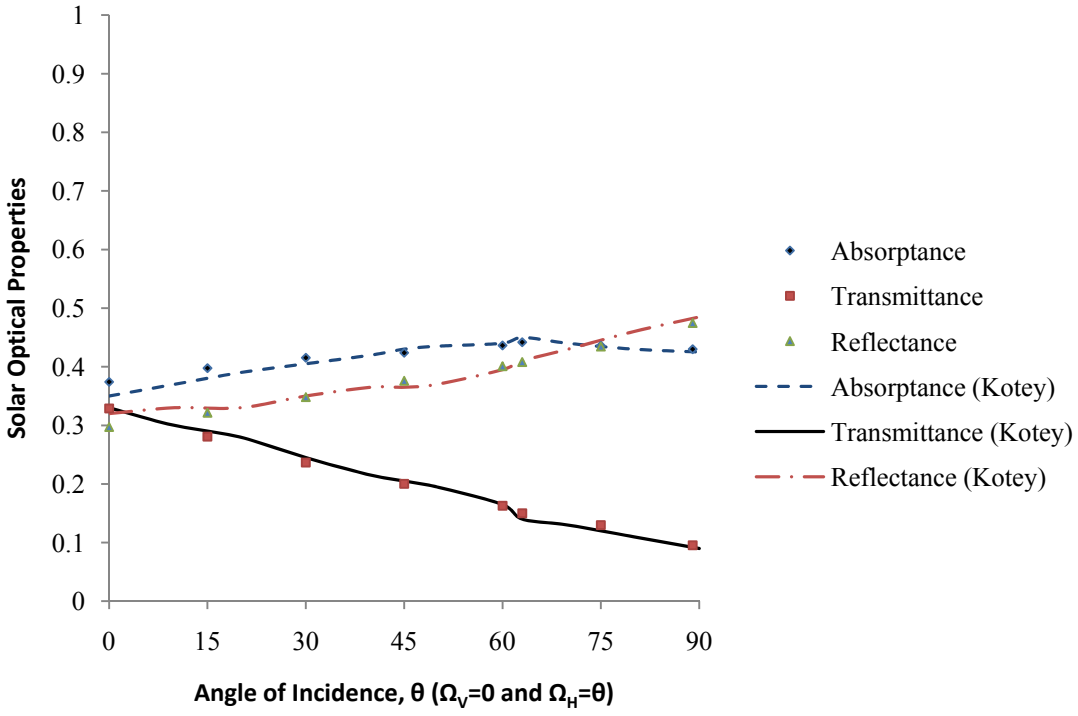

Figure 3.12 - Solar Optical Properties of Light Coloured Drapes (Kotey data taken from (Kotey 2009))

3.8.1 Comparison of Results

A model to calculate the effective solar optical properties of pleated drapes using Monte Carlo ray tracing methods has been presented. The objective of this study was to give further confidence the view factor approach to determining layer effective optical properties presented in (Kotey 2009), of which were implemented in ESP-r. Experimental validation of pleated drape properties has been established through a full complex fenestration system analysis at the NSTF, however the effective optical properties of the pleated drape was not looked at. Though the Monte Carlo analysis is not experimental validation of the models, it alleviates the assumptions made by the view factor method which allow it to be computationally efficient, thereby providing an extra degree of accuracy. Based on the drapery fabric optical property models presented in (Kotey 2009), and assuming the same uniform rectangular pleat representation of a drapery, a comparison of the two models was performed. The results presented in Figures 3.10-3.12 show that the data points at each incidence angle for which the effective optical properties were within two percent of each other. As a result, it can be said that the view factor method, given the improved computational efficiency, provides sufficient accuracy for modelling purposes.

Discrepancies could possibly be accounted for by the different approach the respective models take in dealing with diffuse radiation. Where the Monte Carlo analysis tracks a beam, either as a beam interaction or as a diffuse interaction until it is absorbed, the view factor model of Kotey only allows a beam transmission for the first interaction, and assumes diffuse transmission in subsequent interactions. However, this is a minor discrepancy and it can be concluded that the Monte Carlo analysis gives confidence to the view factor model presented in (Kotey 2009) based on these results.

The CPU time required for the increase from 1000 bundles to 5000 bundles increased significantly, going from ~30 seconds to ~500 seconds. The increased bundle size resulted in a decrease of the standard deviation by .2 percent and the optical properties changing in the tenths of a percent, though it can't be said for certain this is a negligible difference depending on the intended use.

Since the governing equation of the model is defined by the intersection of two lines, the surface definition can easily be changed to better define the shape of a pleated drape. By redefining the surface, for example as a wave function, it might be possible to return an even more accurate value of the solar optical properties a pleated drape exhibits.

Chapter 4

Implementation of New Shading Models to ESP-r

ESP-r is a comprehensive building simulation software built with the purpose of integrating all relevant building component processes including; thermal processes, inter-zone airflow, intra-zone airflow, HVAC and electrical power flow, etc. ESP-r employs a partitioned solver approach, where each domain is solved individually then passed to a global solver, see Figure 4.1. for building design and analysis. Since the software was first designed in the 1970s, it has been made readily available, at no expense, with an open source license, and has since been under constant development. ESP-r was established as a research and teaching tool, however it is now being implemented as a consulting tool used by engineers, architects and building designers (Crawley, et al. 2005). ESP-r is actively supported by users and developers producing training courses and tutorials, a developer's guide, support and validation, see (ESP-r 2011). The Complex Fenestration Construction (CFC) module is a subcomponent of the thermal analysis domain. Similar to how the airflow and thermal process are analysed first then put into a global solver, the CFC module is run externally from the thermal analysis until an input is required for the fenestration system. This section will provide a brief overview of the ESP-r thermal simulation methodology, and further expand into the CFC module methodology.

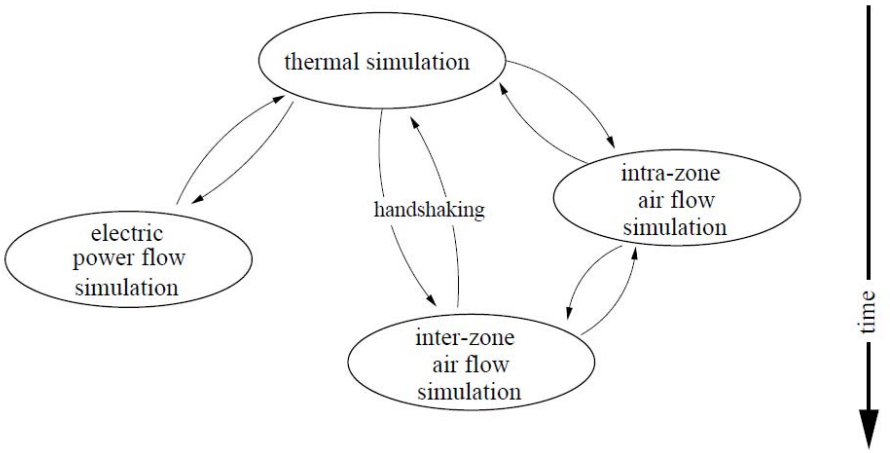

Figure 4.1 - Handshaking between Partitioned Solvers - From (Beausoleil-Morrison 2000)

4.1 ESP-r Thermal Model – Finite Control Volume Heat Balance

The methodology described here and in the subsequent subsections is a brief summary of the work presented in (Lomanowski 2008, Clarke 2001 and Beausoleil-Morrison 2000).

ESP-r is based on the discritization of building components by finite-difference control volumes used in the formulation of a heat balance from which numerical solutions can be generated. These balances represent the thermal interaction between a node and the adjacent nodes linking the heat flow over time and space. For example, Figure 4.2 illustrates a discretized system where element I is in thermal communication with elements 1-3.

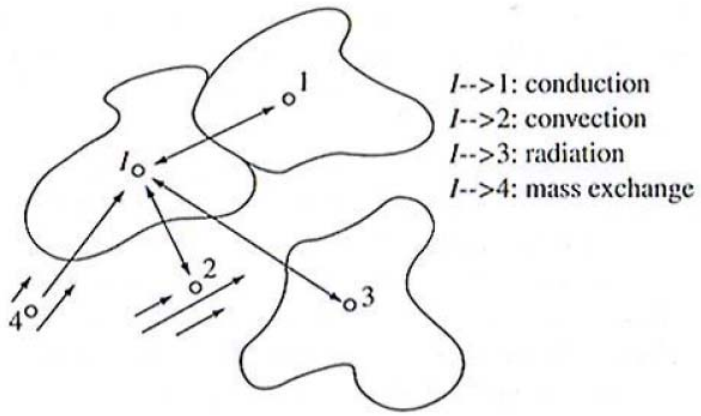

Figure 4.2 - Energy Flow between Nodes in a Discretized System - From (Clarke 2001)

Evaluation of the heat exchange through layers can be quite complex, and can be further complicated by factors like multi-dimensional heat flow and moisture. Therefore ESP-r characterizes materials with effective thermal conductivities to reduce the problem to a one dimensional conduction problem.

The heat balance for the intra-constructional layer element node I's control volume can simply be described as,

$$\left\{\begin{matrix} storage\ of \\ heat\ in\ CV \end{matrix}\right\} = \left\{\begin{matrix} net\ conduction \\ into\ CV \end{matrix}\right\} + \left\{\begin{matrix} source\ of\ heat \\ within\ CV \end{matrix}\right\} \quad (4.1)$$

4.1.1 Multi-Layer Constructions

Layers are stacked together to produce what is known as a multi-layer construction (MLC).

The heat balance for a surface node, for example at node 1 or S_i in Figure 4.3, becomes slightly more complex with the addition of radiative and convective terms,

$$\begin{Bmatrix} storage\ of \\ heat\ in\ CV \end{Bmatrix} = \begin{Bmatrix} net\ conduction \\ into\ CV \end{Bmatrix} + \begin{Bmatrix} source\ of\ heat \\ within\ CV \end{Bmatrix} + \begin{Bmatrix} net\ longwave \\ radiation \\ into\ CV \end{Bmatrix} + \begin{Bmatrix} net\ convection \\ into\ CV \end{Bmatrix} \quad (4.2)$$

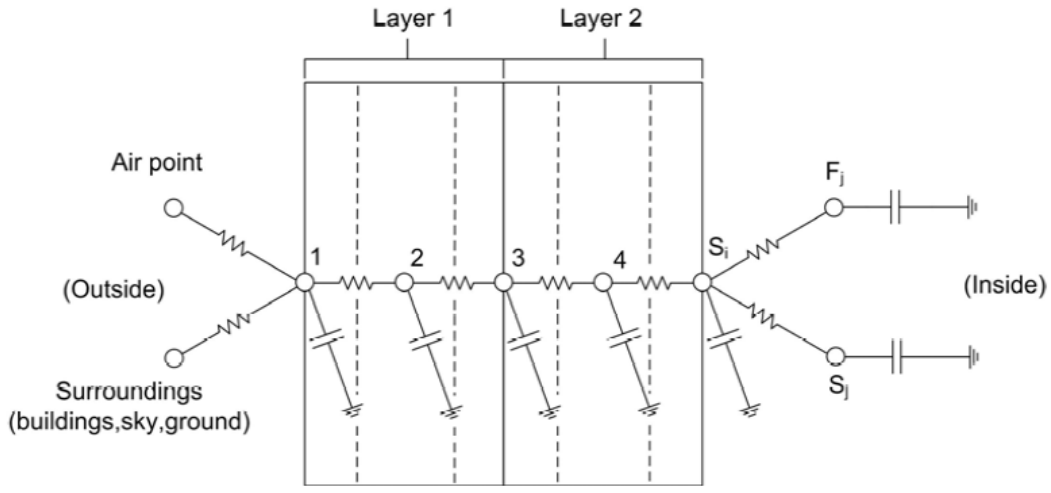

Figure 4.3 - Multi-Layer Construction Nodal Scheme - From (Lomanowski 2008)

ESP-r then employs the Crank-Nicolson difference formulation for each node to evaluate the energy balance numerically, where past, future and present time-row terms are coupled to evaluate the future time-row. To preserve computational efficiency, constraints were placed on MLC analysis which limit it to handling only opaque layers, and communication with adjacent nodes. Without the ability to account for transparent layers or jump resistors, it is not suitable for the analysis of (complex) fenestration constructions.

4.1.2 Transparent Multilayer Constructions

The following is a summary of transparent multilayer constructions (TMC) in ESP-r. Detailed analysis can be found in (Lomanowski 2008).

The TMC is an extension of the MLC designed with the intent to handle transparent layers, determining solar absorption and transmission on a time-step basis based on the sun's position. ESP-r allows a set of optical properties, one at normal incidence and five at off-normal incidence angles, to be associated with the TMC. By interpolating between these data points, the TMC can then determine the off-normal optical properties at each time step.

4.1.3 Simulation Flow

The flow of thermal zone simulation at each time-step is presented in Figure 4.4. No other domains are considered to interact with the thermal domain in this simplification. See (Lomanowski 2008) for further details.

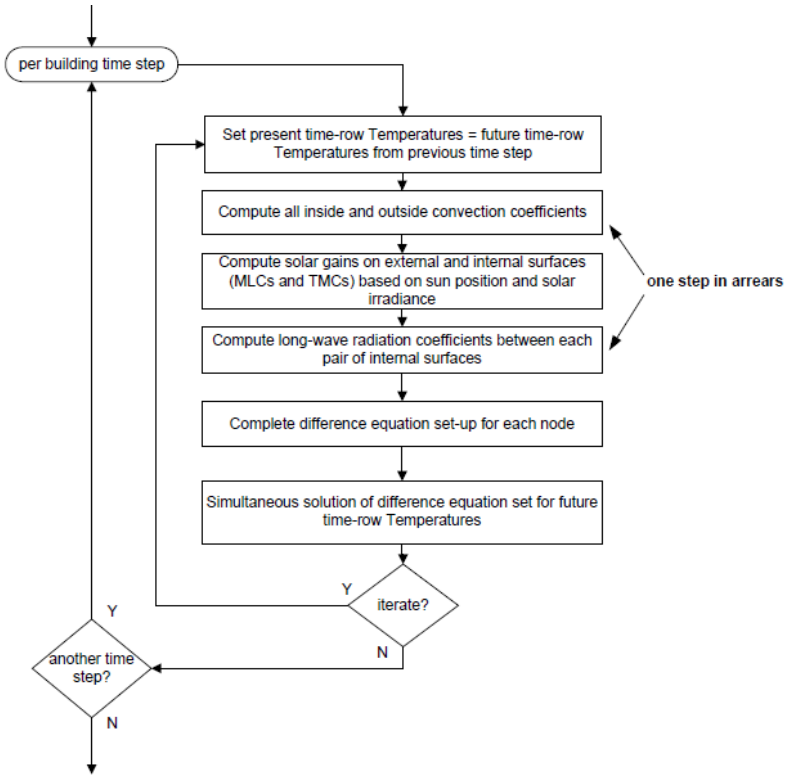

Figure 4.4 - Simplified ESP-r Thermal Zone Simulation Flow at Each Time-Step

– Reproduced from (Lomanowski 2008)

4.2 The Complex Fenestration Construction

The complex fenestration construction (CFC) was designed and implemented into ESP-r by Lomanowski (2008). The following is a summary of the CFC module, the details of which are provided in (Lomanowski 2008).

The shortcomings of the MLC and TMC modules are that the former can only handle opaque materials, while the latter can only handle transparent layers. CFC is a self-contained module designed with the intent of handling the analysis of multi-layer glazing systems with attached shading devices (i.e. calculating solar properties and heat transfer). However, the shading models which were implemented in ESP-r were not specifically designed for this purpose. As a result, the CFC was designed to treat the fenestration systems as a black box, handling the inputs for shading device models as well as ESP-r

boundary conditions and the analysis and communication of the results to ESP-r. This modular approach allows for additional shading device models to be handled with relative ease.

4.2.1 Solar Processing

The CFC is further capable of handling dynamic control of shading devices. This requires solar optical analysis of each layer of the fenestration system at each time-step. Each layer in the CFC is characterized by the 12 effective material optical properties described in Section 1.3.1.2 above, returning a set of effective optical layer properties. Solar processing details can be found in (Lomanowski 2008).

4.2.2 Thermal Processing

When the solar processing of the fenestration system is complete, the resulting absorbed flux at each layer can be determined. This is returned to the nodal difference equations in the thermal heat balance, causing temperature elevations in the layer. It is them possible to determine the effects this will have on the resulting thermal processes, i.e. conduction, convection and radiation to adjacent layers and through jump resistors to non-adjacent nodes, see Figure 1.8. Thermal processing details can be found in (Lomanowski 2008).

4.3 Using the CFC module

Detailed instructions on the general application of the CFC types are referenced in detail in Appendix F of (Lomanowski 2008). Further, the use of the GSLedit tool (Wright et al. 2009), developed at the UW AGSL, which is used to create the input data for shading layers at normal incidence, is also described in (Lomanowski 2008).

GSLedit, or Glazing Shading Layer Editor, is a graphical user interface tool which accepts databases of fill gas, glazing and shading layer optical properties, and outputs them in a file which can then be read by other programs such as ESP-r. This allows for the quick construction of a fenestration systems and allows users to view and manipulate properties. Details on the use of the newly implemented shading models (i.e. roller blinds, pleated drapes and insect screens) are provided in (Kotey 2009).

Chapter 5

Preliminary Simulation - Testing Flat Shading Layer Configurations

It has been established that shading devices are an integral component in the control of solar heat gain and to improve thermal comfort. Further, windows represent one of the largest and most variable sources of heat gain, having a major influence on the energy consumption and peak cooling load of a building. It stands to say that the appropriate configuration and application of shading devices can be used advantageously to reduce the energy consumption of a building.

Having undergone several levels of testing, the CFC capability and operable venetian blind shading layer models incorporated by Lomanowski (2008) provided valuable capabilities to building simulation. Slat-type shades can be placed on the indoor side, between-panes or on the outdoor side. The opportunity to adjust slat angle at the time-step level is especially useful. Efforts in this research comprised a follow up to the work of Lomanowski (2008) with the implementation of the roller blind, pleated drape and insect screen models to ESP-r.

A logical approach to the preliminary analysis of the newly implemented model functionalities was a comparison of the performance of flat shading devices. Using a venetian blind at high slat angle as a metric, the performance of the roller blind and drapery fabric were compared; however the insect screen did not suit this test because each of the shading layers was required to have zero openness in order to mimic the venetian blind. Suitably, the building simulation used in (Lomanowski 2008) was replicated and the roller blind and drapery fabric subsequently replaced the venetian blind. The cooling demand and peak cooling load were used for comparison.

5.1 Background

The task of model validation is as important as the development of the model. Shading model development and validation are still in the early phases, and various organizations (e.g., TNO in the Netherlands, LBNL in the US, the Fraunhoffer Institute in Germany, Lund University in Sweden) have taken an active role in researching this topic. Although all the aforementioned organizations have contributed to the task, few measurements are available for comparison. However, a set of measurements

was made by the Swiss Federal Laboratories for Material Testing and Research (EMPA) for the analysis of venetian blinds, and has since been studied giving confidence to building simulations tools such as ESP-r (e.g. Lomanowski and Wright 2011, Lomanowski 2008) and EnergyPlus (Loutzenhiser et al. 2008).

The models presented in (Kotey 2009), which are the basis for the current ESP-r implementation, have been developed incrementally such that validation could occur at each phase of the project. Further, the AGSL has performed measurements on the heat gain through a complex fenestration, see (Kotey 2009) for further details. In doing so, a comprehensive set of reliable shading device models have been established. The convective heat transfer in glazing cavities is well understood, even considering a venetian blind in the cavity. However less is known about the convective heat transfer at shading attachments and this is a topic suitable for future research (Wright 2008).

5.1.1 Shading Device Model Validation

To accommodate the demand for empirical data to which the shading device models could be compared, experiments were performed at the indoor solar simulator and solar calorimeter at the National Solar Test Facility (NSTF), the details the experiments can be found in (Kotey 2009), while the NSTF details can be found in (CANMET 1993 and Harrison and Dubrous 1990). This measurement facility is capable of imposing a variety of weather conditions in a controlled environment including adjusting incident solar flux, indoor temperature, outdoor temperature and wind speed using a solar simulator arc-lamp, environmental chamber and variable speed fan. In return, the measurement apparatus is used to determine solar heat gain coefficient (SHGC), U-value and solar transmittance of the shaded or unshaded window.

A series of measurements were completed to examine the four shading layer types currently available in ASHWAT, which as previously discussed are identical to those used in ESP-r. Simulations using the same parameters as the NFRC test cell were then performed using ASHWAT for comparison. Figure 5.1 shows very good agreement with minimal discrepancies, in most cases well below 0.05, between the calculated and measured SHGC. Note that there is mild sensitivity with respect to the surface convection heat transfer coefficients. A comparison of U-value and transmission showed similar agreement, (Kotey 2009), giving confidence to the shading device optical models implemented in ESP-r.

At the Swiss Federal Laboratories for Material Testing and Research (EMPA) a test cell was established for the purpose of empirical validation of venetian blind shading layer models used in building energy simulation programs. Within the framework of the International Energy Agency (IEA), Loutzenhizer et al. (2006) conducted a series of experiments and took measurements for the purpose of empirically validating building energy simulation codes. (Loutzenhiser 2008) presents the results of an EnergyPlus

simulation comparison with the test cell measurements. Taking into consideration the complexities of appropriately modelling venetian blind slat optical and convective properties, and heat transfer between the shading devices and glazing surfaces, it was found that the mean differences between the simulation and measurement results were all within 6.1%, with the simulation under predicting measured results.

Lomanowski (2008) conducted a comparison of the CFC glazing and shading system analysis capabilities with the TMC analysis to establish that both functions predicted the same performance for unshaded glazing systems. Preliminary testing could then be undertaken to determine whether the CFC capability would function with the venetian blind shading models. The empirical validation of EnergyPlus performed by Loutzenhiser et al. (2006, 2008) gave credence to the EnergyPlus model, and as a result, provided a valuable basis for comparison of the CFC ESP-r capabilities. A comparison of slat-type blind models analyzing solar transmission and cooling loads with different blind configurations was conducted using the two programs, the results of which are provided in (Lomanowski and Wright 2011), with good agreement giving confidence to the CFC models in ESP-r.

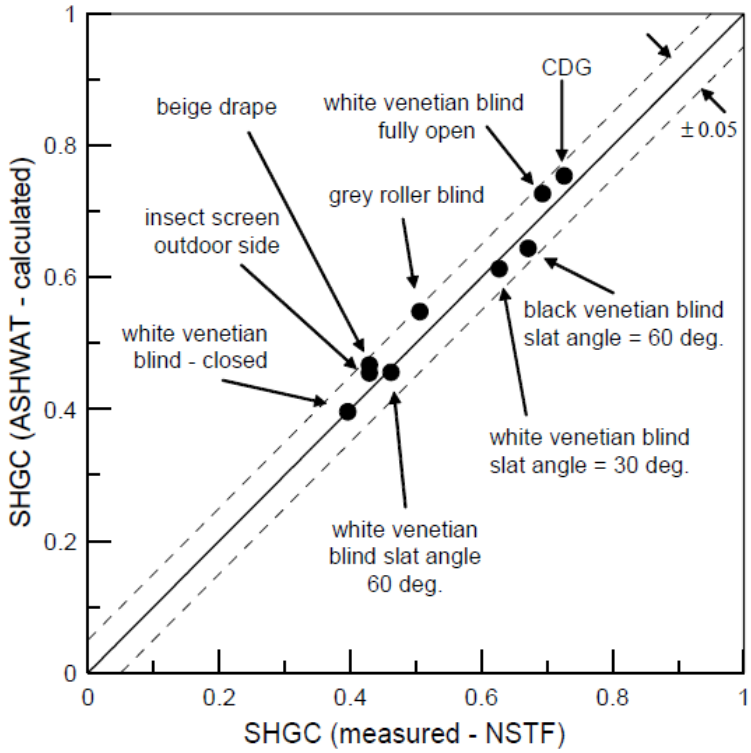

Figure 5.1 - SGHC Comparison between ASHWAT Simulation Results and NSTF Measurements – Reproduced from (Wright et al. 2009)

5.2 Effective Solar Properties of the Flat Configuration

A flat shading layer configuration was chosen for a preliminary as each of the shading device models in ESP-r could be represented with this simple geometry. The concept of effective layer optical properties

was introduced in Chapter 3, further discussed in Chapter 4, and will now briefly be reviewed. By defining shading layers with effective optical properties, a generic layer is created, and the CFC function is able to evaluate a shading layer as if it were any other layer in the system. All the newly implemented shading device models in ESP-r require only a few inputs at normal incidence, A_o, $\tau_{tot}^f$and ρ_{tot}^f, which can easily be determined. This information is used to determine the fabric location on Keyes Chart (Figure 5.2). Further details on all the subsequent models can be found in (Kotey 2009). Some of these details are described in the following subsections.

5.2.1 Transmission

In order to compare the performance of flat shading layer configurations, each shading layer had to have the same fabric or material properties defined. Venetian blind slats were assumed to have zero transmittance. Accordingly, the drapery fabric and roller blinds were defined to have zero openness, however this model did not suit the insect screen and as a result the insect screen was not included in this study. This assumption greatly simplifies the model as there is no beam-beam or beam-diffuse transmission. It should be noted that although there is no direct transmission through the shading layer material, there was some transmission as a result of slat gaps in the venetian blind model.

5.2.2 Reflection

Having replicated the building simulation used in (Lomanowski 2008), an arbitrary value of 0.5 was selected for the beam-total reflectance at normal incidence, $\rho_{bt}(\theta = 0)$. None of the shading device models implemented in ESP-r exhibit any specular reflectance (ASHRAE 1311-RP).

5.2.2.1 Roller Blinds

The reflectance is independent of incidence angle; hence it is equal to the material reflectance at normal incidence, $\rho_{bd}(\theta) = \rho_{bt}(\theta = 0)$. Further, the roller blind diffuse-diffuse reflectance, $\rho_{dd} = \rho_{bt}(\theta = 0)$.

5.2.2.2 Drapery Fabrics and Pleated Drapes

Kotey (2009) defines pleated drapes as a drapery fabric with rectangular pleats. Drapery fabric angle-dependent properties are first determined; see Chapter 3 for details. The effects of the pleating are handled with three cases which represent all possible geometric effects of pleats on solar incident radiation on the system. In this case the drapery has a folding ratio, Fr = 1 corresponding to a fullness of 0%, i.e. the fabric is flat/not pleated. Further details can be found in (Kotey 2009).

5.2.2.3 Venetian Blinds

The simplified models developed by Kotey et al. (2008) for slat-type blinds are based on previous work by (Yahoda and Wright 2005), but eliminate the need for computationally demanding ray tracing

techniques. Assuming slat material solar properties are independent of incidence angle and perfect diffusers, four and six surface enclosure models represent all cases of radiation incident on the blind used in determining layer effective optical properties, where $\rho_{bd}(\theta) = \rho_{bt}(\theta = 0)$. Further, the model corrects for slat curvature, however the model does not account for slat thickness. See (Kotey et al. 2008) for further details. In this case the slats were fully closed, slat angle = 88^o (90^o cannot be used in ESP-r as it accounts for the physical limitations of the slats).

5.3 Preliminary Test Configuration for the Current Study

A study was conducted to examine the functionality of the newly implemented shading devices. A shoebox model was used to illustrate an insulated envelope with a south facing window (Figure 5.2). An atypical wall construction of brick, insulation and concrete was selected to represent the wall, floor and roof constructions, the material properties can be found in Table 5-1. Although it does not accurately represent a real building construction, it serves the purpose of providing thermal mass, and aside from the window, is opaque to radiation. As a result, the cooling load will emphasize the effect of solar gain through the fenestration area.

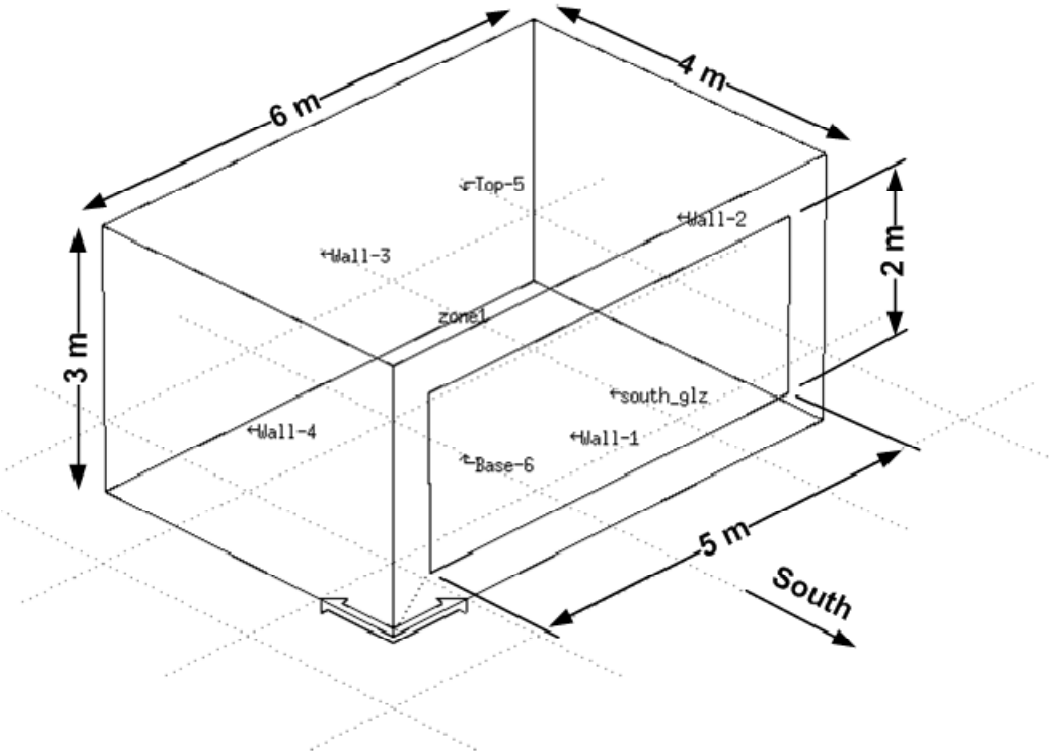

Figure 5.2 - Geometry of Test Cell (Courtesy of Lomanowski 2008)

The walls, roof and windows describing the thermal zone are modelled with an outdoor surface condition which considers shortwave and longwave radiation, wind exposure and other outdoor factors, and the

floor is exposed to a constant near-ground temperature of 22.3℃. Weather data for the simulation period, July 7th, is based on hourly CWEC (Canadian Weather for Energy Calculations) data for Toronto, Ontario. An ESP-r routine interpolates this data to fit the time-step in the simulation case. The site exposure describes the ground reflectance at the site considered. An ideal thermostatic control has a cooling set point of 25℃, and no heating set point as heating is not desirable in the summer months.

Table 5-1 - Wall, Floor and Ceiling Material Properties

Material	**Breeze Block**	**Brown Brick**	**Glasswool**
Roughness	MediumRough	MediumRough	Rough
Thickness (m)	0.1	0.1	0.075
Conductivity (W/mK)	0.44	0.96	0.04
Density (kg/m^3)	1500	2000	250
Specific Heat (J/kgK)	650	650	840
Thermal Absorptance	0.9	0.9	0.9
Solar Absorptance	0.65	0.7	0.3
Visible Absorptance	0.65	0.7	0.3

There is no infiltration and no ventilation from adjacent zones as there are none in this model. A warm-up period of 4 days was used for this model. The results will only be influenced by changes in solar gain, radiant and convective gain/losses through the fenestration. Model parameters are described in Table 5-2.

Table 5-2 - Simulation Model Parameters

Parameter	**Description**	**Value**
Simulation Period	July 7th	0-24 hours
Time Steps per Hour		6
Warm-up Period		4 days
Wall, Floor and Roof Construction	Exterior Layer	Brown Brick (10 cm)
	Middle Layer	Glasswool (7.5 cm)
	Interior Layer	Breeze Block (10 cm)
Climate Data	CWEC Toronto, Canada	
Site Exposure	Rural/Country	
Ground Reflectivity		0.2
Ground Temperature		22.3℃
Thermostatic Control	Basic Ideal thermostat with cooling set point	25℃
Ventilation and Infiltration	No ventilation or Infiltration Default ESP-r interior convection correlations Simple EnergyPlus interior and exterior convection models	

Shading device material and glazing optical properties at normal incidence are described in Table 5-3. The glazing and venetian blind material properties are identical to those used in (Lomanowski 2008). The drapery fabric and roller blind material properties were defined to mimic those of the venetian blind.

Table 5-3 - Fenestration Construction Material Properties Provided at Normal Incidence where Applicable

Glazing/Shading Device	**CLEAR 6MM Glazing**	**Venetian Blind**	**Drapery Fabric**	**Roller Blind**
Layer Thickness (mm)	6.00	12.7	1.00	1.00
τ_{bb}	0.775	0.000	0.000	0.000
$\tau_{f,bt}$	0.775	0.000	0.000	0.000
$\tau_{b,bt}$	0.775	0.000	0.000	0.000
$\tau_{f,bd}$	0.000	0.000	0.000	0.000
$\tau_{b,bd}$	0.000	0.000	0.000	0.000
$\rho_{f,bt}$	0.071	0.500	0.500	0.500
$\rho_{b,bt}$	0.071	0.500	0.500	0.500
τ_{vis}	0.881	0.000	0.000	0.000
$\rho_{f,vis}$	0.080	0.500	0.500	0.500
$\rho_{b,vis}$	0.080	0.500	0.500	0.500
τ_{lw}	0.000	0.000	0.000	0.000
$\varepsilon_{f,lw}$	0.840	0.850	0.850	0.850
$\varepsilon_{b,lw}$	0.840	0.850	0.850	0.850
Conductivity (W/mK)	0.9	0.9	0.9	0.9
Slat Orientation		Horizontal		
Slat Width (mm)		12.70		
Slat Spacing (mm)		10.58		
Slat Crown (mm)		0.00		
Slat Thickness (mm)		0.33		
Slat Angle (degrees)		88		
Opening Multipliers (EnergyPlus only)		1	1	1

5.3.1 Methodology

A preliminary comparison was performed to establish confidence in the newly implemented models. The results from the test room used in (Lomanowski 2008) to compare the performance of a conventional double glazing, 12.7 mm air gap, fenestration system using the TMC and CFC functions established a baseline for comparison. Figure 5.3 and Figure 5.4 show the solar transmission and cooling load as a function of time for the current model and the model used in (Lomanowski 2008), illustrating that the CFC functions, as well as other model parameters are the same.

Having chosen a specified the same material properties for each shading device as well as a baseline model, it is now appropriate to compare a closed venetian blind to a roller blind and drapery fabric.

Further, the placement of the shading layers in indoor, between-pane and outdoor configurations will be analyzed to determine the influence this has on building performance.

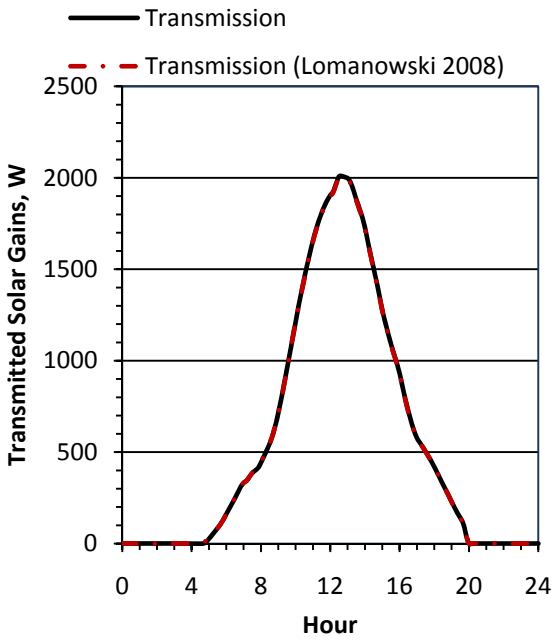

Figure 5.3 - Solar Transmission of Test Cell with Double Glazing

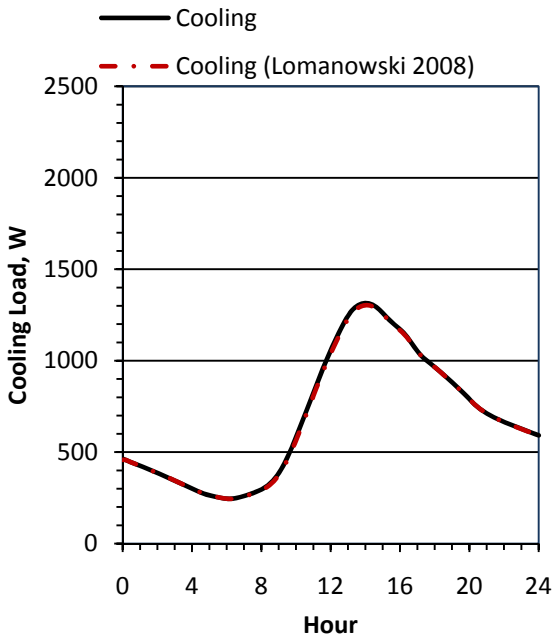

Figure 5.4 - Cooling Load of Test Cell with Double Glazing

5.4 Results

Having discussed the fabric optical properties of the various shading layers (Section 5.2.2), it can be noted that each layer has zero transmittance and a beam-total reflectance of 0.5 at normal incidence. This suggests that solar incident radiation will only be transmitted in the venetian blind model through the slat gaps. Kotey (2009) shows how a small amount of false transmission occurs even if the slats are fully closed.

All shading layer surfaces (i.e. slats, fabric and roller blind material) are considered hemispherically diffuse with respect to incidence diffuse radiation, hence ρ_{dd} is constant. The beam-diffuse reflectivity, ρ_{bd}, is the only optical property which changes as a function of time (i.e. incidence angle) (Figure 5.5), ρ_{bd} as a function of time, and Figure 5.6, ρ_{bd} as a function of θ. As a result ρ_{bd} is the only optical property to produce noticeable discrepancies in the results. The venetian blind slats are considered perfectly diffuse, so there is no change in ρ_{bd} as a function of incidence angle. Similarly, the roller blind uses ρ_{bd} = constant. The drapery fabric ρ_{bd} is however a function of incidence angle.

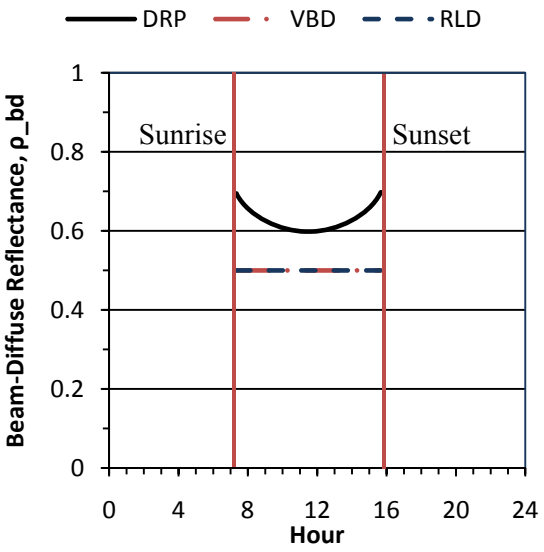

Figure 5.5 - Shading Layer Beam-Diffuse Reflectance as a Function of Time

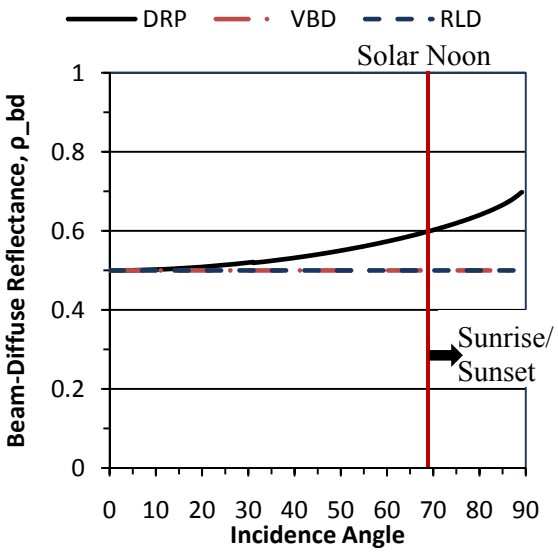

Figure 5.6 - Shading Layer Beam-Diffuse Reflectance as a Function of Solar Incidence Angle

Figure 5.7, Figure 5.8 and Figure 5.9 illustrate the effects of shading layers on the cooling load in the zone considered on the simulation day, July 7th, in Toronto. The shading layers considered include a drapery fabric (DRP), roller blind (RLD) and venetian blind (VBD). A comparison of the three graphs clearly illustrates the effects of shade placement in the complex fenestration system. It can be noted that as the shading layer placement moves from indoor, to between-pane to outdoor, the cooling load is reduced appreciably.

The indoor placement of the shading layer inherently allows solar gain through the fenestration construction to the zone prior to the shading layer having any effect. Since there is zero openness in the fabrics used in this study, solar incident radiation is either absorbed or reflected. Consequently solar gain manifests itself through the energy absorbed by the shading layer which is redistributed via longwave radiation to the walls and adjacent glazing layer and convection to the zone, resulting in a higher peak load.

The indoor shade cooling load is nearly halved when the shading layer is moved between-panes. Since the transmission is limited by the fabric openness, the solar radiation incident on the fenestration construction is either absorbed between-panes or reflected before it enters the zone. The results show that incident radiation on the fenestration construction is reflected to the surroundings, or absorbed and largely redistributed by convective heat transfer to the outdoor side.

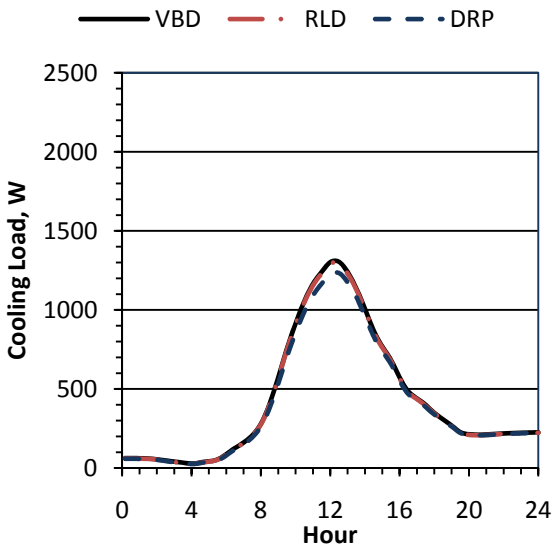

Figure 5.7 - Indoor Shade Cooling Load

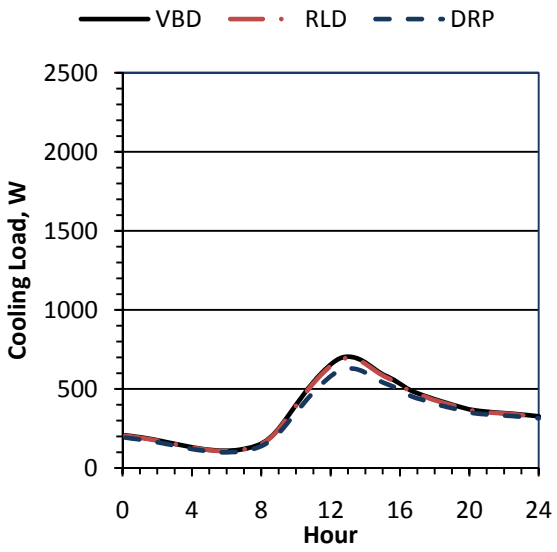

Figure 5.8 - Between-Pane Shade Cooling Load

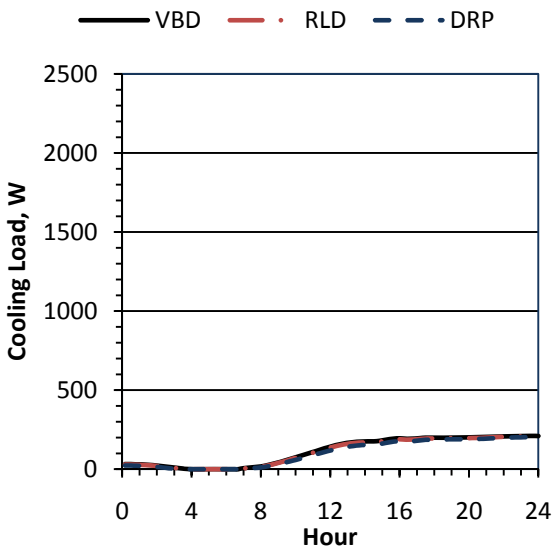

Figure 5.9 - Outdoor Shade Cooling Load

The outdoor shading scheme is able to intercept the majority of solar radiation before it even enters the conditioned zone. As little solar radiation is transmitted directly through the shading layers, solar gain is strictly a result of heat transfer from the shading layer to the zone. Hence the majority of the gain seen in Figure 5.9 is actually a result of solar gain through the walls of the envelope and not the fenestration system. The same effect is seen in the way Figure 5.7 and Figure 5.8 are skewed.

Having discussed the effects of the shade placement on cooling load, the results can be further analyzed to see the effects of shading devices on the cooling load prediction. Referring back to the earlier discussion on effective layer properties, it is clear that direct transmission is a negligible, since all the shading

devices have zero openness. However, it is clear that reflectance does have an influence on the cooling load. Figure 5.5 and Figure 5.6 illustrate the beam-diffuse reflectance, $\rho_{bd}(\theta)$, of the shading devices and how it changes as a function of time or incidence angle. It is clear that the venetian blind and roller blind were expected to perform near identically, while the flat drapery fabric would perform slightly better based on this criterion. This result is reflected, particularly, in Figure 5.7 and Figure 5.8, where it is seen how the shading layer influences the cooling load. It can be seen that the venetian blind and roller blind models predict a near identical performance while the drapery fabric incident angle dependent solar optical properties result in slightly better performance. However, for the outdoor case, it was noted earlier that the shading layer had little effect n the cooling load. This too is reflected in the Figure 5.9 where the cooling load is essentially identically for all three shading devices.

5.5 Discussion

As the shade moves from the indoor side to between-panes to the outdoor side, the cooling load decreases significantly. In this particular model we see the peak demand occur at the same time in the indoor and between-pane shade configurations, while outdoors, the cooling load does not peak. This result was as expected considering zero beam radiation was transmitted through the layers and hence we expect to see significant differences in the different cooling loads based on shading layer placement in the construction.

It was also anticipated, provided an understanding of the models used to convert normal incidence fabric optical properties to off-normal effective layer properties, that the venetian blind and roller blind layers with the same fabric optical properties would perform nearly identically. Meanwhile, the drapery fabric was expected to have a lower cooling load as a result of a beam-diffuse reflectivity dependence on the incidence angle. This was seen in the performance of the shading device and glazing constructions regardless of shading layer placement.

The purpose of this chapter was to provide preliminary testing of the newly implemented shading layer models introduced to the CFC function in ESP-r. The new shading model results were analyzed in terms of a comparison of the existing and established venetian blind shading layer, given confidence to the newly implemented subroutines. Subsequent simulation work has uncovered no difficulty with the performance of the new shading models.

It should be noted that the drapery fabric model is incorporated in the pleated drape model, and is actually defined as a pleated drape with zero fullness. Having established the functionality of the drapery fabric model has by extension given confidence to the pleated drape model in ESP-r. Further, the insect screen, although not analyzed in this particular study, was implemented in the same fashion as the other shading

device model. Given the success of the preliminary analysis of the roller blind and pleated drape models gives confidence to the functionality of the insect screen model.

Chapter 6

Comparison Study of ESP-r and EnergyPlus Shading Layer Analysis

Chapter 5 established the successful implementation of three additional shading device models (e.g. roller blinds, pleated drapes and insect screens) into ESP-r. The new simulation capabilities will be further investigated with a comparison of the EnergyPlus and ESP-r roller blind and pleated drape models. It has previously been mentioned that slat-type shading in EnergyPlus has undergone validation by comparison with EMPA measurements (Loutzenhiser, Manz and Carl, et al. 2008 and Loutzenhiser, Manz and Strachan, et al. 2006). Further, the CFC capabilities were tested against the TMC function in ESP-r for a conventional double-glazing system (Lomanowski 2008) and against EnergyPlus for the effects of venetian blinds on building performance (Lomanowski and Wright 2011) with close agreement. The newly implemented shading devices could not be compared with EMPA results as measurements only exist for slat-type shading; however the new ESP-r models were scrutinized with a comparison to EnergyPlus simulations.

6.1 EnergyPlus Models

Using EnergyPlus, glazing system solar optical and thermal calculations can be completed from two different approaches. In the first method, properties are based on WINDOW 4 and WINDOW 5 algorithms (Finlayson, Arasteh, et al. 1993 and Arasteh, Reilly and Rubin 1989). However, EnergyPlus has a simplified model for glazing systems which can determine off-normal properties based on design condition U-Value and $SHGC$ values, although with slightly less accurate results (ISO 15099 2003 and Finlayson, Arasteh, et al. 1993).

EnergyPlus is also capable of determining the effects of shading layers on the fenestration system. Thermal models are based on (ISO 15099 2001). The shading device models employed by EnergyPlus are described in the subsequent sections, the details of which can be found in the engineering reference. Some of the material is paraphrased from the engineering reference for clarification.

Testing is an ongoing process in the development of EnergyPlus. Analytical testing is based on ASHRAE research project (865-RP and 1052-RP), comparative testing is performed against ANSI/ASHRAE

Standard 140-2007 and the International Energy Agency Solar Heating and Cooling Programme (IEA SHC) BESTEST (Building Energy Simulation Test) and release tests are also part of release development. Further details on testing modules and development can be found in the EnergyPlus Testing and Validation (U.S. Department of Energy 2011).

6.1.1 Solar Properties

Shading devices affect the transmittance, reflectance and absorptance of solar radiation through a fenestration system. The effect depends on the shade position relative to the glazing layers and the interaction between the adjacent layers in the system (Engineering reference). EnergyPlus much like the CFC capability in ESP-r divides shading devices into four categories; shades, blinds, screens and switchable glazings; however switchable glazing models do not exist in ESP-r and insect screens will not be considered in this study.

6.1.1.1 Shades

Roller blinds and drapery fabrics are categorized as “Shades” in EnergyPlus. Shades are characterised as perfect diffusers, meaning beam radiation which is reflected or transmitted is hemispherically uniform diffuse radiation. Additionally, the transmittance, reflectance and absorptance are the same for the front and back of the shade and are independent of incidence angle. Thus, the effective layer properties are the same as the fabric optical properties at normal incidence. It should be noted that pleated drape models are not available in EnergyPlus.

6.1.1.2 Blinds

Venetian blinds are defined as “Blinds” in EnergyPlus, and unlike shades, their solar properties heavily depend on incidence angle and slate geometry including; slat angle, width and spacing, based on (Simmler, Fischer and Winkelmann 1996). Beam radiation may be transmitted directly through slat gaps, horizontal flat slats are considered prefect diffusers and absorption is independent of incidence angle as well. Inter-reflections between the shading layer adjacent glazing layers or walls near the periphery of the shade are ignored. Further, EnergyPlus has the capability to schedule slat angles as well as retractable shading.

6.1.1.3 Screens

Screens, or insect screens are made up of metallic or non-metallic materials and can sometimes be used as a shading device. EnergyPlus models screens as orthogonal cylinders which are diffusely reflecting and dependent on incidence angle, wire diameter and spacing to determine the openness. The insect screen transmittance algorithm is comprised of two components; the direct beam transmission and diffuse transmission caused by the scattering of beam radiation hitting the screen material. Additionally, the

inward reflected beam radiation can be modelled in three ways based on user input. The user can elect to model or not model inward reflected beam transmission or model the incoming direct beam radiation as hemispherically-diffuse radiation depending on material reflectivity and thus properties are independent of incidence angle. However, the screen can only be placed as an outdoor shading layer.

6.1.2 Heat Balance Algorithm

The conduction transfer function (CTF) module is a simple linear equation with constant coefficients which can calculate the conduction heat transfer through any element. The conduction transfer functions need to be calculated once for each construction type. They represent an efficient method of computing surface heat fluxes as they do not require the temperature and fluxes within a surface. However, they become more unstable with decreasing time-steps or heavy constructions due to round-off and truncation errors (EnergyPlus Engineering Reference 2010). Other heat balance algorithms are available in the (EnergyPlus Engineering Reference 2010).

Note that since the glass layers are substantially thin, little heat storage is likely to occur and therefore is neglected in the heat transfer analysis. This, however, can be problematic in heavily glazed facades with very thick glass layers. In a similar fashion, thermal storage is also neglected for shading layers. As such, the glazing and shading layer temperatures are calculated iteratively at each time step. Further details can be found in the EnergyPlus Engineering Reference (2010).

6.1.3 Convection Models

EnergyPlus supplies an array of convection correlations for both the indoor and outdoor fenestration construction calculations. The outdoor Thermal Analysis Research Program (TARP) method was developed by Walton (1983) and is a comprehensive model which takes correlations from both ASHRAE and flat plate experiments by Sparrow et al. (1979) and are a function of both natural and forced convection. The indoor TARP method is comprehensive natural convection model correlating the convective heat transfer to surface orientation and temperature difference between the surface and zone air. This method can be found in the ASHRAE Handbook (ASHRAE 2001).

Other indoor side convection models available in EnergyPlus include; forced ceiling diffuser convection mixed with natural convection, an adaptive convective algorithm, and a simple ASHRAE model for natural convection. On the outdoor side, convection can also be modelled by a simple combined natural convection coefficient with forced outdoor air using ASHRAE's model, correlation measurements by Klems and Yazdanian, MoWiTT for smooth surfaces and DOE-2 for rough surfaces or an adaptive convection algorithm which dynamically selects correlations based on the conditions of the simulation, the details of which are available in the (engineering reference document).

6.2 ESP-r Models

The shading device and glazing systems in ESP-r are modelled via the CFC module.

6.2.1 Solar Properties

The solar optical models used in CFC models are described in Chapter 5.

6.2.2 Heat Balance Algorithm

Glazing and shading layers are explicitly (i.e. some information is lagged by one iteration, referring to "past" time-step data) treated within the nodal scheme of the thermal zone in which they are located; details can be found in Chapter 4. That is to say the fenestration layer nodes are linked to all zone surface nodes via convective and radiative heat transfer. The governing equations are then solved simultaneously by the ESP-r solution routines to determine nodal temperatures. In the CFC model, the thermal mass of glazing and shading layers are treated in the same fashion as any opaque construction. In fact, the thermal mass of the CFC layers is required to obtain solution stability (Lomanowski 2008).

Note: Both the EnergyPlus and ESP-r glazing and shading models neglect edge and frame effects, rather they only consider the center-of-glass region. It is however possible to model the edge and frame regions in either EnergyPlus or ESP-r as separate constructions knowing the U-value of these regions. This information can be obtained from various sources e.g. (ASHRAE 2009).

6.2.3 Convection Models

The task of predicting convective heat transfer coefficients is non-trivial; particularly when dealing with indoor and outdoor shading devices which effectively triple the surface area for convection.

Convection at indoor horizontal and vertical surfaces is represented by buoyancy driven natural convection, using correlations developed by Alamdari and Hammond (1983). A model for determining the convective flow in glazing cavities has been developed by Wright et al. (1996). However, accounting for the convective flow at the indoor and outdoor shading attachments is an ongoing topic of research e.g. (Naylor, et al. 2006, Shahid and Naylor 2005 and M. Collins 2004).

The convective flow between panes for venetian-blinds is well understood. Huang et al. (2006) studied the effects of slat-type shades on convective flow and radiative heat transfer in a glazing cavity, and characterized the convective component by applying a modification factor to spacing thickness based on slat angle. This model is reliable for cavities up to 25 mm thick.

An outdoor convection model applies a user supplied (i.e. supplied by the calling routine) outdoor heat transfer coefficient to the glazing and shading layers. Since the shading layer is exposed on two surfaces,

this effectively triples the exposed surface area. The interaction between the shading layer and outdoor glazing is ignored since both are generally exposed to forced convection.

6.2.4 ESP-r CFC Module Validation

CFC module validation was previously covered in Chapter 5.

6.3 ESP-r and EnergyPlus Simulation Comparison

ESP-r and EnergyPlus are both long standing and industry proven energy simulation tools. The added functionality of modelling shading device influence on building performance has greatly improved their ability to represent real building performance. This is especially important in the design of energy-efficient buildings. As is the case, it seems ideal to do a model comparison between the two programs and determine whether they will reach the same conclusion as to the influence of different shading configurations. As in (Lomanowski and Wright 2011) the TARP convective model option was chosen for use in EnergyPlus, other pertinent simulation parameters were described in Section 5.3.

The intent of this study was to give further confidence to the newly implemented ESP-r models through a comparison of shading models to EnergyPlus. It was previously established through work by Loutzenhiser et al. (2006, 2008) that EnergyPlus has proven capabilities in simulating the effects of slat-type shading. Presumably, a correct model for drapery fabric and roller blind solar optical properties would produce similar comparison results.

To ensure the EnergyPlus model was properly configured, a preliminary test was performed using a venetian blind on the indoor side of the complex fenestration. The cooling load as a function of time throughout the test date, July 7th, in Toronto, was determined for the current study, and compared with the results of (Lomanowski and Wright 2011). Figure 6.1 establishes that the two models coincide and that the current model was properly configured. Subsequently, all further comparisons made in this chapter are of cooling load as a function of time.

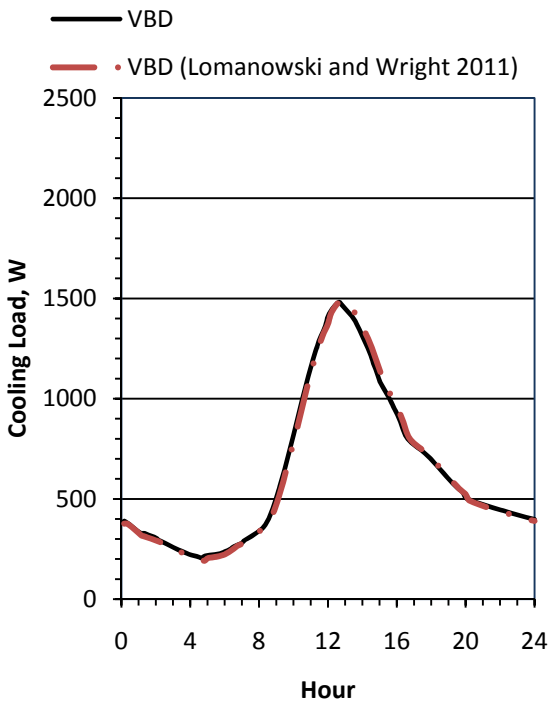

Figure 6.1 - EnergyPlus Model Configuration -
Cooling Load for Venetian Blind from Current Model and (Lomanowski and Wright 2011)

6.4 Results

A comparison of simulations including the roller blind and pleated drape models implemented in ESP-r and blinds in EnergyPlus are presented in Figure 6.2, Figure 6.3 and Figure 6.4. In each case, the horizontal axis shows the time-of-day in hours, and the vertical axis shows the cooling load for roller drapes (RLD), pleated drapes (DRP) and venetian blinds (VBD).

Immediately it can be noted that although the indoor shade case seems in close agreement through the daylight hours when solar gain influences the model, it does not agree in the evening and at night. Additionally, the between pane case possesses a large discrepancy between the peak-loads predicted by EnergyPlus and ESP-r models. In the outdoor case there is again disagreement leading from the night to the morning, however the cooling loads converge towards the end of the day. Discrepancies in the cooling load profile were thought to be a result of differences in the convection models employed by the two programs. Differences in the initial cooling load at 0 hour are thought to be a result of the manner in which the two programs handle the start-up of the simulation. Consequently, more detailed analysis on these discrepancies was performed.

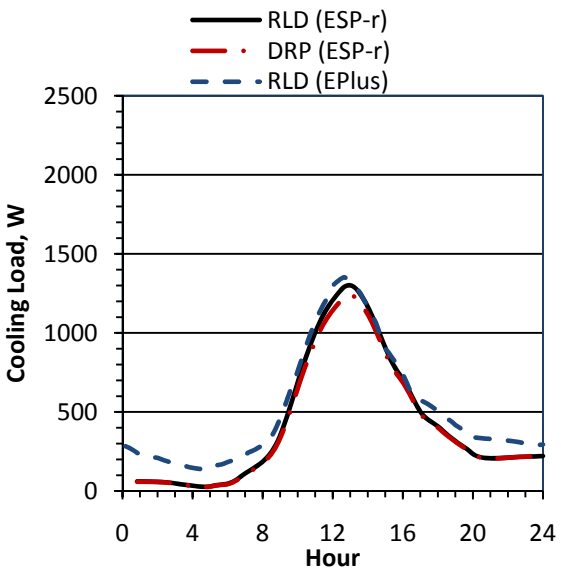

Figure 6.2 - Cooling Load versus Time-of-Day – Indoor shade

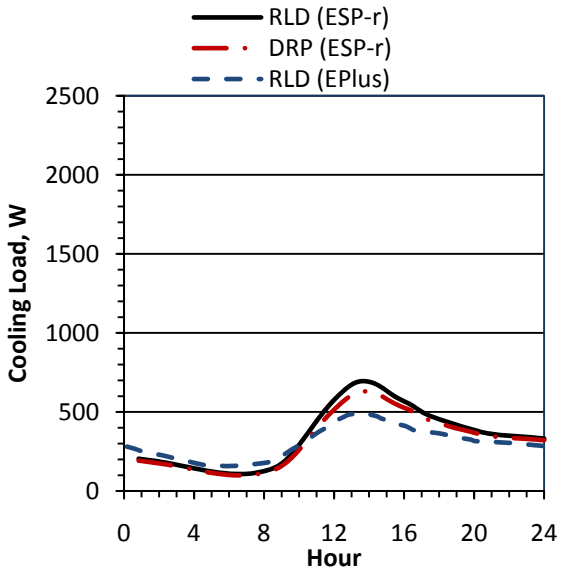

Figure 6.3 - Cooling Load versus Time-of-Day – Between Pane Shade

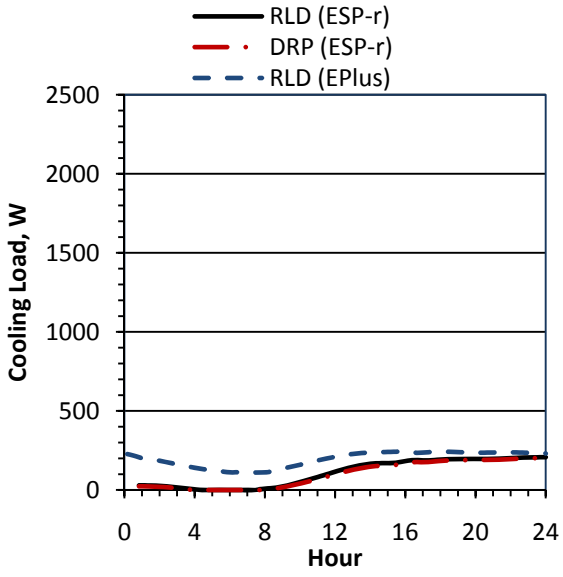

Figure 6.4 - Cooling Load versus Time-of-Day - Outdoor Shade

6.4.1 Convection model

The test cell used for this comparison was selected to minimize the influence the outdoor factors through the floor, walls and ceiling, while emphasizing the effect of the glazing on the simulation results. However, the array of convective models provided in EnergyPlus highlights the fact that convective modelling of airflows around indoor and outdoor shading is still not well understood see Section 6.1.3 above. Figure 6.5, Figure 6.6, Figure 6.7 and Figure 6.8 illustrate the extent to which differing

combinations of indoor and outdoor convective models influence the predicted cooling load of an indoor roller blind with $\tau_{bt}(\theta = 0) = 0$ and $\rho_{bt}(\theta = 0) = 0.5$ in EnergyPlus, as compared with ESP-r (RLD) performance. Again, each figure shows cooling load versus time-of-day.

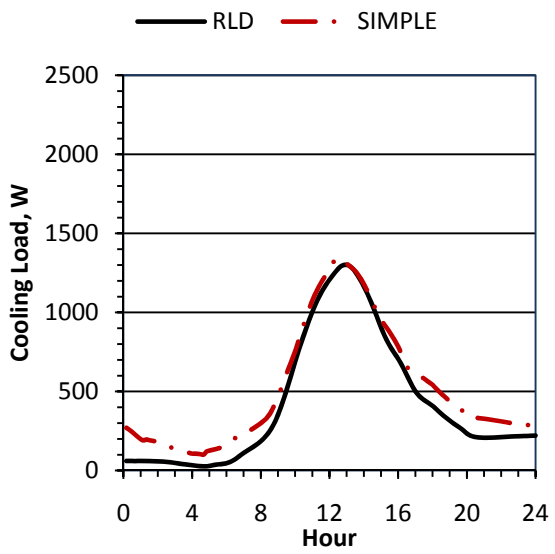

Figure 6.5 - ESP-r RLD and EnergyPlus Roller Blind Shade Model with Simple Indoor and Outdoor Convective Model comparison

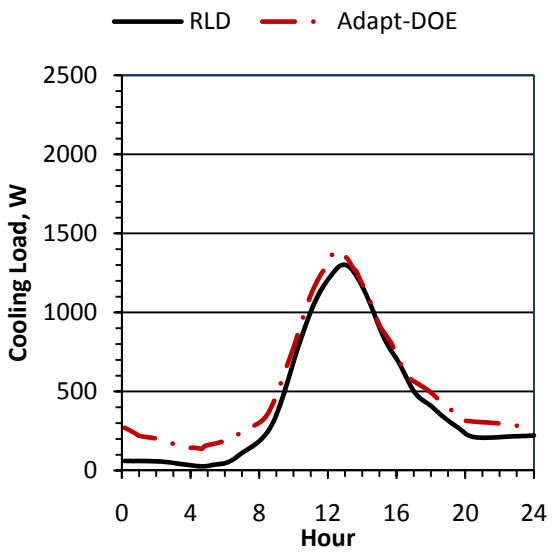

Figure 6.6 - ESP-r RLD and EnergyPlus Shade Model with Adaptive Indoor and DOE-2 Outdoor Convective Model comparison

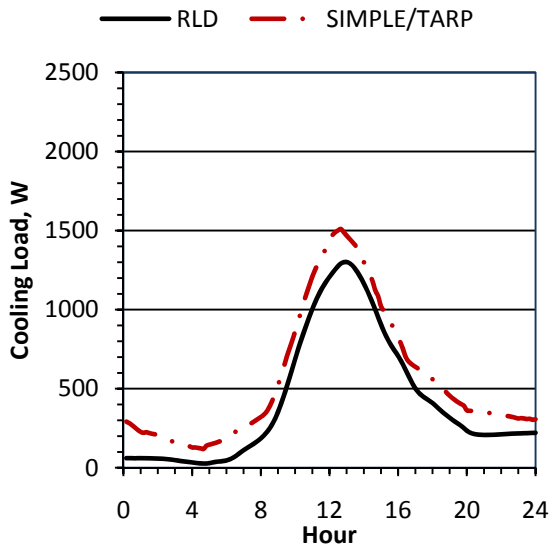

Figure 6.7 - ESP-r RLD and EnergyPlus Shade Model with Simple Indoor and TARP Outdoor Convective Model comparison

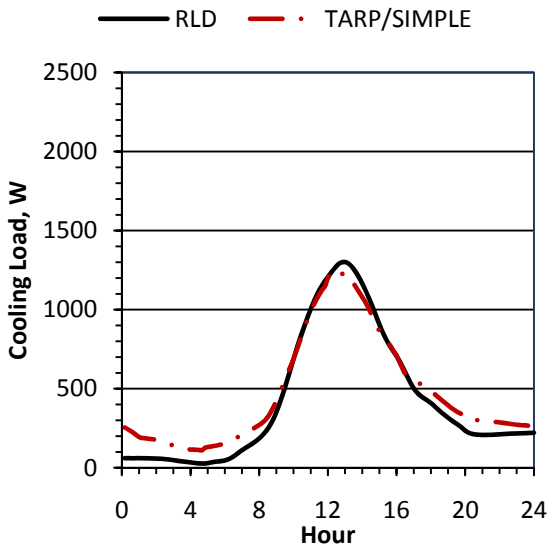

Figure 6.8 - ESP-r RLD and EnergyPlus Shade Model with TARP Indoor and Simple Outdoor Convective Model comparison

For this particular scenario, ESP-r agrees more closely with a Simple model rather than the TARP model. Further, note in Figure 6.6 and Figure 6.7 that, while the discrepancy gets worse with a Simple convection

model for the indoor side and TARP for the outdoor convection; the agreement is good when the TARP model is used for the indoor side and a Simple convection model for the outdoor side. Additionally, an Adaptive indoor model paired with the DOE-2 outdoor convection model over predicts relative to the ESP-r cooling load.

6.4.2 Start-up

The model parameters discussed in Section 5.3 defined a start-up period which applied to ESP-r; however a start-up period definition was not available in EnergyPlus. ESP-r starts the simulation with all the surfaces in the zone at a defined temperature, and the start-up days are used to get all the surfaces temperatures to reach the dynamic near-equilibrium. An investigation into how EnergyPlus determined this parameter indicated that the Conduction Transfer Function (CTF) method (see Section 6.1.2 above) it employs does not begin simulating until a dynamic near-equilibrium state of temperatures at each of the surfaces in a given zone is reached. This is achieved by iteratively cycling the model through the first test day of the simulation. It should be noted that this is also the reason for which the EnergyPlus model predict similar cooling loads at 0 hour (refer to Figures 6.2-6.4) with respect to cooling load regardless of the shading layer.

The study presented in Section 6.3 imposed the ESP-r definition of a “Start-up” period on the EnergyPlus model. This was performed by running the simulation for five days, corresponding to four start-up days and the test day. **Error! Reference source not found.**, illustrates the comparison of EnergyPlus results with a start-up period, “Start-up”, without a start-up period, “No Start-up” and the ESP-r results. It can be seen that although there was a slight discrepancy in the late evening to early morning between the No Start-up case and ESP-r results for an indoor venetian blind, the peak had better agreement than the Start-up case relative to the ESP-r results. The outcome of this study was used as a baseline and all of the simulations were modelled in a similar fashion.

However, analysis of the roller blind model was completed following initial testing and the same procedure was performed, see Figure 6.10. It is clear in the case of an indoor roller blind that the EnergyPlus model with a Start-up period better correlates to the simulation results from the ESP-r model. The varied outcomes of these models yielded further questions into how both programs handled the start-up period.

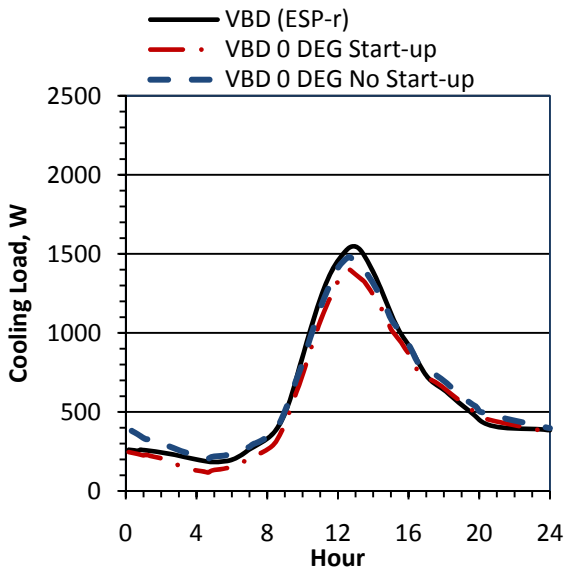

Figure 6.9 - Indoor Venetian Blind with 0 Degree Slat Angle Cooling Load, ESP-r vs. EnergyPlus with and without an ESP-r defined 'Start-up' Period

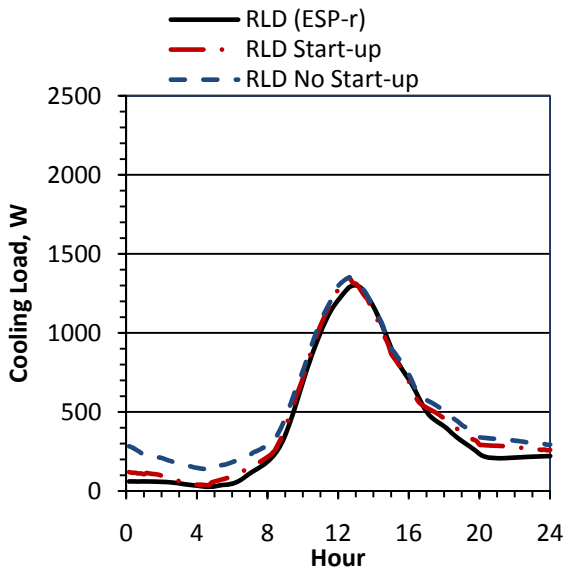

Figure 6.10 - Indoor Roller Blind Cooling Load, ESP-r vs. EnergyPlus with and without an ESP-r defined 'Start-up' Period

A final study was performed, and is presented below, this time imposing the EnergyPlus definition of a "Start-up" period on the ESP-r model. This was achieved by defining the weather data files in each program such that all the simulation days would be the same as the test day, July 7th.

It should be noted at this point that the term "No Start-up" referred to in Figures 6.9 and 6.10 for the EnergyPlus results refers to the EnergyPlus definition of a "Start-up" period, referred to in the subsequent discussions.

6.4.2.1 The Outdoor Shade Case

The outdoor shade was initially considered as the cooling load is not influenced by transmission to the zone; therefore the results are most heavily influenced by gain through the walls. Figure 6.11 demonstrates the fashion in which the individual programs handle the start-up period definition. The CTF function in EnergyPlus has already converged on a dynamic near-equilibrium state as required by the CTF function, therefore the simulation results are the same for each day in the EnergyPlus simulation. This is the process that is being imposed on ESP-r, where it was found that the solution was close to convergence near day four for the outdoor roller blind; however seven days were used for testing.

Figure 6.12 focuses in on the results of the test day. It can be seen that when both programs apply the same technique in regard to handling the start-up period definition that they reach nearly the same conclusion for an outdoor shade, particularly in regards to the cooling load trend. It is however evident there was a minor discrepancy in the magnitude of the simulation results.

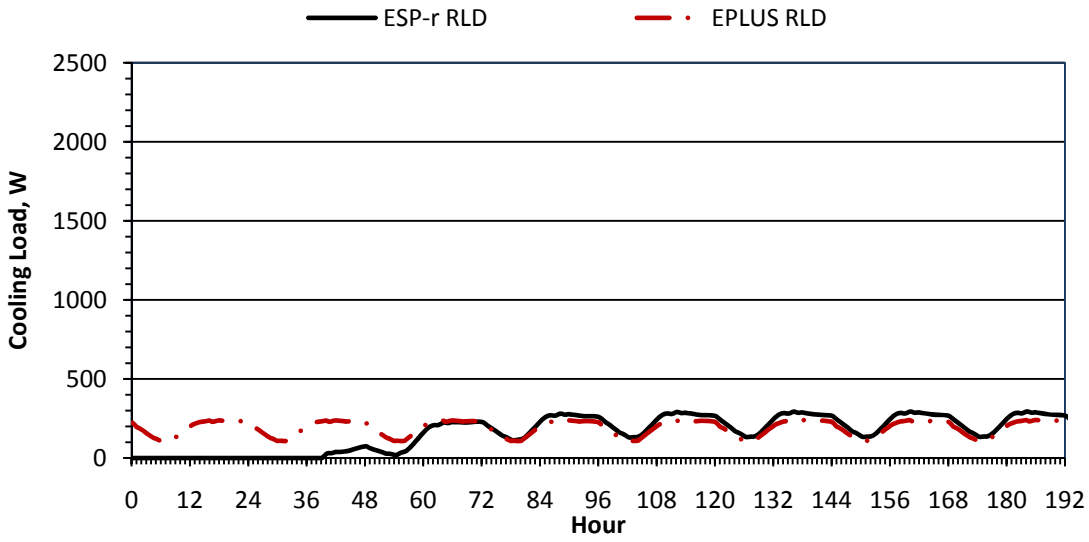

Figure 6.11 - Cooling Load for an Outdoor Roller Blind - 7 Start-up Days before Model Solutions Converge

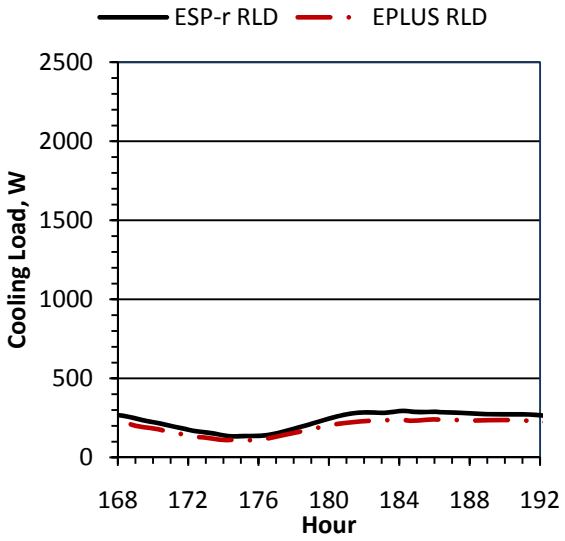

Figure 6.12 - Cooling Load for an Outdoor Roller Blind - Test Day

6.4.2.2 The No Window Case

The magnitude discrepancy of the Indoor Shade case was further investigated by repeating this test for the same shoebox model, this time without a window. Figure 6.13 illustrates that the concern in regards to the magnitude of cooling loads is not a result of the fenestration system analysis, rather a difference in the handling of the heat transfer through the walls.

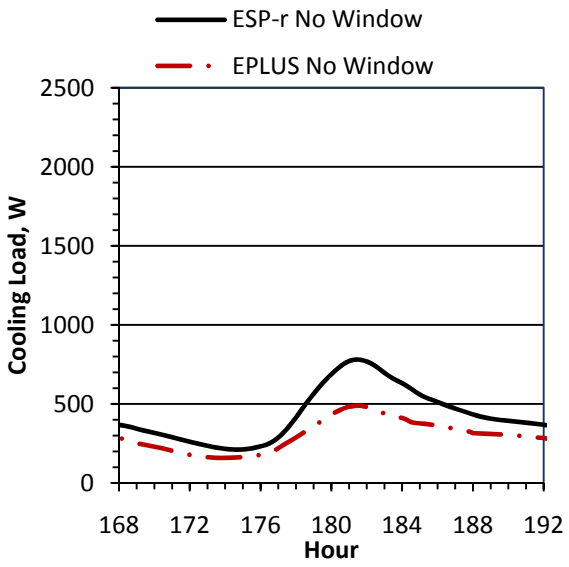

Figure 6.13 - Cooling Load for Shoebox without a Window - Test Day

6.4.2.3 The Indoor Shade Case

The indoor shade case was analysed to determine whether the transmission through the fenestration system would be sensitive to some other influence, causing further discrepancy in the results. Figure 6.14 has been included for reference purposes, again we see that ESP-r results nearly converge after four days, but seven days are used for the test. It can be noted that the discontinuity in the evening hours is a result of inconsistency in the weather trends as the same day is being cycled.

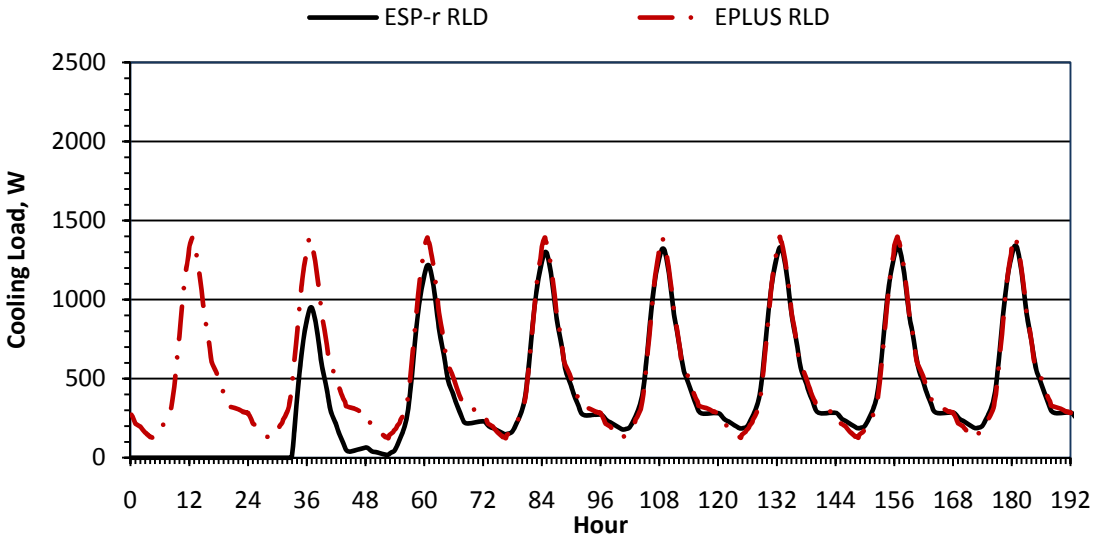

Figure 6.14 - Cooling Load for an Indoor Roller Blind - 7 Start-up Days before Model Solutions Converge

A closer look at the indoor shade case is presented in Figure 6.15, where it can be seen that the contribution of solar gain through the fenestration system far outweighs the effects of gain through the walls. The close correlation puts emphasis on the fact that the two programs are predicting near similar shading device optical properties.

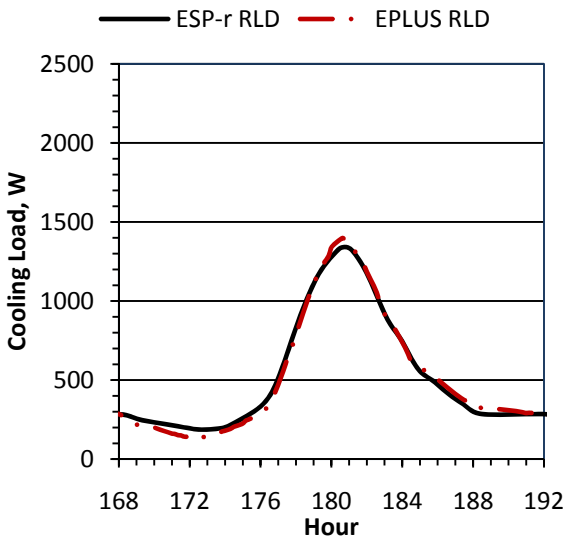

Figure 6.15 - Cooling Load for an Indoor Roller Blind - Test Day

6.4.2.4 The Between Pane Shade Case

The between pane case was also examined, the result of which is presented in Figure 6.16. Unlike in the indoor and outdoor roller blind models, a much larger discrepancy is seen in the between pane results.

Firstly, it can be noted that both models follow a similar trend, however with different levels of cooling load. In the evening hours, a similar trend can be seen to that of the outdoor case or no window case, suggesting that this does not need to be investigated. It has also been established that the solar optical models are near similar in that the indoor and outdoor shade cases have yielded promising results. The cause for discrepancy in this case is likely attributed to the modelling of convection through shading layer between panes used by the respective programs.

EnergyPlus models the convective heat transfer of a shading device between panes as per the ISO15099 pressure balance equation (EnergyPlus engineering reference 2010). The convection model for a venetian blind in ESP-r is based on models developed by Huang et al. (2006) and are implemented in the same way (i.e. Huang et al. 2006) if placed in a glazing cavity. The reason for the Huang et al. models being used is that they have experimental validation for a range of gap spaces, where the ISO15099 models do not. As two different models are being used to model the convection of a shading device between panes, this is

likely that the discrepancy arises. As a result, it is evident that more work needs to be done on the modelling of convective flow through a shading device between panes. However, it is unlikely that drapes, roller blinds or insect screens can be used in a practical way in a glazing cavity.

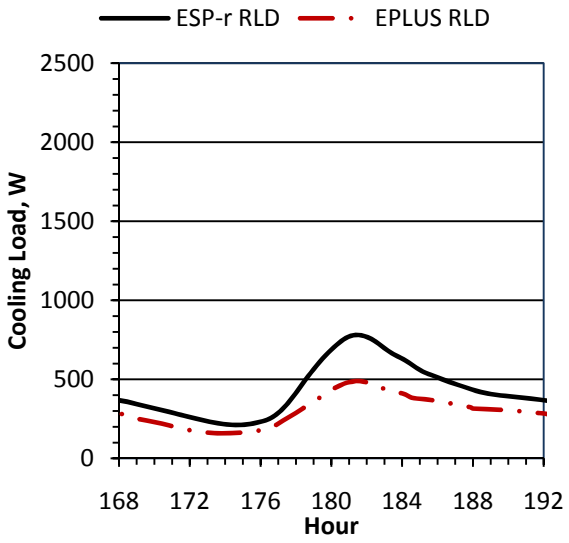

Figure 6.16 - Cooling Load for an Between Pane Roller Blind - Test Day

6.5 Discussion

The comparisons made in this study give confidence to the shading device models implemented in ESP-r. In most cases the EnergyPlus and ESP-r simulations produced close results, particularly and most importantly in regards to the trend of shading device influence on cooling load. This can also be said of the effects of shading layer placement in the complex fenestration constructions.

By forcefully replicating the start-up method employed by EnergyPlus in ESP-r, the cooling load profiles for the indoor and outdoor shading layers were nearly identical, varying mildly in level of cooling load but with the same trend. As a result, it appears that the optical models are predicting similar effective layer properties. However, a comparison of Figure 6.3 and Figure 6.16 emphasizes that the modelling between pane shading devices still remains an issue. As the indoor and outdoor roller blind models yielded such promising results, it is unlikely that the optical models could cause such a discrepancy in the between pane shade case. Further, the indoor and outdoor surface convection models, although likely attributing to a difference in magnitude of the results, did not seem to have a major effect on the cooling load trend, as seen in the no window case. As a result, the likely cause for this discrepancy is in the modelling of convection through a shading layer between panes. It should however be noted that between pane roller blinds, drapes and insects screens are not practical applications.

The modelling of convective flows near shading devices remains one of the most challenging issues in regard to all building energy simulation software. As seen in Figures 6.5-6.8, simply changing the convection models presented to EnergyPlus users can yield a 15% difference in the peak load. This uncertainty is also evident in the discrepancies between the ESP-r and EnergyPlus convection models. The assumptions made in the various convection models can have noticeable influence on the energy demand predictions. Therefore, the modelling of convective flows near shading devices remains an area which requires further detailed analysis. However, the close correlation between results is promising given that the ESP-r results for indoor and outdoor shades fall within the ~7.5% error presented in EnergyPlus alone.

Chapter 7

Conclusions and Recommendations

The focus of the current research was to successfully implement additional shading device models, i.e. drapery fabrics, pleated drapes, roller blinds and insect screens, to the ESP-r framework and further to demonstrate the successful implementation through model comparisons. To do so an understanding of the ESP-r framework, the Complex Fenestration Construction module (Lomanowski 2008) as well as the shading device models (Kotey 2009) had to be established.

Before model implementation, an analysis of the pleated drape solar optical property models was performed, giving further confidence to the view factor or net reduction method used by Kotey (2009) to improve computational time. The characteristic off-normal fabric solar property models used by Kotey were used in a Monte Carlo simulation and a simulation was performed. In reproducing near similar results to those determined by Kotey (2009), the solar-optical shading devices models, including the pleated drape, roller blind and insect screens could be implemented with confidence.

Extensive testing, using a shoebox approach, was completed after the implementation of each shading device model to ESP-r to establish each module was properly interfaced. As a preliminary analysis, flat shading layers were compared in a test cell simulation. The Venetian blind model, which was previously implemented by Lomanowski (2008), was used as a baseline to compare the relative performance of a roller blind and drapery fabric on a test cell's cooling load. The insect screen could not be used in this comparison since the material parameters were not suitable. The effect on performance yielded by the simulations suggested the models were properly implemented and further testing could ensue.

Work by Loutzenhiser (2006, 2008) demonstrated that given the correct convection coefficients, the venetian blind models in EnergyPlus could accurately predict the effects of the shading layer on building performance. As a result, the newly implemented roller blind and drapery fabric models were compared with the roller blind/drapery fabric model available in ESP-r. Using a test cell which would emphasize the effects of solar gain, a comparison was performed. The results suggested that although the trend of the effects of shading layers was near similar between the two programs, it further emphasized the general inability for modelling tools to accurately represent or model some convective flows in buildings. Rather,

without specific parameters input to the two programs, energy consumption varied quite heavily between the two programs.

To strengthen confidence in the newly implemented pleated drape, roller blind, drapery fabrics and insect screen models, continued investigation of convection near shading devices is recommended. In the meantime, it is also vital that convection models of airflow between shading layers placed indoors be established to streamline the results between various modelling programs. It is anticipated that in doing so, this comprehensive package will be of great value to building designers and promote the use of building energy simulation earlier in the design phases of future projects.

References

Alamdari, F., and G. P. Hammond. "Improved data correlations for buoyancy-driven convection in rooms." *Building Services Engineering Research & Technology* 4, No. 3 (1983).

Arasteh, D. K., J. C. Kohler, and B. T. Griffith. *Modeling Windows in EnergyPlus with only U, SGHC, and optionally VT.* Report No. LBNL-2804E, Lawrence Berkley National Laboratory, 2009.

Arasteh, D. K., M. S. Reilly, and M. D. Rubin. "A versatile procedure for calculating heat transfer through windows." *ASHRAE Transactions* 95, Pt. 2 (1989).

ASHRAE. *ASHRAE Handbook - Fundamentals.* Atlanta: ASHRAE, 2009.

—. *ASHRAE Handbook - Fundamentals.* Atlanta: ASHRAE, 2001.

Beausoleil-Morrison, I. *The adaptive coupling of heat and air flow modelling within dynamic whole-building simulation.* Glasgow, University of Strathclyde: PhD thesis., 2000.

Breitenbach, J., S. Lart, I. Langle, and J. L.J. Resenfeld. "Optical and Thermal Performance of Glazing with Integral Venetian Blinds." *Energy and Buildings* 33 (2001): 433-442.

CANMET. *The determination of fenestration solar heat gain coefficient using simulated solar irradiance.* The Solar Calorimetry Laboratory, Queen's University, Kingston: Natural Resources, Canada, 1993.

Clake, J. A. "Prospects for Truly Integrated Building Performance Simulation." *Building Simulation '99.* Kyoto: Int. Building Performance Simulation Association, 1999. (3) 1147-1154.

Clarke, J.A. *Energy Simulation in Building Design, 2nd Edition.* Oxford: Butterworth-Heinemann, 2001.

Collins, M. R., and J. L. Wright. "Calculating Center-Glass Performance Indices of Windows with a Diathermanous Layer." *ASHRAE Transactions, Vol. 112, Pt. 2*, 2006: 22-29.

Collins, M. R., and S. J. Harrison. "Calorimetric Analysis of the Solar and Thermal Performance of Windows with Interior Louvered Blinds." *ASHRAE Transactions* 110, Pt. 1 (2004a): 474-485.

Collins, M. R., and S. J. Harrison. "Estimating the Solar and Thermal Gain from a Windows with an Interior Venetian Blind." *ASHRAE Transactions* 110, Pt. 1 (2004b): 486-500.

Collins, M.R. "Convective heat transfer coefficients from an internal window surface and adjacent sunlit Venetian blind." *Energy and Buildings 36*, 2004: 309-318.

Crawley, D. B., J. W. Hand, M. Kummert, and B. T. Griffith. *Contrasting the Capabilities of Building Energy Performance Simulation Programs.* Washington, DC, USA; Univeristy of Strathclyde, Glasgow, Scotland; University of Wisconsin, Madison, Wisconsin, USA; National Renewable Energy Laboratory, Golden, Colorado: A Joint Report by DOE (U.S. Department of Energy), 2005.

Edwards, D. K. "Solar absoption by each element in an absorber-coverglass array." *Solar Energy*, no. 19 (1977): 401-402.

ElSherbiny, S. M., G. D. Raithby, and K. G.T. Hollands. "Heat transfer by natural convection across vertical and inclined air layers." *Journal of Heat Transfer* 104 (1982): 96-102.

EN 13363-2 E. "Solar protection devices combined with glazing - Calculation of total solar energy transmittance and light transmittance - Part2: Detailed calculation method." EN Standard, 2004.

EN 410. "Glass in buildings - Determination of luminous and solar characteristics of glazing." EN Standard, 1998.

EN 673. "Glass in buildings - Determination of thermal transmittance (U-value) - Calculation method." EN Standard, 1997.

EN ISO 10077-1. "Thermal performance of windows, doors and shutters - Calculation of thermal transmittance - Part 1: Simplified method." EN/ISO Standard, 2000.

EnergyPlus Engineering Reference. DOE (U.S. Department of Energy), 2010.

EnergyPlus Input Output Reference. DOE (US Department of Energy), 2010.

eQUEST Introductory Tutorial, version 3.64. Camarillo: James J. Hirsch & Associates, 2010.

ESP-r. 2011. http://www.esru.strath.ac.uk/Downloads/downloads.htm#ESP-r.

Farber, E. A., W. A. Smith, C. W. Pennington, and J. C. Reed. "Theoretical analysis of solar heat gain through insulating glass with inside shading." *ASHRAE Journal*, 1963: 79.

Finlayson, E. U., D. K. Arasteh, C. Huizenga, M. D. Rubin, and M. S. Reilly. *WINDOW 4.0: documentation of calculation procedures.* Report No. LBL-33943, Lawrence Berkeley National Laboratory, 1993.

—. *WINDOW 4.0: Documentation of Calculation Procedures.* Berkley: Lawrence Berkley Laboratory, 1993.

Gebhart, B. "A New Method for Caculating Radiant Exchanges." *ASHRAE Transactions* 65 (1959): 321-332.

—. *Heat Transfer.* New York: McGraw-Hill, 1961.

Gebhart, B. "Unified Treatment for Thermal Radiation Transfer." Paper 57-A-34, ASME Annual Meeting, 1957.

Government Grants UK. *Government Grants.* 2011. https://www.government-grants.co.uk/.

Government of Canada. *ecoACTION - Grants and Rebates.* February 2011. http://www.ecoaction.gc.ca/grantsrebates-subventionsremises/index-eng.cfm.

Harrison, S. J., and F. Dubrous. "Determination of Window Thermal Characteristics Using a Solar Simulator Based Test Method." *ASHRAE Transactions* 96, Pt. 1 (1990): 912-919.

Hollands, K. G.T. *Thermal Radiation Fundamentals.* New York: Begell House, Inc., 2004.

Hollands, K. G.T., J. L. Wright, and C. G. Granqvist. "Ch. 2 (Glazings and Coatings)." In *Solar Energy – The State of the Art - ISES Position Papers*, 26-107. James & James Ltd., 2001.

Huang, N. Y.T., J. L. Wright, and M. R. Collins. "Thermal Resistance of a Window with an Enclosed Venetian Blind: Guarded Heater Plate Measurements." *ASHRAE Transactions* 112, Pt.2 (2006): 13-21.

ISO 15099. *Thermal Performance of Windows, Doors and Shading devices - Detailed Calculations.* 2001.

ISO 15099. "Thermal Performances of Windows, Doors, and Shading Devices—Detailed Calculations." ISO Standard, 2003.

Kotey, N. A. "Measurements and Models Related to Solar Optics in Windows with Shading Devices." Master's Thesis, Waterloo, On, 2009.

Kotey, N. A., J. L. Wright, and M. R. Collins. "A simplified method for calculating the effective solar optical properties of a drapery." *Proceedings of the 32nd Conference of the Solar Energy Society of Canada Inc. (SESCI) and 2nd Conference of the Solar Building Research Network (SBRN), Calgary, Alberta Canada, June 9-13, 2007.* Calgary, 2007.

Kotey, N. A., M. R. Collins, J. L. Wright, and T. Jiang. "A Simplified Method For Calculating The Effective Solar Optical Properties Of A Venetian Blind Layer For Building Energy Simulation." *ASME Journal of Solar Energy Engineering*, 2008.

LBNL. *International Glazing Dddatabase (IGDB).* http://windows.lbl.gov/materials/igdb/.

Lomanowski, B. A. "Implementation of Window Shading Models into Dynamic Whole-building Simulation." Master's Thesis, Waterloo, On, 2008.

Lomanowski, B. A., and J. L. Wright. "The Complex Fenestration Construction: a practical approach for modelling windows with shading devices in ESP-r." *Journal of Building Performance Simulation*, 2011.

Loutzenhiser, P. G., et al. "An empirical validation of modeling solar gains through a glazing unit using building energy simulation programs." *HVAC&R Research 12*, 2006: 1097-1116.

Loutzenhiser, P. G., H. Manz, S. Carl, H. Simmler, and G. G. Maxwell. "Empirical validations of solar gain models for a glazing unit with exterior and interior blind assemblies." *Energy and Buildings 40*, 2008: 330-340.

Manz, H., P. Loutzenhiser, T. Frank, P. A. Strachan, R. Bundi, and G. Maxwell. "Series of experiments for empirical validation of solar gain modeling in building energy simulation codes—Experimental setup, test cell characterization, specifications and uncertainty analysis." *Building and Environment 41*, 2006: 1784-1797.

Mitchell, R., et al. "WINDOW 6.2/THERM 6.2 Research Version User Manual." Program Description LBNL-941, 2008.

Naylor, D., H. Shahid, S. J. Harrison, and P. H. Oosthuizen. "A simplified method for modeling the effect of blinds on window thermal performance." *International Journal of Energy Research* 30 (2006): 471-488.

Parmelee, G. V., and W. W. Aubele. "The shading of sunlit glass: an analysis of the effect of uniformly spaced flat opaque slats." *ASHVE Transactions* 58 (1952): 377-398.

Pennington, C. W., W. A. Smith, E. A. Farber, and J. C. Reed. "Experimental analysis of solar heat gain through insulating glass with indoor shading." *ASHRAE Journal 2:27.*

Pfrommer, P., K. J. Lomas, and C. Kupke. "Solar Radiation Transport through Slat-Type Blinds: a New Model and its Application for Thermal Simulation of Buildings." *Solar Energy* 57, No. 2 (1996): 77-91.

Rheault, S., and E. Bilgen. "Heat Transfer Analysis in an Automated Venetian Blind System." *ASME Journal of Solar Energy Engineering* 111 (1989): 89-95.

Rosenfeld, J. L.J., W. J. Platzer, H. Van Dijk, and A. Maccari. "Modeling the Optical and Thermal Properties of Complex Glazing: Overview of Recent Developments." *Solar Energy* 69 Supplement, No. 1-6 (2000): 1-13.

Shahid, H., and D. Naylor. "Energy performance assessment of a window with a horizontal Venetian blind." *Energy and Building* 37 (2005): 836-843.

Shewen, E., K. G.T. Hollands, and G. D. Raithby. "Heat Transfer by Natural Convection Across a Vertical Cavity of Large Aspect Ratio." *Journal of Heat Transfer* 118 (1996): 993-995.

Simmler, H., U. Fischer, and F. Winkelmann. *Solar-Thermal Window Blind Model for DOE-2.* Simulation Research Group internal report, Lawrence Berkeley National Laboratory, 1996.

Sparrow, E. M., and V. K. Johnson. "Thermal radiation absorption in rectangular grooves." *ASME paper 62-WA- 52*, 1962.

Sparrow, E. M., J. W. Ramsey, and E. A. Mass. "Effect of Finite Width on Heat Transfer and Fluid Flow about an Inclined Rectangular Plate." *Journal of Heat Transfer* 101 (1979): 204.

U.S. Department of Energy. *Testing and Validation.* Mar 11, 2011. http://apps1.eere.energy.gov/buildings/energyplus/energyplus_testing.cfm.

U.S. Department of Health and Human Services. *Grants.gov.* 2011. http://www.grants.gov/.

Walton, G. N. *Thermal Analysis Research Program Reference Manual.* NBSSIR 83-2655, National Burea of Standards, 1983.

Wilcox, B. "New California Simulation Engine (CSE) for residential building energy modeling." *California Energy Commission.* June 21, 2011. http://www.energy.ca.gov/title24/2013standards/prerulemaking/documents/2011-06-21_workshop/presentations/New_California_Simulation_Engine_for_residential_building_energy_modeling.pdf (accessed July 12, 2011).

Wright, J. L. "A Correlation to Quantify Convective Heat Transfer Between Vertical Window Glazings." *ASHRAE Transactions* 102, Pt. 1 (1996): 940-046.

Wright, J. L. "Calculating Center-Glass Performance Indices of Glazing Systems wth Shading Systems." *ASHRAE Transactions* 114, Pt. 2 SL-08-020 (2008).

Wright, J. L. "Calculating Center-Glass Performance Indices of Windows." *ASHRAE Transactions* 1004, 1B, SF-98-12-4 (1998): 1230-1241.

Wright, J. L., and A. McGowan. "Calculating Solar Heat Gain of Window Frames." *ASHRAE Transactions* 105, Pt. 2 (1999): 1011-1021.

Wright, J. L., and N. A. Kotey. "Solar Absorption by Each Element in a Glazing/Shading Layer Array." *ASHRAE Transactions* 112, Pt. 2 (2006): 3-12.

Wright, J. L., C. S. Barnaby, P. Niles, and C. Rogalsky. "Efficient Simulation of Complex Fenestration Systems in Heat Balance Room Models." *12th International Conference of the International Building Performance Simulation Association* In Review (2011).

Wright, J. L., M. R. Collins, N. A. Kotey, and C. S. Barnaby. *Improving Cooling Load Calculations for Fenestration with Shading Devices.* 1311-RP, ASHRAE, 2009.

Yahoda, D. S., and J. L. Wright. "Heat Transfer Analysis of a Between-Panes Venetian Blind Using Effective Longwave Radiative Properties." *ASHRAE Transactions* 110, Pt. 1 (2004b): 463-473.

Yahoda, D. S., and J. L. Wright. "Methods for Calculating the Effective Longwave Radiative Properties of a Venetian Blind Layer." *ASHRAE Transactions* 110, Pt. 1 (2004a): 455-462.

Yahoda, D. S., and J. L. Wright. "Methods for Calculating the Effective Solar-Optical Properties of a Venetian Blind Layer." *ASHRAE Transactions* 111, Pt. 1 (2005): 572-586.

Appendix A

Modifications to CFC Sub-Modules in ESP-r Framework

To accommodate for the introduction of the new shading layers, modifications to the existing ESP-r and CFC subroutines needed to be made. As such, many of the details provided in Appendix D-F of (Lomanowski 2008) still apply; this document will then reference the Sections which were altered.

A.1 Modifications to ESP-r Solar Processing Flow Chart

Refer to Appendix D of (Lomanowski 2008).

In Section 1.5 of Appendix D, modifications were made to the "profile_angle" and "cfc_eff_opt_prop" subroutines.

A.1.1 "profile_angle" (in Esrubld/complex_fenestration.F)

Previously, profile_angle determined the profile angle of incident solar radiation to slat-type shades based on slat orientation (i.e. horizontal or vertical configuration).

The pleated drape properties are also modelled with profile angle dependence, however due to the geometry of pleated drapes, it requires both the horizontal and vertical profile angles simultaneously. As a result, slat orientation is no longer determined in this routine, rather both angles are calculated for any shading layer. The slat orientation is handled in a subsequent routine.

A.1.2 "cfc_eff_opt_prop" (in Esrubld/complex_fenestration.F)

The cfc_eff_opt_prop subroutine is used to determine effect solar optical properties of the layers which comprise the CFC. The subroutine has been expanded to determine whether the shading layer type and further, determine the effect layer properties of the three new shading layer (roller blind, pleated drape and insect screen) models implemented.

A.1.3 Subroutine “cfc_eff_opt_prop”

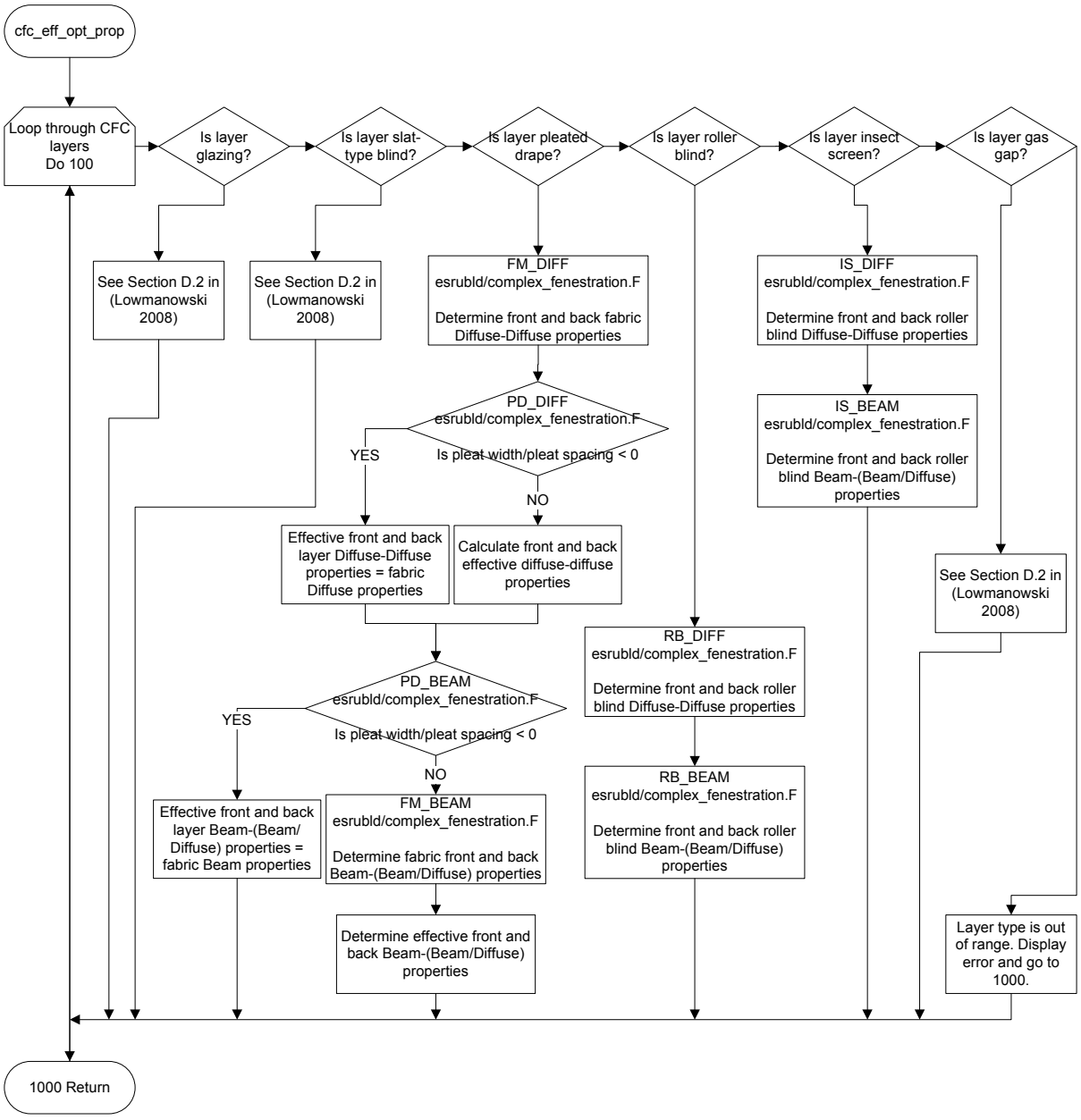

A.2 Modifications to ESP-r Thermal Simulation Flow Chart

Refer to Appendix E of (Lomanowski 2008).

In Section 1.6 of Appendix E, modifications were made to the "cfc_thermal_processing" and "cfc_convection" subroutines.

"cfc_thermal_processing" (in esrubld/complex_fenestration.F)

Previously, cfc_thermal_processing was setup to accommodate for the slat-type shading model (vb_eff_diff_properties), computing longwave properties based on venetian blind longwave models.

This subroutine has been modified to include the newly implemented shading device longwave model subroutines:

- Pleated Drape
    - PD_LW
        - Determines front and back side longwave emittance and transmittance
        - OPENNESS_LW
            - Determines material longwave emittance and transmittance based on fabric openness
        - PD_DIFF
            - Determines effective front and backside longwave diffuse-diffuse transmittance and reflectance
- Roller Blind
    - OPENNESS_LW
        - Determines material longwave emittance and transmittance based on fabric openness
- Insect Screen
    - OPENNESS_LW
        - Determines material longwave emittance and transmittance based on fabric openness

"cfc_convection" (in esrubld/complex_fenestration.F)

The cfc_convection subroutine is used to determine the temperature and time dependent gap resistances. Indoor and outdoor correlations were used to account for slat-type shading.

In order to accommodate for the newly implemented shading layer models, the modified gap width correlation used had to be modified for the new shading layer types. In the case of the roller blind, an effective value was required to give sufficient mass to the drape in order to account for stability issues.

Appendix B

Monte-Carlo Simulation Data and Code

B.1 MC Simulation Data

The following data was derived from Monte-Carlo simulation at fixed angles of incidence of incoming solar radiation. A mean standard deviation was used to determine the accuracy of the results. At each angle of incidence calculated, 30 trials of 5000 rays were used.

The standard deviation of the mean was calculated by, $SD_{\overline{x}} = \frac{\sigma}{\sqrt{n}}$.

Table B-1 - Dark Coloured Drape Effective Solar Optical Properties

Dark Coloured Material Effective Drape Solar Optical Properties (Beam-Total)						
θi	Absorptance		Transmittance		Reflectance	
	Mean	SD	Mean	SD	Mean	SD
0	0.6431	0.0012	0.1141	0.0006	0.2428	0.0011
15	0.6489	0.0011	0.0924	0.0007	0.2587	0.0012
30	0.6477	0.0012	0.0724	0.0007	0.2799	0.0011
45	0.6452	0.0013	0.0581	0.0007	0.2968	0.0011
60	0.6342	0.0011	0.0481	0.0006	0.3177	0.0009
63	0.6319	0.0014	0.0463	0.0005	0.3218	0.0014
75	0.6174	0.0014	0.0398	0.0004	0.3428	0.0015
89	0.5842	0.0011	0.0307	0.0003	0.3851	0.0011

Table B-2 - Medium Coloured Drape Effective Solar Optical Properties

Medium Coloured Material Effective Solar Optical Properties (Beam-Total)						
θi	Absorptance		Transmittance		Reflectance	
	Mean	SD	Mean	SD	Mean	SD
0	0.5845	0.0012	0.2057	0.0008	0.2098	0.001
15	0.6038	0.0014	0.1686	0.0009	0.2276	0.001
30	0.6215	0.0012	0.134	0.0008	0.2445	0.001
45	0.6273	0.0012	0.1059	0.0007	0.2668	0.0008
60	0.6336	0.001	0.0777	0.0006	0.2887	0.0009
63	0.6393	0.0017	0.068	0.0007	0.2928	0.0016

75	0.6303	0.0014	0.0563	0.0006	0.3133	0.0014
89	0.6017	0.0013	0.0432	0.0005	0.3551	0.0013

Table B-3 - Light Coloured Drape Effective Solar Optical Properties

Light Material Coloured Solar Optical Properties (Beam-Total)						
θi	Absorptance		Transmittance		Reflectance	
	Mean	SD	Mean	SD	Mean	SD
0	0.3741	0.0011	0.3287	0.001	0.2972	0.0014
15	0.3976	0.0014	0.2809	0.0009	0.3215	0.0012
30	0.4154	0.0011	0.2365	0.0012	0.3481	0.0009
45	0.4239	0.0012	0.2001	0.001	0.376	0.0013
60	0.4364	0.0012	0.1627	0.0011	0.4009	0.0015
63	0.4419	0.0014	0.15	0.0008	0.408	0.0011
75	0.4358	0.0012	0.1299	0.001	0.4343	0.0011
89	0.43	0.0013	0.0955	0.0006	0.4745	0.0011

B.2 MC Simulation Code

B.2.1 Pseudocode

```
declare arrays which describe the drape

for ray = 1:number of bundles

  strike = 0

  while (no surface has absorbed any rays)

    if(strike = 0)
      the ray is described by the incoming solar radiation in terms
      of omega_h and omega_v

      theta is calculated at this point

    elseif(strike>0)
      the resulting position vector from the ray's last interaction
      is the new ray origin

      the direction vector was also previously determined
    end
```

```
for surface 1:7
   calculate u and t
end

if (strike = 0)
   case 1: surface 4 is struck
      calculate the resulting position vector
   case 2: surface 1 is struck
      calculate the resulting position vector
   case 3: surface 2 is struck
      calculate the resulting position vector
   case 4: surface 3 is struck
      calculate the resulting position vector
   get theta (incidence angle)

elseif (strike > 0)
   find out which surface is struck
   if (surface 6 is struck)
      absorb_surface = absorb_surface+1
   elseif (surface 7 is struck)
      absorb_surface = absorb_surface+1
   get theta
   end
end

calculate the absorptivity, reflectivity and transmissivities

if (ray absorbed)
   absorb_surface = absorb_surface+1
   break

elseif (ray transmitted as a beam)
   if(strike > 0 and transmitted through surface 4)
      absorb_surface = absorb_surface+1
   elseif(transmitted through surface 2)
      absorb_surface = absorb_surface+1
   end

   the direction vector stays the same

   if(transmitted through surface 1)
      then need to change y_o = 0 to y_o = 2*s
   elseif(transmitted through surface 5)
      then need to change y_o = 2*s to y_o = 0
   end

elseif (ray transmitted diffusely)
   if(strike > 0 and transmitted through surface 4)
      absorb_surface = absorb_surface+1
   elseif(transmitted through surface 2)
      absorb_surface = absorb_surface+1
```

```
        end

        the direction vector is determined here through the function
        determining_geometries

        if(transmitted through surface 1)
           then need to change y_o = 0 to y_o = 2*s
        elseif(transmitted through surface 5)
           then need to change y_o = 2*s to y_o = 0
        end

      elseif (ray reflected diffusely)
        if (strike == 0 and reflected at surface 4)
           absorb_surface = absorb_surface+1
        end

        the direction vector is determined here through the function
        determining_geometries
      end

   strike=strike+1
   end

end
```

Appendix C

CFC User Reference for New Shading Layers

The following description is tailored towards the use of the new shading layers introduced to ESP-r. As such some of the following is paraphrased from (Lomanowski 2008) and further background in regards to the general application of the CFC module is available in Appendix F of (Lomanowski 2008).

The Complex Fenestration Construction (CFC) module extends the capabilities previously offered by ESP-r through the transparent multilayer constructions (TMC), with the added capability of not only analyzing glazing systems, but glazing and shading systems. The CFC achieves this though the external handling of solar, convective and radiant exchanges through the layers at each time-step, and subsequently returning the results in a nodal structure which can be read by ESP-r. This additionally introduces the possibility of modelling controlled operable shading at each time-step.

Basic controls are available via the subroutine "CFC_control" in esrubld\complex_fenestration.F.

C.1 Modelling Procedure

A CFC model is composed of glazing and/or shading layers separated by gas gaps. The newly implemented shading models further extend the capabilities of the CFC to support the modelling of roller blinds, pleated drapes, drapery fabrics and insect screens in addition to venetian blind models previously established. Layers can be arranged in any fashion, however only one shading layer may exist in a particular CFC model.

The general procedure to modelling a CFC in ESP-r is as follows:

1. Create a CFC composition in the ESP-r construction database.
2. Create an import (*.GSL) file via the Glazing Shading Layer Editor GSLedit, and modify the glazing and/or shading layer optical properties and fill gas properties as desired.
3. Attribute the properties from the *.GSL file to ESP-r via the CFC module to create a ESP-r CFC input file (*.cfc) for each of the zones containing a CFC.

C.1.1 Creating a CFC Shading Layer

See Appendix F.2 of (Lomanowski 2008).

C.1.2 Creating an Import (*.GSL) file using the Glazing Shading Layer Editor (GSLedit)

See Appendix F.3 of (Lomanowski 2008) for further details.

Open GSLedit and click "New" and select the number of layers in the system. Gas gaps do not count as layers, and the number and order of layers must correspond to the ESP-r CFC construction. Refer to Figure C.1.

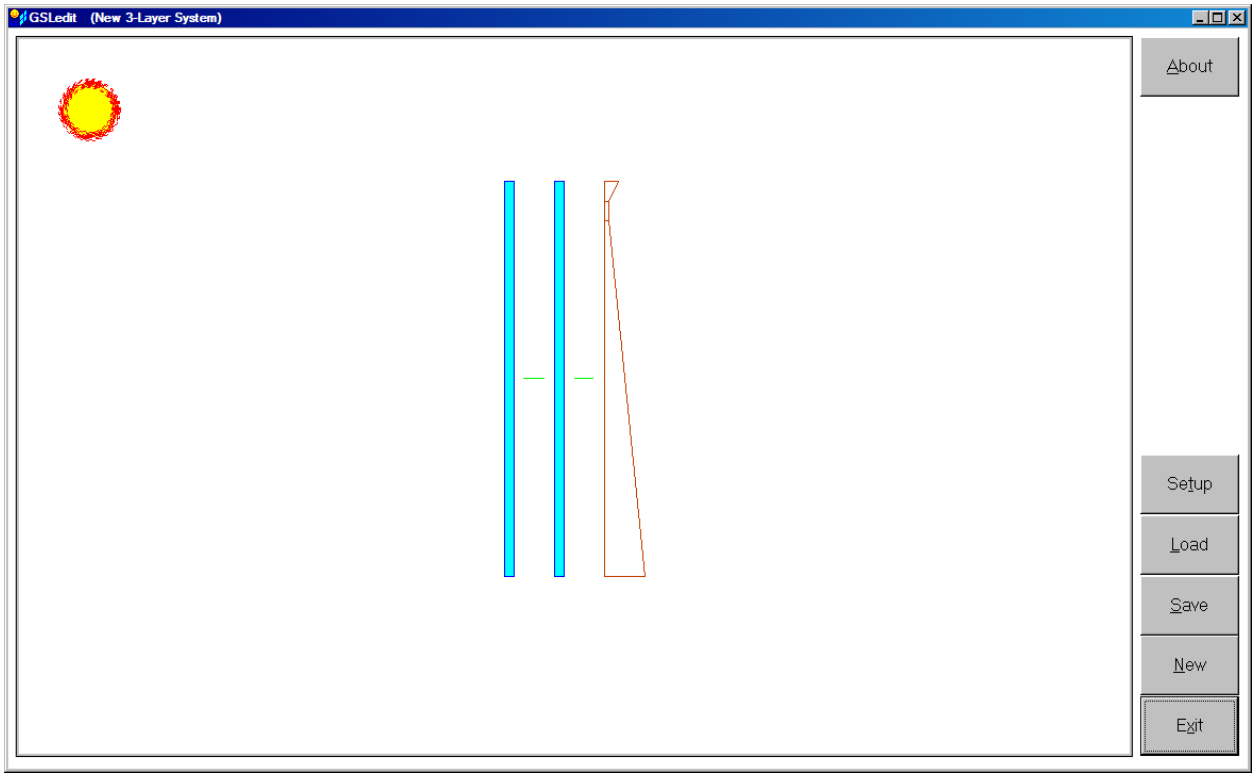

Figure C.1 - Layout for GSLedit

- Left clicking on a layer allows the user to select the layer type, or change certain properties.
  - The glazing databases are based on the International Glazing Database (IGD) (LBNL 2008)
  - Fill gas composition/mixtures can be edited in GSLedit
  - Additional shading layer or glazing or gas type entries can be entered by editing the database text files located in the respective \ GSLedit_v1*files directories.
- Right clicking on a layer allows to user to view the solar optical, longwave, geometric or fill gas properties of the layer which is selected.

Note: Make sure the shading layer position and gas gap thicknesses match those in the CFC construction in ESP-r.

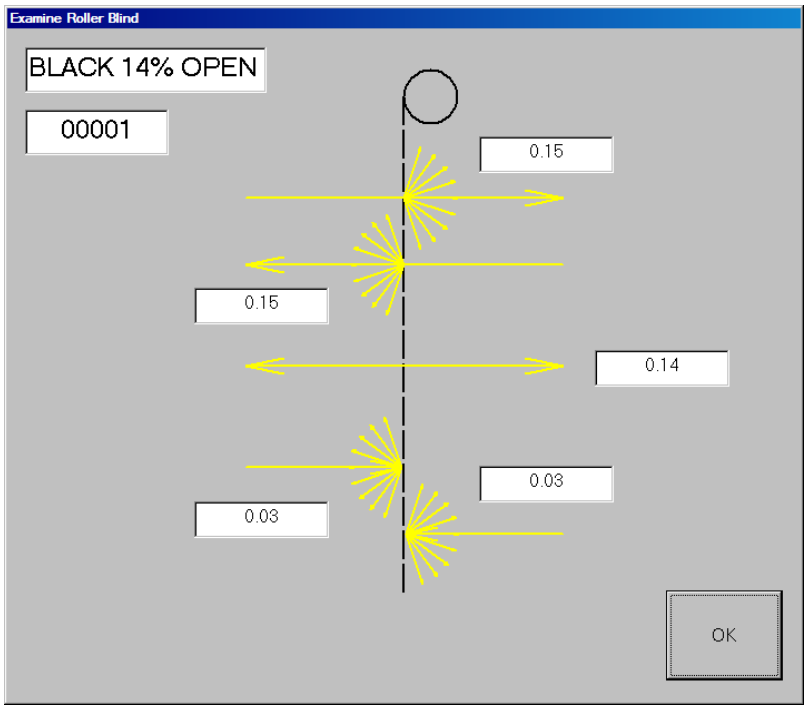

Figure C.2 - Property Display Window of Roller Blind Layer

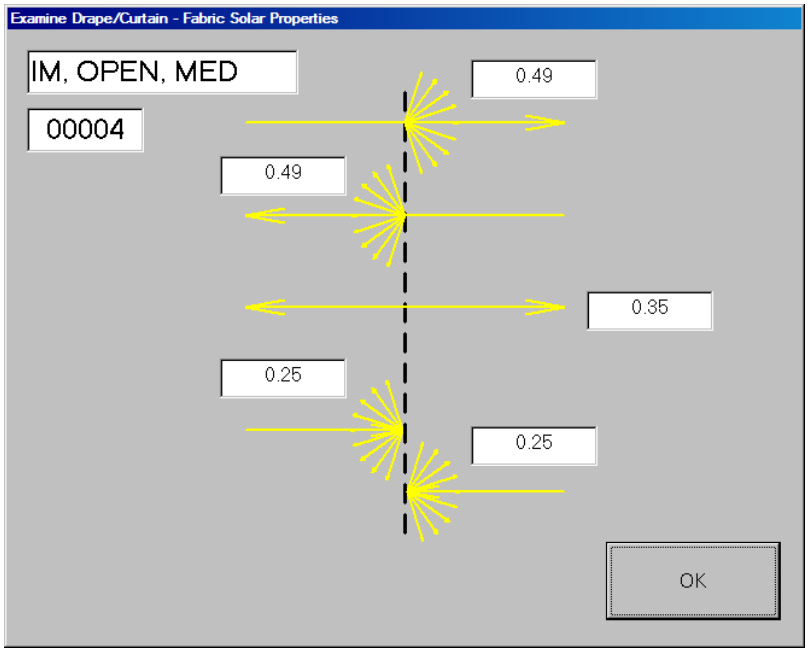

Figure C.3Property Display Window of Drapery Fabric Layer

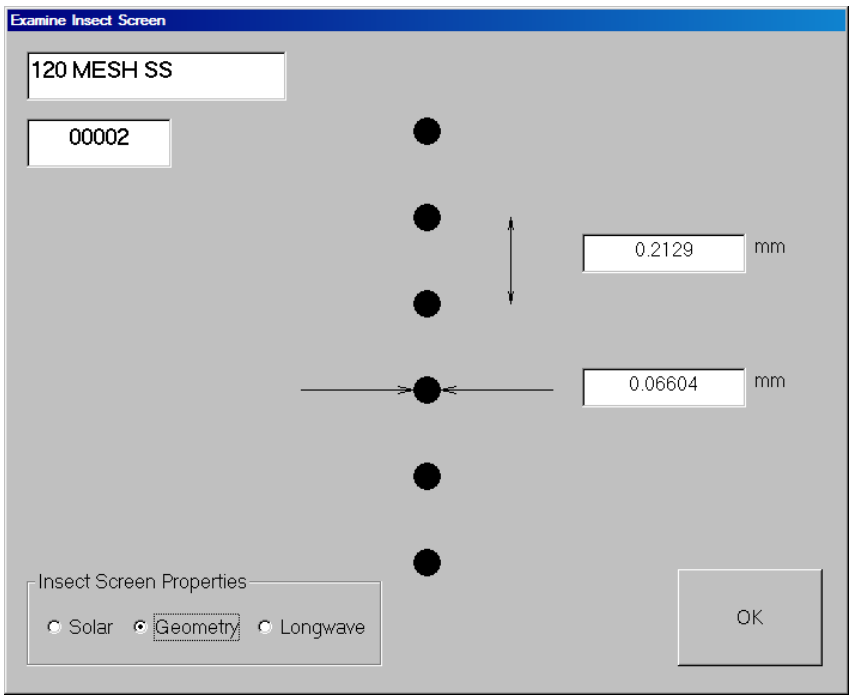

Figure C.4 - Property Display Window of Insect Screen Layer

- Save the GSLedit system in the appropriate ESP-r format for use in the CFC module.
    - Click “Setup”, see Figure C.1, then click “Output File Format” and select “ESP-r (#marks comments)”. This will save the file in the correct *.GSL format which can be handled by ESP-r.
- Copy the *.GSL file from \GSLedit_v1\GSLsystems to the \zones folder in the ESP-r model.

C.1.3 The Addition of CFCs to the ESP-r Model

See Appendix F.4 of (Lomanowski, Implementation of Window Shading Models into Dynamic Whole-building Simulation 2008) for further details.

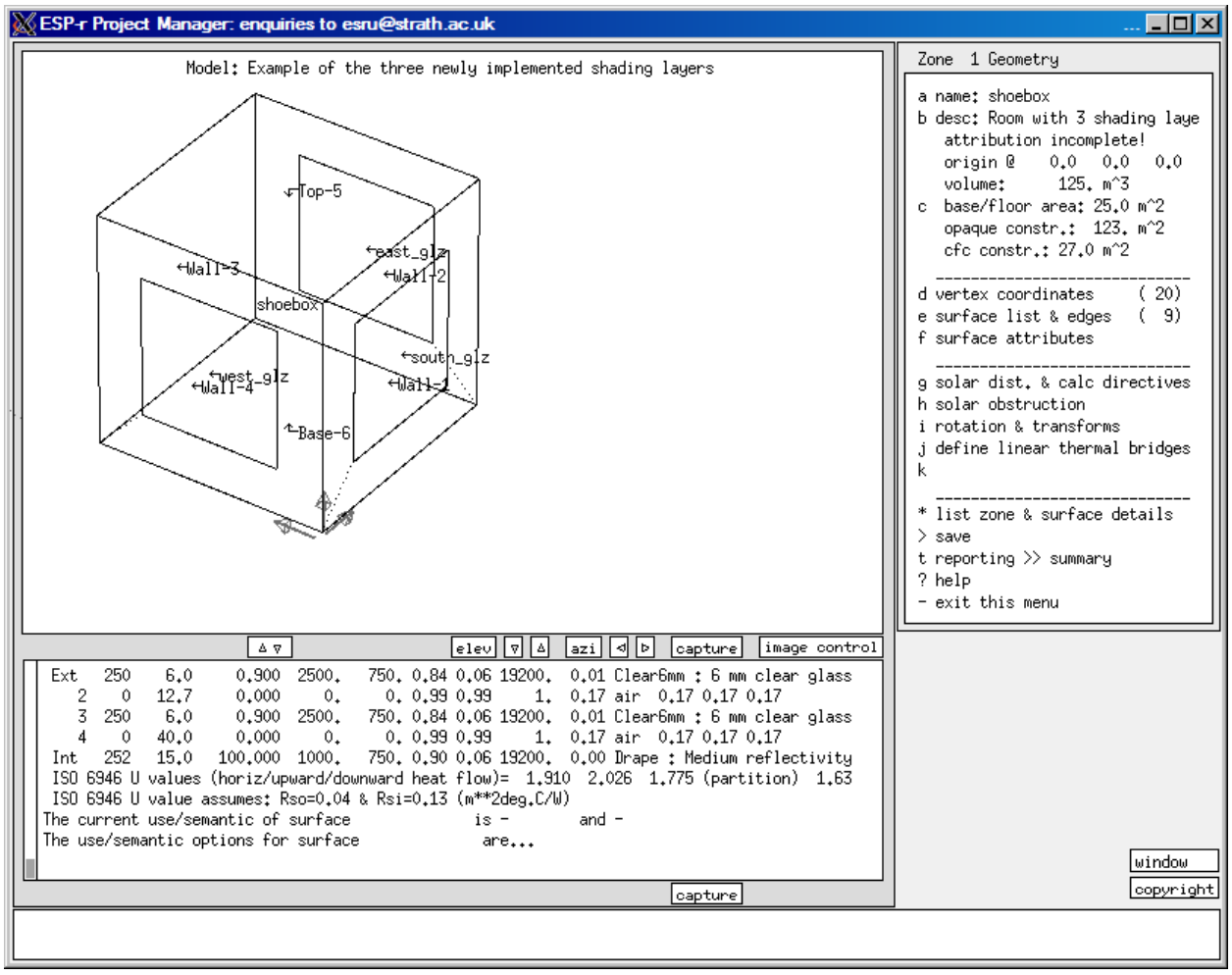

Figure C.5 - Geometry, Composition and Boundary Conditions of Example Model

Click “Import GSLedit files”

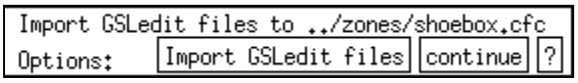

Enter the number of CFC types. (3 will be used for this example, one for each newly implemented shading layer type (i.e. roller blind, pleated drape and insect (bug) screen).

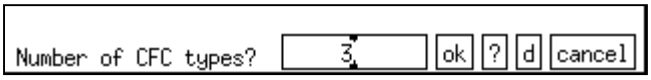

Assign the CFC type for each CFC surface:

- South Glazing Surface (Roller Blind)

- West Glazing Surface (Pleated Drape)

- East Glazing Surface (Insect Screen)

Assign the respective *.GSL edit file for the CFC type referenced:

- For CFC type 1, a roller drape is selected.

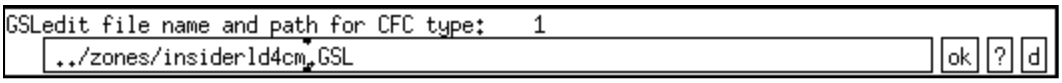

- For CFC type 2, a pleated drape is selected.

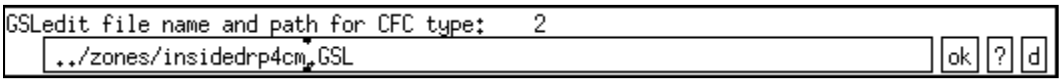

  - Specify the pleated drape width (a width of 0 mm corresponds to a drapery fabric)

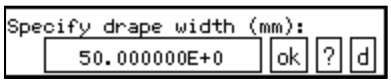

  - Specify the pleated drape spacing (for a drapery fabric any spacing size > 0 mm can be applied)

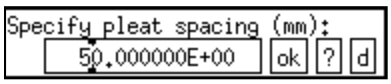

- For CFC type 3, a insect screen is selected.

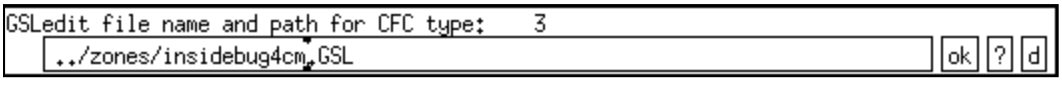

The *.cfc file will subsequently be created with all the necessary data to carry out the simulation.

Note 1: The user will be prompted to “Import GSLedit files” each time there is a change made to the model construction or geometry. However, this can be skipped once the *.GSL files are initially imported once for the model construction being used.

Note 2: the insect screen wire diameter and spacing can be edited manually in \GSLedit_v1\BUGfiles before creating the *.GSL file, or in the *.GSL once created:

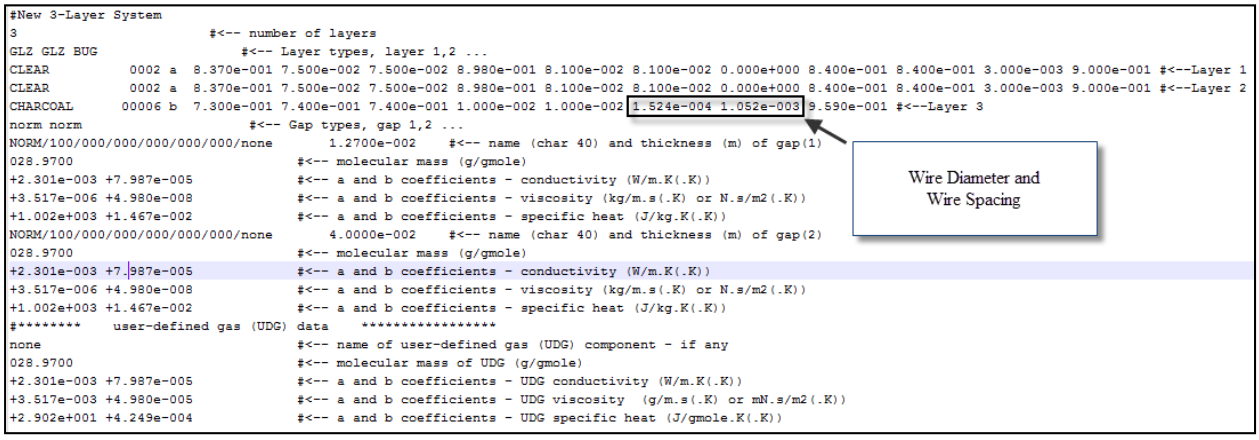

Figure C.6 - Modifying Wire Diameter and Spacing in the *.GSL File

Simulations can subsequently be carried out.

C.2 CFC input file

Each zone in the ESP-r model is assigned a *.cfc input file much like the other ESP-r input files (*.tmc and *.con). The shoebox.cfc file presented below is an example of the *.cfc file which was created for the model illustrated in Figure C.1. There are three CFC types presented in this file, representing the south, west and east glazing and shading systems, with a roller blind, pleated drape and insect screen respectively. Once created, the .cfc model can be modified manually to suit the needs of the user, and can also be modified to bypass the “Import GSLedit files” process.

The shoebox.cfc file is broken down into its respective components to clearly define the cfc type definitions in the file. Further explanations are provided in the text boxes.

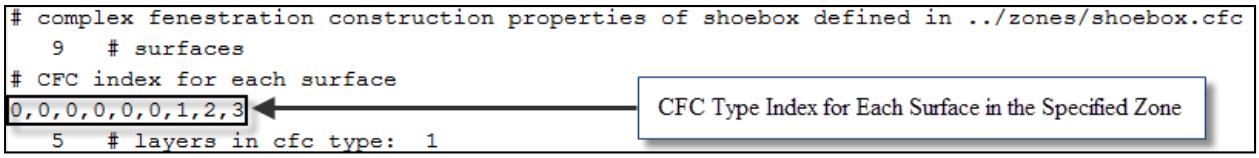

```
# For each layer: normal solar optical properties - R_fr, R_bk, Tran., (T_f_tot, T_b_tot, T_f_bd, T_b_bd)
   0.071   0.071   0.775   0.775   0.775   0.000   0.000   # glazing
   0.000   0.000   0.000   0.000   0.000   0.000   0.000   # gas gap
   0.071   0.071   0.775   0.775   0.775   0.000   0.000   # glazing
   0.000   0.000   0.000   0.000   0.000   0.000   0.000   # gas gap
   0.500   0.500   0.000   0.000   0.000   0.000   0.000   # roller drape
# For each layer: normal visible optical properties - R_fr, R_bk, Tran. CU
   0.080   0.080   0.881   # glazing
   0.000   0.000   0.000   # gas gap
   0.080   0.080   0.881   # glazing
   0.000   0.000   0.000   # gas gap
   0.500   0.500   0.000   # roller drape
# For each layer: normal longwave radiative properties - EmisF, EmisB, Tra
   0.840   0.840   0.000   # glazing
   0.000   0.000   0.000   # gas gap
   0.840   0.840   0.000   # glazing
   0.000   0.000   0.000   # gas gap
   0.912   0.912   0.050   # roller drapes
```

Solar Optical, Visible Optical (Currrently Not Used) and Longwave Properties for Each Layer in CFC type 1: (Double Clear Glazing with Air Gaps and Indoor Roller Blind)

R_fr = Front Reflectance
R_bk = Back Reflectance
Tran = Transmittance
T_f_tot = total Front Transmittance
T_b_tot = Totoal Back Transmittance
T_f_bd = Front Beam-Diffuse Transmittance
T_b_bd = Back Beam-Diffuse Transmittance
EmisF = Front Emissivity
EmisF = Back Emissivity

```
# For each layer: normal solar optical properties - R_fr, R_bk, Tran., (T_f_tot, T_b_tot, T_f_bd, T_b_bd)
   0.071   0.071   0.775   0.775   0.775   0.000   0.000   # glazing
   0.000   0.000   0.000   0.000   0.000   0.000   0.000   # gas gap
   0.071   0.071   0.775   0.775   0.775   0.000   0.000   # glazing
   0.000   0.000   0.000   0.000   0.000   0.000   0.000   # gas gap
   0.500   0.500   0.000   0.000   0.000   0.000   0.000   # drape
# For each layer: normal visible optical properties - R_fr, R_bk, Tran. CU
   0.080   0.080   0.881   # glazing
   0.000   0.000   0.000   # gas gap
   0.080   0.080   0.881   # glazing
   0.000   0.000   0.000   # gas gap
   0.500   0.500   0.000   # drape
# For each layer: normal longwave radiative properties - EmisF, EmisB, Tran.
   0.840   0.840   0.000   # glazing
   0.000   0.000   0.000   # gas gap
   0.840   0.840   0.000   # glazing
   0.000   0.000   0.000   # gas gap
   0.874   0.874   0.050   # drapes
```

Solar Optical, Visible Optical (Currrently Not Used) and Longwave Properties for Each Layer in CFC type 2: (Double Clear Glazing with Air Gaps and Indoor Pleated Drape)

```
   5   # layers in cfc type:  3
# For each layer: normal solar optical properties - R_fr, R_bk, Tran., (T_f_tot, T_b_tot, T_f_bd, T_b_bd)
   0.075   0.075   0.837   0.837   0.837   0.000   0.000   # glazing
   0.000   0.000   0.000   0.000   0.000   0.000   0.000   # gas gap
   0.075   0.075   0.837   0.837   0.837   0.000   0.000   # glazing
   0.000   0.000   0.000   0.000   0.000   0.000   0.000   # gas gap
   0.010   0.010   0.730   0.740   0.740   0.010   0.010   # insect screen
# For each layer: normal visible optical properties - R_fr, R_bk, Tran. CU
   0.081   0.081   0.898   # glazing
   0.000   0.000   0.000   # gas gap
   0.081   0.081   0.898   # glazing
   0.000   0.000   0.000   # gas gap
   0.010   0.010   0.730   # insect screen
# For each layer: normal longwave radiative properties - EmisF, EmisB, Tran.
   0.840   0.840   0.000   # glazing
   0.000   0.000   0.000   # gas gap
   0.840   0.840   0.000   # glazing
   0.000   0.000   0.000   # gas gap
   0.251   0.251   0.735   # insect screen
```

Solar Optical, Visible Optical (Currrently Not Used) and Longwave Properties for Each Layer in CFC type 2: (Double Clear Glazing with Air Gaps and Indoor Pleated Drape)

```
# gas layer   2
 0.290E+02        # molecular mass of gas mixture (g/gmole)
 0.230E-02  0.799E-04        # a and b coeffs.- gas conductivity (W/m.K)
 0.352E-05  0.498E-07        # a and b coeffs.- gas viscosity (N.s/m2)
 0.100E+04  0.147E-01        # a and b coeffs.- specific heat (J/kg.K)
# gas layer   4
 0.290E+02        # molecular mass of gas mixture (g/gmole)
 0.230E-02  0.799E-04        # a and b coeffs.- gas conductivity (W/m.K)
 0.352E-05  0.498E-07        # a and b coeffs.- gas viscosity (N.s/m2)
 0.100E+04  0.147E-01        # a and b coeffs.- specific heat (J/kg.K)
```

Gas Composition for Two Fill Gas/Mixture Gap Layers in CFC Type 1

```
# layer type index for cfc type:  2
1,0,1,0,3
# Gas mixture properties for cfc type:  2
# gas layer   2
 0.290E+02        # molecular mass of gas mixture (g/gmole)
 0.230E-02  0.799E-04        # a and b coeffs.- gas conductivity (W/m.K)
 0.352E-05  0.498E-07        # a and b coeffs.- gas viscosity (N.s/m2)
 0.100E+04  0.147E-01        # a and b coeffs.- specific heat (J/kg.K)
# gas layer   4
 0.290E+02        # molecular mass of gas mixture (g/gmole)
 0.230E-02  0.799E-04        # a and b coeffs.- gas conductivity (W/m.K)
 0.352E-05  0.498E-07        # a and b coeffs.- gas viscosity (N.s/m2)
 0.100E+04  0.147E-01        # a and b coeffs.- specific heat (J/kg.K)
# pleated drape attributes for cfc type:  2
# pleated drape: width(mm); spacing(mm);
  50.000  50.000
```

Gas Composition for Two Fill Gas/Mixture Gap Layers in CFC Type 2

Pleated Drape Specific Properties in CFC Type 2

```
# Gas mixture properties for cfc type:  3
# gas layer   2
 0.290E+02        # molecular mass of gas mixture (g/gmole)
 0.230E-02  0.799E-04        # a and b coeffs.- gas conductivity (W/m.K)
 0.352E-05  0.498E-07        # a and b coeffs.- gas viscosity (N.s/m2)
 0.100E+04  0.147E-01        # a and b coeffs.- specific heat (J/kg.K)
# gas layer   4
 0.290E+02        # molecular mass of gas mixture (g/gmole)
 0.230E-02  0.799E-04        # a and b coeffs.- gas conductivity (W/m.K)
 0.352E-05  0.498E-07        # a and b coeffs.- gas viscosity (N.s/m2)
 0.100E+04  0.147E-01        # a and b coeffs.- specific heat (J/kg.K)
# insect screen attributes for cfc type:  3
# insect screen: width(mm); spacing(mm); Wire Emissivity
   0.152    1.052    0.959
```

Gas Composition for Two Fill Gas/Mixture Gap Layers in CFC Type 3

Insect Screen Specific Properties in CFC Type 3